Very Large Telescope

SPHERE

User Manual

Reference	PDM-ESO-254263
	VLT-MAN-SPH-14690-0430
Issue	P100.0
Status	7th public release (P100 Phase 1)
Date of Issue	2017-03-06

Prepared	*Date*	*Signature*
J. Girard , Z. Wahhaj, J.Milli, A. Vigan, M. van den Ancker, H. Boffin *Early contributors: D. Mouillet, D. Mawet, M. Kasper, R. Siebenmorgen and the SPHERE consortium*	*2017-03-06*	
Approved *S. Mieske*	*Date*	*Signature*
Released *A. Kaufer*	*Date*	*Signature*

The SPHERE consortium:

Institut de Planétologie et d'Astrophysique de Grenoble, France (PI institute)
Max-Planck-Institut für Astronomie, Heidelberg, Germany (co-PI institute)
Laboratoire d'Astrophysique de Marseille, France
Observatoire de Genève, Switzerland
Laboratoire Lagrange, Nice, France
The Italian National Institute for Astrophysics coordinated by the
Osservatorio Astronomico di Padova, Italy
Laboratoire d'Etudes Spatiales et d'Instrumentation en Astrophysique, Paris, France
Eidgenössische Technische Hochschule (ETH) Zürich, Switzerland
The Astronomical Institute Anton Pannekoek, University of Amsterdam, the Netherlands
Office National d'Etudes et de Recherches Aérospatiales, Châtillon, France
The Netherlands Research School for Astronomy (NOVA-ASTRON), the Netherlands
The European Southern Observatory (ESO)

Change Record

Issue	Section	Comments
V95	All	First public draft
V95.1	8, Appendix	Added description of templates in Chapter 8 and associated tables in the Appendix.
V96.1	Many	Science Calibration Plan overview Beta ETC: + links IRDIS Astrometry IFS data reduction Inconsistencies Removed 4Q mask, Added ALC_YH_S mask Large NDIT Warning Added ZIMPOL saturation limits Comment on ND filters Warning about current ETC Clarification about provided flat field in IRDIS/LSS Updated IRDIS filters section Updated IFS dispersive elements information Added information on astrometry in Section 7 Several additions for LSS Corrected execution time calculation and overheads for IRDIFS observations IRDIS DPI mode Quality Assessment Low Wind Effect (LWE)
V97.1	Many	IRDIS_LSS mode offered in service if time critical (section 1.7) More information on the low wind effect (section 5.2) SPARTA files to review image quality now available in ESO archive (section 5.3) IRDIFS mode can now use BB_H filter. IRDIFS_EXT mode can now use BB_Ks filter (section 12.6) Getting calibration files from ESO archive (section 10.1)

Issue	Section	Comments
V99.0	Many	General reformatting Information on astrometric calibration More information on IRDIS DPI & link to the dedicated page
V100.0	5, 6, 8, Appendix.	Table 4: R>11 GS are now offered in SM as well as SAM as a new setup for IRDI(F)S (all modes but LSS) Updated information on coronagraphic transmission (section A6), sky offsets (section 7.4), SPARTA files (section 5.3) and true north determination (section 8). SAM: Sparse Aperture Masking (several sections) GoTo acquisition template

LIST OF ACRONYMS

ADC	Atmospheric Dispersion Corrector
ADI	Angular Differential Imaging
AO	Adaptive Optics
APLC	Apodized Pupil Lyot Coronagraph
BB	Broadband
CI	Classical Imaging
CLC	Classical Lyot Coronagraph
CP	Common Path
DBI	Dual Band Imaging
DD	Double Difference
DIT	Detector Integration Time
DM	Deformable Mirror
DMS	Detector Motion Stage
DPI	Dual Polarization Imaging
DRH	Data Reduction and Handling
DTTP	Differential Tip Tilt Plate
DTTS	Differential Tip Tilt Sensor
ESP	Extra-Solar Planet
ETC	Exposure Time Calculator
FF	Flat-field
FLC	Ferro-electric Liquid Crystal
FoV	Field of View
FP	Focal Plane
HA	Hour Angle
HAR	High angular resolution
HF	High Frequency
HODM	High Order Deformable Mirror
HW	Hardware
HWP	Half Wave Plate
IFS	Integral Field Spectrometer
INS	Instrument Software
IRDIS	IR Differential Imaging Spectrometer
ITTM	Image Tip-Tilt Mirror
IWA	Inner Working Angle
LOCI	Locally Optimized Combination of Images
LRS	Low resolution spectroscopy
LSS	Long Slit Spectroscopy
LWE	Low Wind Effect
mas	milli-arcseconds
MRS	Medium Resolution Spectroscopy
NB	Narrowband
NCPA	Non Common-Path Aberrations
NDIT	Number of DIT
NGC	New Generation Controller
NIR	Near Infrared
NRM	Non-Redundant Masking, also called SAM (Sparse Aperture Masking)
PCA	Principal Component Analysis

PDI	Polarimetric Differential Imaging (data reduction technique applied for data obtained in DPI mode)
PCOM	Polarization Compensator
PSF	Point Spread Function
PTTM	Pupil Tip-Tilt Mirror
QWP	Quarter-Wave Plate
RON	Readout Noise
RTC	Real-Time Computer
RTD	Real-Time Display
SAM	Sparse Aperture Masking, also called NRM (Non-Redundant Masking)
SAXO	Sphere AO for eXoplanet Observation
SC	Science Case
SD	Simple Difference
SDI	Spectral Differential Imaging
SNR	Signal to Noise Ratio
SP	Spectral type
SPHERE	Spectro-Polarimetric High contrast Exoplanet REsearch
SR	Strehl Ratio
tbc	to be confirmed
tbd	to be defined
WFE	WaveFront Error
WFS	WaveFront Sensor
ZIMPOL	Zurich Imaging POLarimeter
ZP	ZeroPoint

Table of contents

1. INTRODUCTION

The aim of the SPHERE User Manual is to provide information on the technical characteristics of the instrument, its performance, observing, calibration and data reduction procedures.
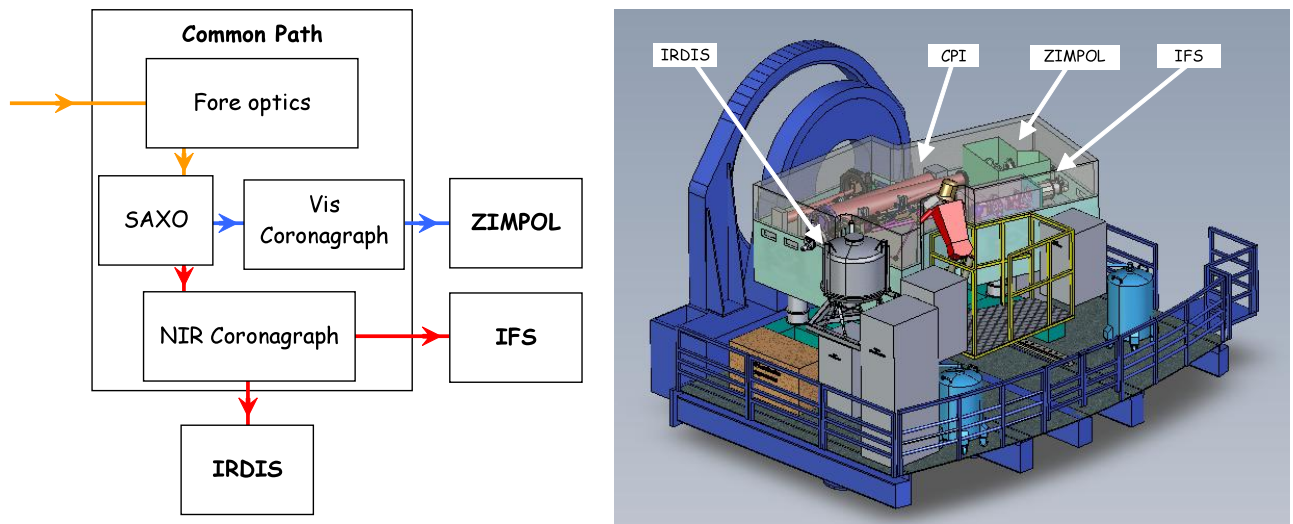
Figure 1: SPHERE sub-systems (left) including the common path (CPI) with adaptive optics system SAXO, coronagraphs, and sub-instruments IRDIS, IFS and ZIMPOL. Left: schematic view of the instrument on the Nasmyth platform.

SPHERE in a nutshell

The primary science goals of SPHERE are imaging, low-resolution spectroscopic, and polarimetric characterization of exoplanets. The instrument design is driven to provide highest image quality and contrast performance in a narrow field around bright targets observed in the visible or near infrared. SPHERE is installed at one of the UT3 Nasmyth foci of the VLT and consists of four subsystems:

CPI: The common path and infrastructure receives direct light from the telescope, and provides highly stabilized, AO-corrected, and coronagraphic beams to the three sub-instruments, described below.

IFS: The integral field spectrograph provides a data cube of 38 monochromatic images either at spectral resolution of R~50 between 0.95 - 1.35µm (Y-J) or at R~30 between 0.95 - 1.65µm (Y-H).

IRDIS: The infrared dual-band imager and spectrograph provides classical imaging (CI), dual-band imaging (DBI), dual-polarization imaging (DPI), and long slit spectroscopy (LSS) either between 0.95 – 2.32µm, with resolving power of R~50 (LRS with 0".12 wide slit) or between 0.95 - 1.65µm with R~350 (MRS with 0".09 wide slit).

ZIMPOL: the Zurich imaging polarimeter provides near diffraction limited classical imaging and dual-polarization imaging (DPI) below 30 mas resolution in the visible.

Dichroic splitters allow simultaneous observations with IRDIS and IFS (IRDIFS modes).

Table 1: IFS

Observing mode	Integral field spectroscopy	
Spectral range	0.95–1.35 µm: R~50	0.95 – 1.65 µm: R~30
Sampling	(12.25 mas)^2 / spaxel (hexagonal grid), Nyquist at 0.95 µm. Resampled by the pipeline on a square with (7.4 mas)^2 / pixel.	
FOV	~ 1.73" x 1.73"	
Detector type	Hawaii II RG 2048x2048	

Coronagraph	None, or with classical or apodized pupil Lyot coronagraphs.
Stabilization	Pupil- or Field-stabilized
WFS	Visible light

Table 2: IRDIS

Observing modes	DBI, DPI, CI	LSS
Spectral range	0.95 – 2.32 μm: NB and BB filters	0.95 - 2.32 μm: R~50 0.95 - 1.65 μm: R~350
Sampling	$(12.25 \text{ mas})^2$ / pixel, Nyquist-sampled at 0.95 μm	
FOV	11" x 11"	11" slit
Detector type	Hawaii II RG 2048 x 1024	
Coronagraph	None, or with classical or apodized pupil Lyot coronagraphs.	Central blocking
Stabilization	Pupil- or Field-stabilized	Field stabilized
WFS	Visible light	

Table 3: ZIMPOL

Observing modes	Imaging (I), differential polarimetric imaging (P1, P2)
Spectral range	500 – 900 nm in broad and narrowband filters
Sampling	$(7 \text{ mas})^2$ / pixel, diffraction-limited at λ >600 nm
FOV	3.5" x 3.5"
Detectors type	Two 4k × 2k pixel, back-illuminated, frame transfer CCD 220 (e2v CCD 44-82 bi) with 15μm × 15μm pixels, equipped with a stripe mask and a micro-lens array.q
Linear polarization	Instrumental polarization <1%, polarimetric sensitivity < 0.1% with fast modulation, simultaneously on two CCDs
Coronagraph	None, or with classical Lyot coronagraphs
Stabilization	- Imaging: pupil or field stabilized. - Polarimetry: field stabilized, or fixed derotator with stable and minimized instrumental polarization.
WFS	Visible light shared between WFS and ZIMPOL: - Dichroic for R-band observation: (100% WFS outside R band / 100% R band to ZIMPOL) - Grey beam splitter: (20% WFS / 80% ZIMPOL), with AO limit lowered by ~1.74 mag

High contrast imaging
When imaging a star one often aims at discovering companions or other faint structures around it. This requires removing the halo produced by the star. However, close to the star, there are point source structures called speckles that evolve over hour long timescales. Speckles are interference images of (atmospheric or instrumental) wavefront corrugations left uncorrected by the AO system, with a typical size of a resolution element (~λ/D). The sensitivity of an exposure is most often limited by these speckles. Subtracting them is the main goal in high contrast imaging. Speckles are a function of wavelength and change with time as optics and atmosphere change.
SPHERE combines various techniques to provide high contrast imaging, with excellent stellar PSF suppression and stability: a high density high frequency AO system that corrects turbulence and

static optical aberrations, coronagraphy, and differential imaging, in which images at different wavelengths or polarization states are observed simultaneously (Figure 2).

The AO corrects the incoming wavefront up to ~20 cycles/aperture (20 = half the number of deformable mirror actuators across the pupil), corresponding to a radius = 20 λ/D in the image plane. Within this correction radius, the coronagraph efficiently suppresses the diffraction pattern down to a much fainter residual halo, which is associated to the uncorrected wavefront errors. Further out (>20 λ/D), the AO system still corrects the PSF of off-axis sources but does not contribute to the suppression of the stellar halo. Far from the star (beyond an arcsecond), the contrast depends on the filter width, number of detector reads and integration time rather than on AO correction, so that at that location SPHERE performance behaves similar to previous instruments (e.g. NACO). Differential imaging techniques are then used to remove the residual stellar halo and/or speckles (see Section 0).

The stability of the PSF becomes critical when combining observations obtained at different times. This is important for angular differential imaging (ADI) or conventional PSF subtraction. The best PSF stability is obtained when observing in pupil-stabilized mode.

Field and pupil rotation

At the Nasmyth focus, both the pupil and the field rotate when tracking an object. The field rotation is the combination of the parallactic angle and altitude of the object. The pupil rotation is directly related to the altitude of the object being tracked. The SPHERE derotator allows stabilization of either the field or the pupil on the detector.

In *pupil-stabilized* observations the PSF variability is minimized because most of the optical elements do not move. The telescope pupil is also aligned with the Lyot stops of the instrument, which cover the M2 shadow and its spider arms. The pupil-stabilized mode provides the highest PSF stability and is recommended for coronagraphic observations and for high contrast imaging close to the star. The field rotates with the parallactic angle, enabling *angular differential imaging* (ADI, see Section 0). The center of rotation is the central star. One should then be aware of the trade-off between rotation rate and the smearing of off-axis PSF (see Exposure Time Calculator).

In *field-stabilized* mode, light from a specific location in the field of view falls on a particular location on the detector, throughout the observation. For SPHERE observations this is:

- Mandatory in long slit spectroscopy. The slit shall not rotate during the observation and is defined by the observer.
- Mandatory for ZIMPOL P2 polarimetric mode (see Table 8).
- Recommended when smearing of the image within a DIT becomes an issue (e.g. at larger separation). This may be caused by a long DIT, selected to reduce the RON, or by fast field rotation, while observing close to zenith.

Field stabilized mode also ensures that a companion image would fall on the same detector pixels (lenslets for IFS). This reduces concern due to flat-fielding; this might improve stability of photometric time series.

For completeness, we mention that instrumental polarization is best understood when the derotator is static and hence does not move.

Coronagraphy

A coronagraph suppresses the coherent light coming from on-axis unresolved source (Figure 2). In SPHERE, all coronagraphs consist of a focal plane mask, followed by a pupil stop and sometimes preceded by an entrance pupil apodizer. SPHERE houses several coronagraphs to accommodate different observational needs such as spectral range or inner working angle. Coronagraph choices and trade-offs are detailed in the Appendix.

Differential Imaging

ADI exploits the fact that the field and the pupil rotate with respect to each other. In pupil-stabilized mode, most speckles are caused by instrumental artifacts and are locked up in the pupil plane, whereas the object of interest, a companion or a disk, will rotate as the field rotates. This allows distinguishing the stellar halo from the object.

Simultaneous observation of several monochromatic images can be used to reduce the impact of speckles (Sparks and Ford, 2002). For a given observation, the location of a companion around a star is constant while the location of speckles from the star increases with wavelength and their intensity decreases. For a wide enough wavelength range this allows subtraction of the speckles. This process is known as *spectral deconvolution* (Thatte et al. 2007). This approach is used in IFS and in IRDIS LSS.

Planets and the host star have different spectral features. This information can be used to suppress speckle noise. For this, one needs simultaneous images at two similar wavelengths at which the brightness of the planet varies, e.g. in and out of a molecular band. This method is called *spectral differential imaging* (SDI). This approach is used in IRDIS DBI. It can also be used with ZIMPOL imaging when different filters are used in ZIMPOL's two arms (e.g., Hα and continuum).
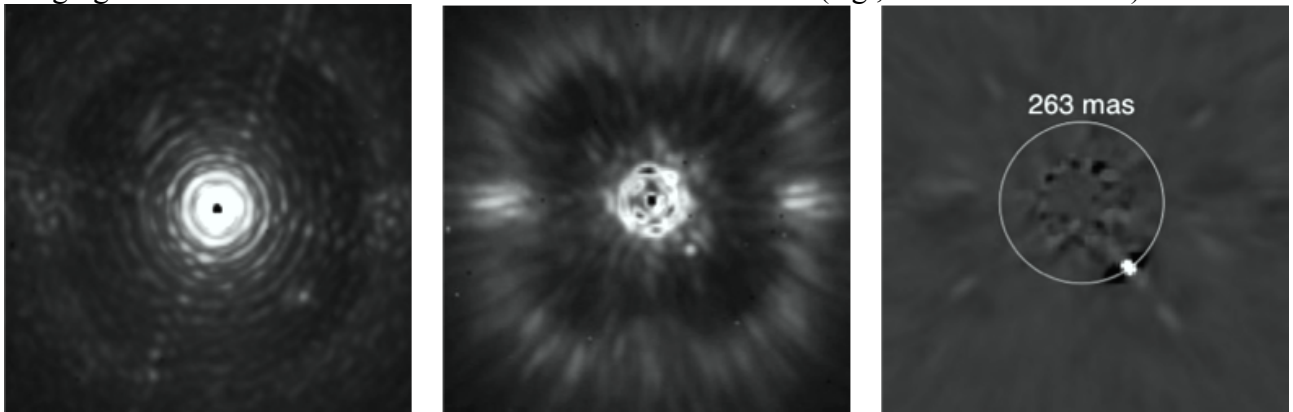
Figure 2: Illustration of the three pillars of high contrast imaging. Left: raw on-sky J-band PSF of SPHERE with IRDIS, showing the diffraction pattern resulting from the almost perfect correction provided by the extreme AO system up to 20 cycles per aperture, and so 20 λ/D in the image (this is half the number of actuators on the deformable mirror on a side). Middle: raw on-sky J-band coronagraphic image of Iota Sgr, illustrating the efficient removal of diffraction rings and pinned speckles by the coronagraph. Note the very visible AO correction radius. Outside the correction radius (r > 20 λ/D), the brighter halo results from the uncorrected wings of the seeing halo. Right: result of angular differential imaging (ADI) strategy, and post-processing using principal component analysis, cleaning the remaining speckles in the field after extreme AO and coronagraphy, revealing a faint off-axis companion.

Stars are often unpolarized, whereas circumstellar environments and planets may be highly polarized. This feature is used to increase the image contrast and is called *dual polarization imaging* (DPI). DPI is used in ZIMPOL polarimetric imaging and in IRDIS DPI.

Sparse Aperture Masking

Sparse Aperture Masking (SAM) is one of the first extended modes offered to the community. SAM is an interferometric technique for recovering high contrast structures at small angular separations. A small opaque pupil-plane mask with 1-meter circular sub-apertures (holes) turns a telescope into a Fizeau interferometer, changing the instrument PSF into an interference "snow flake" pattern.

The primary advantage of observing with SAM is the use of robust observables such as closure phase and kernel phase that are insensitive to residual wavefront errors, allowing high contrasts to be reached at angular separations where these effects typically dominate. Being an interferometric method, SAM allows measurements to be made beyond the Rayleigh diffraction limit, down to separations as small as $0.5\lambda/D$. However, by blocking the majority (~90%) of the incoming light, SAM requires brighter targets (typ. R or H < 8) and the use of longer exposure times. In addition, the field of view of SAM observations is typically limited to ~ 5-6 λ/D (250 mas at H-band) and the contrasts achieved are not comparable to those obtained at larger separations through other techniques (such as coronagraphy).

In summary, SAM is a useful "niche" technique for detecting companions and structures with moderate contrasts at or close to the diffraction limit.

From P100 and on, SAM is offered as a setup for the following modes:

- **IRDIS CI**
- **IRDIS DBI**
- **IRDIFS and IRFIS_EXT**
- **IRDIS DPI (similar to the SAMPOL mode on NACO)**
- **ZIMPOL I**

For IRDIS and IRDIFS, the 7-hole mask is introduced through the "IR coro/mask combination" (previously "IR Coronagraph"): N_SAM_7H.

For ZIMPOL, the 7-hole mask is introduced through the "IR coro/mask combination" (previously "Visible Coronagraph"): V_SAM_7H.

SAM always make use of pupil tracking in order to keep the pupil (and telescope spiders) fixed with respect to the sparse sub-apertures as shown on Figure 3 for each given instrument.
The corresponding masks are located in the respective Lyot wheels.

The derotator angle is the same as for imaging and coronagraphy in pupil tracking and for this reason, SAM shares the same astrometric calibration (true north and plate scale). The POSANG keyword in P2PP does not have any effect when the tracking law is "PUPIL".

For SAM, the same set of calibration files will be provided (flats, darks, backgrounds, etc.). The basic reduction can be performed by the ESO pipeline but the interferometric analysis is left to the users.

DESIGN   IRDIS   IFS   ZIMPOL

H3   YJ   N_R
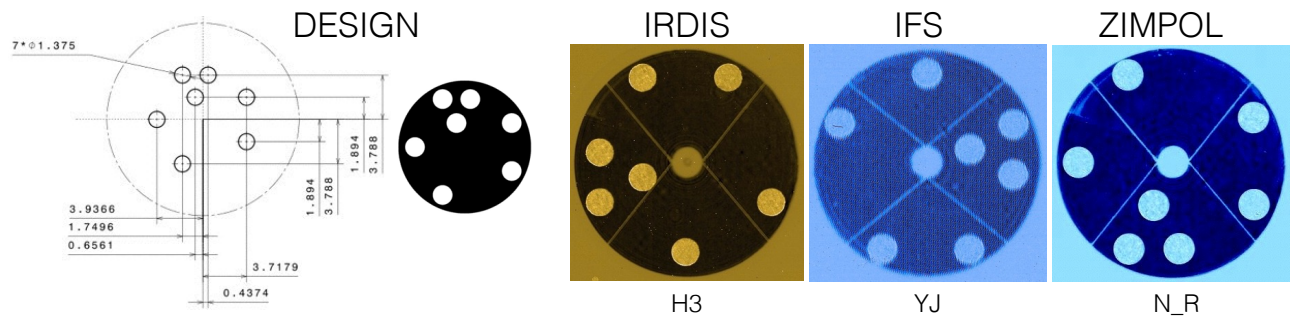
Figure 3: Layout of the SPHERE 7-hole aperture mask design projected on the 8m primary mirror. Each pair of holes (baseline) produces a set of interference fringes. The three images on the right are how the holes are located with respect to the full pupil of the telescope as seen by the 3 instruments. In the case of IRDIS, the mask has been mounted with a 90º offset and one of the holes is tangent with the telescope spider.

Science case examples

Besides imaging of exoplanets and companions around stars, there are other science opportunities opened by SPHERE.

1) The close environment around bright stars

Good/median AO performance is obtained for stars up to R = 11 mag (~9.3 for ZIMPOL with the BS_GREY) . For stars with R > 11 mag, users should apply for observations in visitor mode. For fainter stars performance is likely to degrade (see Section 0 and Section 0). With AO, diffraction limited resolution is obtained for IFS within 1.73''x1.73", for ZIMPOL up to 3.5''x3.5", and IRDIS in an 11''x11" FOV, respectively.

2) Circumstellar emission much fainter than the stellar halo

The suppression of the stellar PSF is for SPHERE much improved compared to previous instruments (e.g., NACO). This is in particular true at small separation angles from the star between 1 and 20 λ/D. Beside the high image quality and PSF stability of the instrument, there are dedicated data reduction techniques based on differential imaging to enhance the contrast of circumstellar emission further (ADI, PDI, SDI).

3) High angular resolution observations will support studies of stellar ejecta, binaries at small separations, stellar proper motions, solar system objects, etc.

Mode offering from P98
Table 4: Modes offered.

Observing Mode	Comment	Service/Visitor
IRDIFS	- Pupil-stabilized (default) or Field stabilized - Coronagraph: N_ALC_YJH_S - SAM: N_SAM_7H	S+V
	- Other coronagraphs	V
IRDIFS_EXT	- Pupil-stabilized (default) or Field stabilized - Coronagraph: N_ALC_YJH_S - SAM: N_SAM_7H	S+V
	- Other coronagraphs	V
IRDIS_DBI	- Pupil-stabilized (default) or Field stabilized - Coronagraph: N_ALC_YJH_S, N_ALC_Ks with K-band filters - SAM: N_SAM_7H	S+V
	- Other coronagraphs	V
IRDIS_CI	- Pupil-stabilized (default) or Field stabilized - Coronagraph: N_ALC_YJH_S, N_ALC_Ks with K-band filters - SAM: N_SAM_7H	S+V
	- Other coronagraphs	V
IRDIS_DPI	- Field stabilized (default) - Coronagraph: N_ALC_YJ_S, N_ALC_YJH_S, N_ALC_Ks - Filters: broad band filters BB_J	S+V
	- Pupil Stabilized - Coronagraph: N_ALC_YJ_S, N_ALC_YJH_S, N_ALC_Ks - Filters: broad band filters BB_Y, BB_H, BB_Ks - SAM: N_SAM_7H (Pupil Stabilized)	V
IRDIS_LSS	Long Slit Spectroscopy in LRS and MRS	V[*]
ZIMPOL_P1/P2	- Derotator: P1 (static) or P2 (Field-Stabilized) - Filters: combination of NB and BB filters not allowed - WFS/ZIMPOL splitter: GREY or DIC-HA - No coronagraph (allowing some saturation) or V_CLC_M_WF - Some saturation allowed - Detector/modulator: FastPol, SlowPol - Field-Position: on-axis	S+V
	- Other coronagraphs - NB and BB filter combination	V
ZIMPOL_I	- Same as P1/P2 but with readout mode StdImaging. - Pupil-stabilized - SAM: V_SAM_7H (Pupil Stabilized)	S+V
	- Other coronagraphs - NB and BB filter combination	V

---

[*] In general, observations using the LSS should be requested in Visitor Mode. However, if very good conditions are critical for the observations, this mode can now also be requested in Service Mode. A clear justification regarding the need for Service Mode should be provided and will be assessed as part of the technical feasibility review: if very good conditions are not required, the programme will be reassigned to Visitor Mode. Observations using the IRDIS_LSS mode in Service Mode should be requested in a separate run from possible other observations.

2. TECHNICAL DESCRIPTION

The SPHERE subsystems CPI, IFS, IRDIS and ZIMPOL are described below.
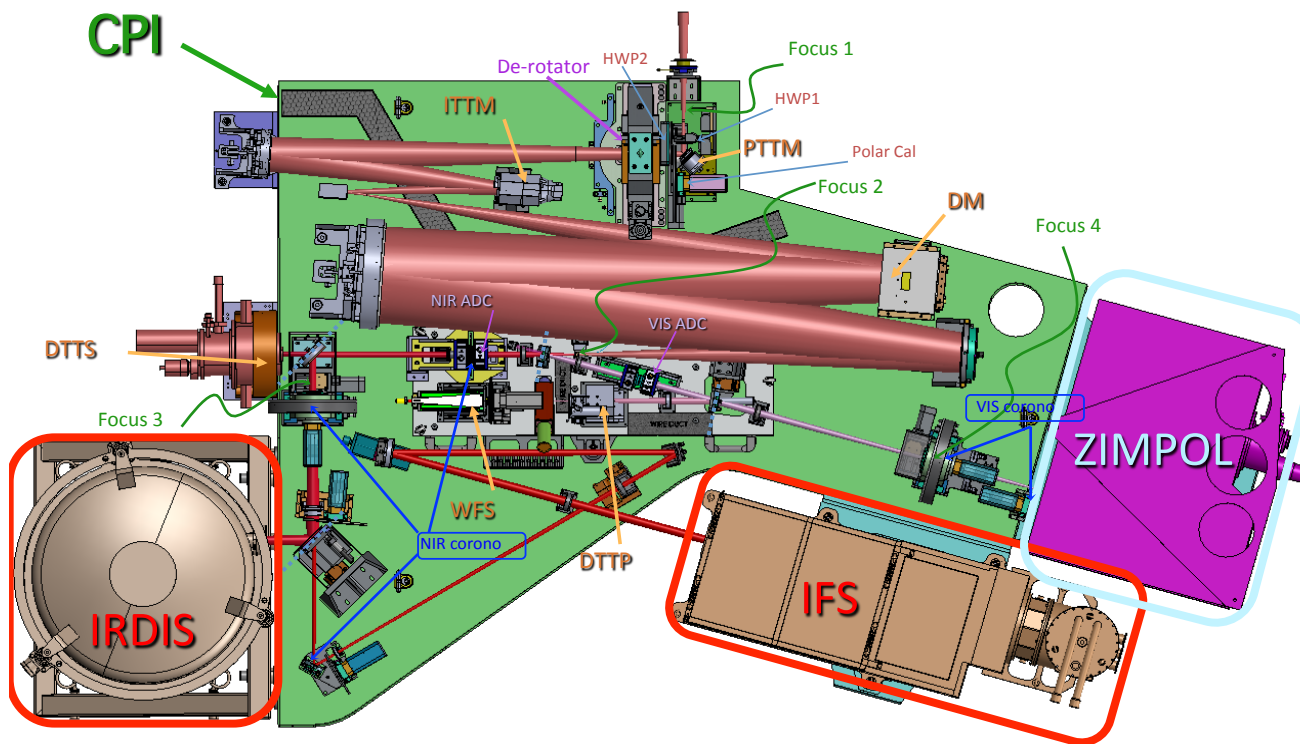
Figure 4: CPI, the common path optical beam on the main optical bench (green) feeding the 3 other sub-systems ZIMPOL (magenta), IRDIS (gray) and IFS (brown).

CPI

CPI includes the main optical bench, connects the other sub-systems to the light path, and guarantees a static alignment of SPHERE to the VLT focus (Figure 4). It feeds the cryostats and motors with power, includes servo-controlled pods, damping vibrations on the Nasmyth platform. An enclosure protects the SPHERE optics from dust and reduces temperature gradients. From the entrance focal plane up to the second focus (FP2; Focus 2) a reflective design propagates the complete spectral range from 450 to 2320 nm through the instrument. It includes the beam derotator, active optics, with pupil and image tilt mirrors, and the high order deformable mirror DM, which is the heart of the system providing a stable AO-corrected image.

CPI also includes visible and infrared half-wave plates for polarization switching/modulation. After FP2, light is split between visible and NIR. The NIR beam path includes refractive optics: the NIR ADC, coronagraphic components, neutral densities filters and an exchangeable splitter between IRDIS and IFS.

In the optical, atmospheric dispersion correction is applied by the VIS ADC, and then the beam is split between ZIMPOL and AO (WFS). If Zimpol is not used, all the light goes to the WFS. If Zimpol is used, one can chose between the grey beam splitter (sending 80% of the light to Zimpol and the remaining 20% to the WFS) and a dichroic beam splitter (DIC_HA) sending the spectral range around the R band to Zimpol and the rest to the WFS. Before ZIMPOL, the beam goes through a coronagraphic focal plane (FP4; Focus 4) and a pupil plane hosting the corresponding Lyot stops.

The adaptive optics module is called SAXO. It is designed to correct for the turbulence perturbation at high frequency (1.2 kHz). The turbulence is measured by a 40x40 lenslet Shack-Hartmann sensor that is equipped with a red-sensitive sub-electron noise EMCCD. It servo controls the pupil

position, and fine-tunes the centering on the coronagraph by means of a dedicated differential tip-tilt sensor (DTTS).

The coronagraphs are set-up by a mask in the focal plane (FP3 for NIR and FP4 for the visible), a Lyot stop in the downstream pupil, and an apodizer in the upstream pupil (before the focal mask). The wheels for the coronagraphs include also field stops and the IRDIS long slit masks. Several set-up combinations are defined for a range of observing conditions and science cases (seeing, inner working angle, wavelength, etc.); they are listed in the Appendix.

IFS

The SPHERE integral field spectrograph (IFS) is a lenslet-based integral field unit (called BIGRE, Antichi et al. 2009), providing a 1.73" x 1.73" FOV that is Nyquist sampled at 0.95 µm (Table 1). The IFS includes a flat calibration source and filters for accurate detector calibrations. The IFS instrument layout is displayed in Figure 4. The raw data 21000 spectra are aligned with the detector columns over a hexagonal grid rotated by ~10.7° with respect to the dispersion. Each spectrum from a spaxel is projected on a rectangular area of 5.1x41 pixels on the detector.

During data reduction, the image is translated into a (x,y,λ) data cube, which has for both available spectral resolutions a constant dimension of (291,291,38). Each image is resampled by the pipeline over a square regular grid at $(7.4 \text{ mas})^2$ / spaxel. Data outside this region are meaningless (see Figure 6).
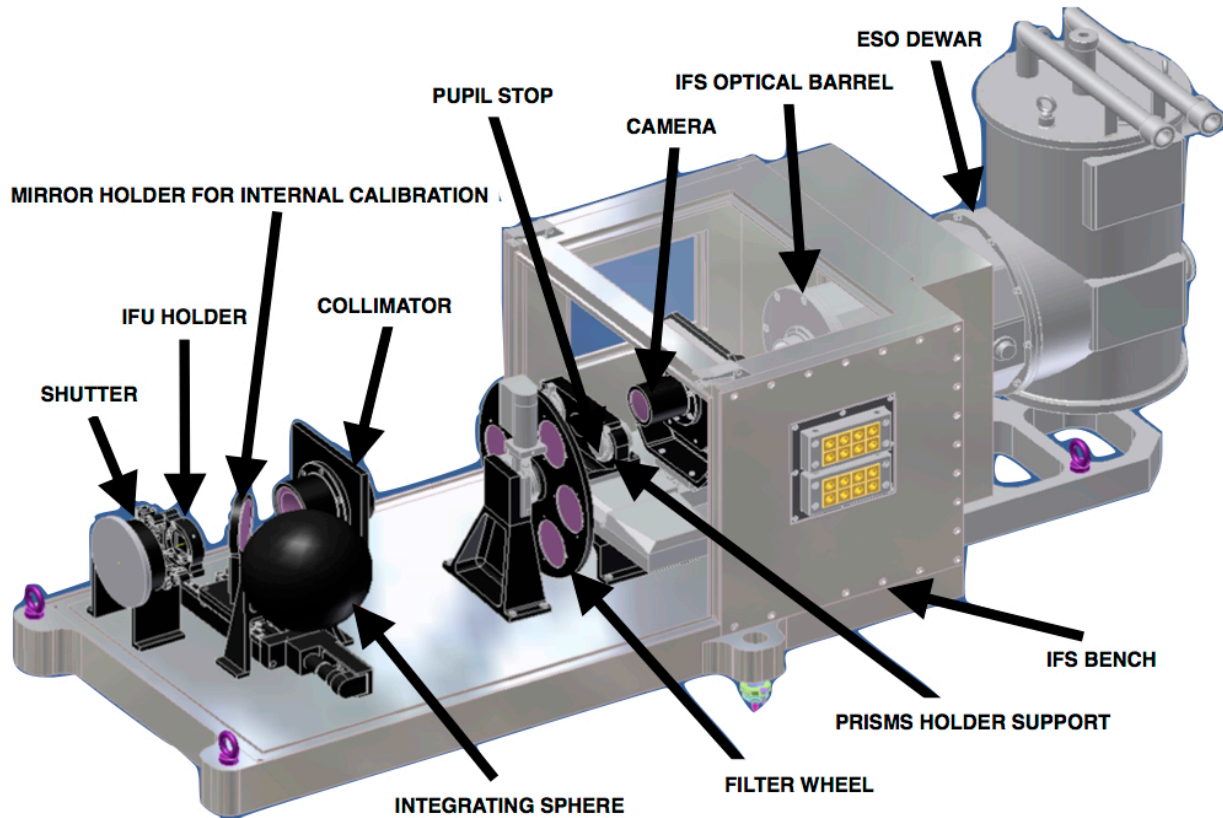
Figure 5: Inside the IFS. Note that the IFS optical bench is not cold, and that it has its own Lyot stop and internal calibration sources.
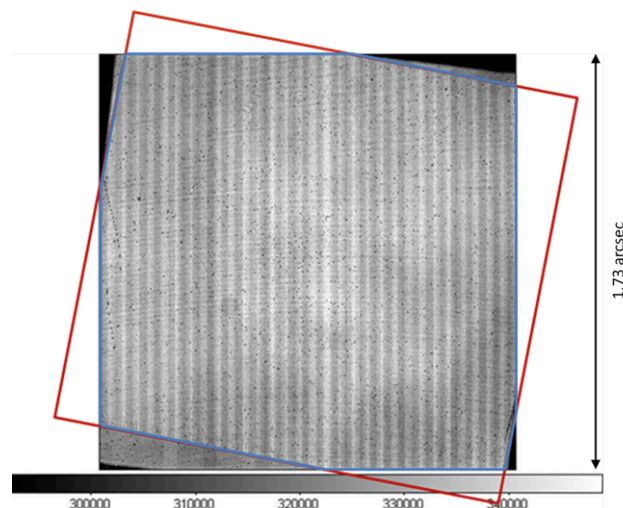
Figure 6: IFS flat-field and projection of the sky on the BIGRE detector (red) and ~1.73" x 1.73" FOV (blue).

IRDIS

The FOV is 11"x12.5" and the pixel scale is 12.25mas matching Nyquist sampling at 0.95 μm. Two parallel beams are projected onto the same 2kx2k detector and each occupies about half of the array. The IRDIS instrument layout is displayed in Figure 6. DBI provides images in two neighbouring filters, simultaneously. Various filter pairs are available for different spectral features. DPI uses crossed polarizers providing images in the two polarization directions at the same time. For LSS, the coronagraph mask is replaced by a coronagraphic slit.

Three wheels are provided within the cryogenic environment:

a. **The Lyot stop wheel, with Lyot stops for the coronagraphs of the CPI, LRS prism, and MRS grism.**
b. **The common filter wheel, with blocking filters, broadband and narrowband filters.**
c. **The dual filter wheel, with DBI and DPI filter pairs, polarizers, and a pupil-imaging lens.**

The complete list of available filters is summarized in the Appendix. Dual imaging separation is done using a beam-splitter combined with a mirror, producing two parallel beams. IRDIS achieves less than 10 nm differential aberrations between the two channels and, as a consequence, allows high contrast differential imaging.
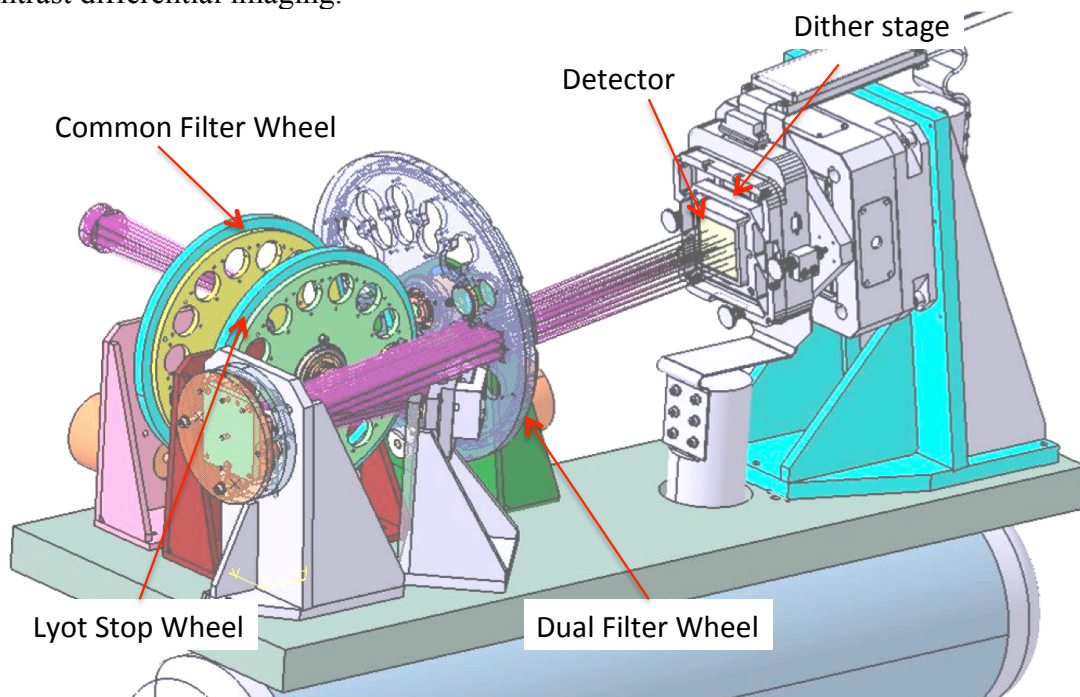
Figure 7: Inside view of the IRDIS cryostat. The CPI beam comes from the left, goes through the common filter and Lyot stop wheels, is split in two, then goes through the dual filter wheel before landing on the infrared detector.

The IRDIS detector is mounted on a detector motion stage (DMS). The DMS enables detector dithering in XY-directions at sub-micron accuracy. Detector dithering is available mainly to improve the flat-field accuracy and to handle cosmetic defects. The recommended pattern is 4x4 pixels (but can be extended up to 10x10).

ZIMPOL
ZIMPOL is designed as high contrast imaging polarimeter with very high polarimetric sensitivity for the visual range. It also provides at the same time imaging capabilities. Another VLT instrument, FORS2, provides a polarimetric mode for the visual range which is however complementary to ZIMPOL. FORS2 is a seeing limited Cassegrain imaging and spectrograph polarimeter for accurate absolute polarization measurements (0.1% in the field center). FORS2 has a very high throughput and is therefore suited for faint objects. ZIMPOL is a diffraction limited imaging polarimeter with a very small field of view centered on a bright target. Because ZIMPOL is a Nasmyth instrument, it provides only a limited absolute polarimetric accuracy (~0.5%). The basic observing strategy for ZIMPOL is a relative polarization measurement of the immediate

surroundings of a central star, which is used as a (zero)-polarization reference for the correction of the instrument polarization.

Atmospheric seeing variations are a key problem when aiming to achieve high image quality. Differential measurements such as DPI with fast (kHz) polarization modulation can solve this problem. DPI is performed quasi-simultaneously by fast modulation revealing, e.g. faint structures around a bright point source.

The ZIMPOL instrument layout is displayed in Figure 8 and its main capabilities are summarized in Table 3. ZIMPOL includes a new concept for imaging polarimetry, which is based on fast polarimetric modulation and on-chip de-modulation by two CCDs (Figure 8). Thanks to a polarimetric beam-splitter, one polarization is sent to CCD1 and the other perpendicular polarization to CCD2. Further, the polarization modulation is synchronized with an innovative reading scheme of the detectors.

By this technique, the polarization of the incoming light is converted by a polarization modulator and the following polarization beam splitter into an intensity modulation with an amplitude proportional to the polarization signal. The de-modulating CCD has every second row covered by a stripe mask and these covered rows can be used as a buffer storage area. With charge shifting on this masked CCD each "open" pixel can measure the intensity of the two alternating states. Photo-charges created during one half of the modulation cycle are shifted for the second half of the cycle to the next masked row and again back for the subsequent illumination during the next first half of the modulation cycle. In this way two frames are build up in alternating pixel rows, corresponding to opposite polarization states. After many modulations the CCDs can be readout and the raw polarization signal is then the difference between "even" and "odd" rows.

A single arm of ZIMPOL provides a full polarimetric measurement. Because a polarizing beamsplitter is used for the polarization analysis, half of the light goes to the other arm, which can perform polarimetry for the same or another filter.
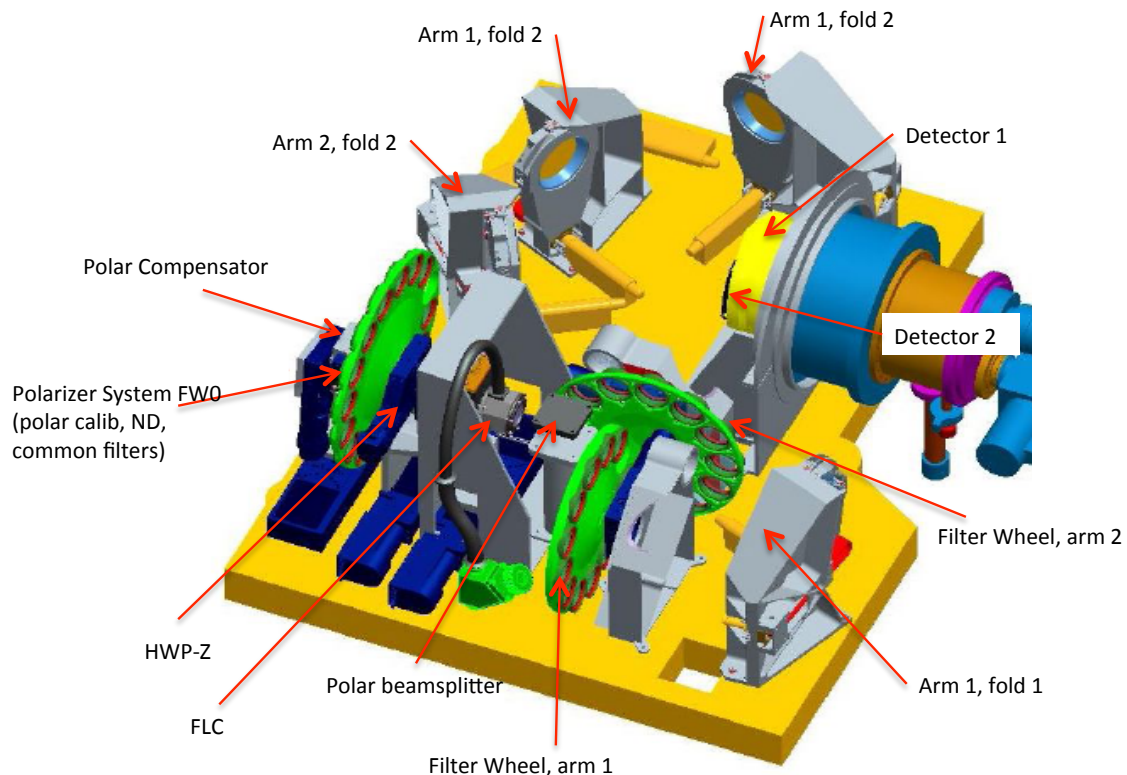
Figure 8: ZIMPOL schematic view showing the main elements of this visible polarimeter, from polarization compensator, common filter wheel, Ferroelectric Liquid Crystal (FLC) modulator to the splitter, filter wheels 1 and 2, and the two detectors.

Advantages of differential polarimetric technique are:

a. **Both images are created *quasi-simultaneously* (the modulation is faster than the seeing variations), and both images are recorded with the *same pixels* reducing significantly flat-fielding issues.**
b. **Differential effects due to the storage of two images in different buffer pixels are compensated with *a demodulation phase-switch* between subsequent images.**
c. **There are only very small *differential aberrations* between the two images with opposite polarization.**
d. **The differential signal does not suffer from *chromatic effects* due to diffraction or speckle chromatism.**

The efficiency of the modulation – demodulation process depends on the modulation frequency. The instrument offers a fast modulation mode with a frequency of about 1 kHz and a polarization efficiency of 80% and a slow modulation mode with a frequency of about 30 Hz and an efficiency of 90%. A simple calibration is foreseen to correct for the polarization efficiency taking into account a slight wavelength dependence and possible small temporal variations in the polarization measurement.
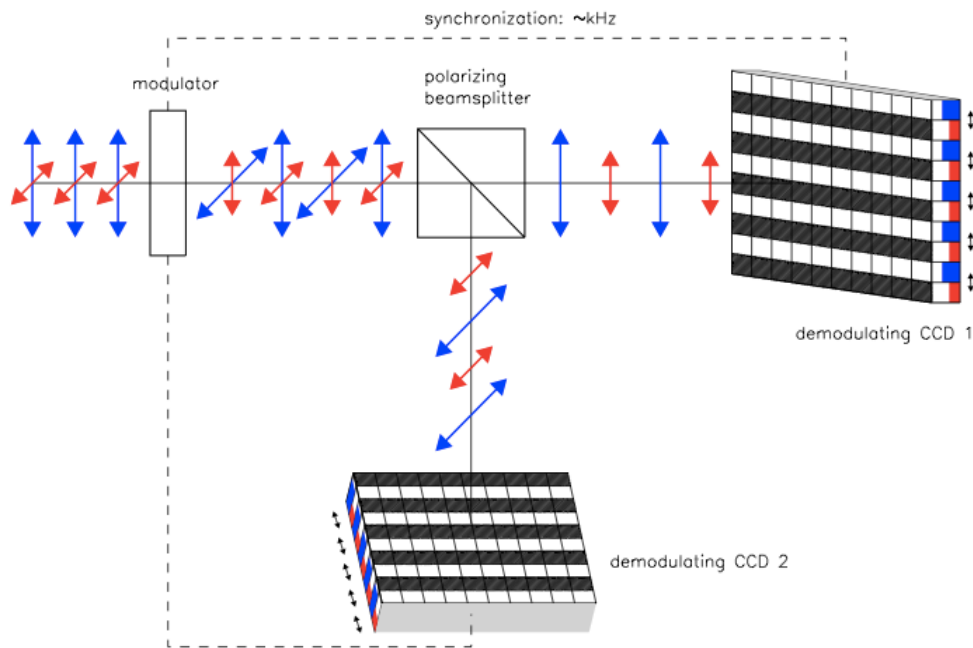
Figure 9: In ZIMPOL the polarized signal is modulated on CCD1 and CCD2. The detectors are read after a charge shifting sequence that is synchronized to the polarization swap.

2.1.1 Hardware

The ZIMPOL sub-system receives the beam from CPI after the visible coronagraph pupil Lyot stop plane. The instrument offers an extended list of broadband (BB) and narrowband (NB) filters that are described in the Appendix. The first filter wheel (FW0) is common to both arms and includes both filters and polarimetric components used to calibrate the intrinsic polarization of ZIMPOL. As a consequence, the filters located in this wheel cannot be calibrated polarimetrically and can therefore be used only for imaging observing mode and not for polarimetric imaging.

Depending on the observing mode, a polarization compensator that can be controlled in orientation and in amplitude, and internal Half-Wave Plates (HWP) are set within the observing template. A Ferro-electric Liquid Cristal polarization modulator (FLC) is inserted in the beam for polarimetric imaging to modulate the polarization direction as selected by the polarization beam-splitter. This splitter then feeds two optical beams of ZIMPOL. Each beam goes through filter wheels FW1 and FW2, the tip-tilt mirror that allows offsetting the FOV, and finally arrives on the detector. Both CCDs are located side by side in the same cryostat. The two filter wheels enable polarimetric observations in two bands. The common filter wheel FW0 contains polarimetric calibration components and additional filters for imaging.

2.1.2 Instrumental polarization

SPHERE includes many optical components that impact the instrumental polarisation. The optical path through the CPI and ZIMPOL is schematized in Figure 10. The polarization signal is measured by ZIMPOL at the position of the modulator and the beam-splitter. The linear polarization intensity is recorded either parallel I_0 or perpendicular I_{90} to the optical bench. Other polarization position angles can be selected by synchronously rotating half-wave plate HWP2 (mounted at the entrance of the CPI) and half-wave plate HWPZ (inside ZIMPOL).

The instrumental polarization is minimized by design. HWP1 and M4 (SPHERE fold mirror) enable reduction of the telescope polarization induced by M3. There is also a tilted, rotatable compensator plate to reduce the instrumental polarization introduced by the derotator.

For a given observation, both orthogonal polarization states are exchanged applying a frequent 45° rotation of HWP2. Thank to this design the introduced instrumental polarization is < 1%. In many science cases, the central bright star can be used as zero-polarization reference allowing for a very

accurate correction of the instrument polarization for measurements of circumstellar sources. Cross-talk effects affect the measured fractional polarization signal p (or Q/I and U/I) by $\Delta p/p < 0.05$ providing very good polarization properties for a Nasmyth instrument.

A model of the instrumental polarization of ZIMPOL is currently built for cases where the central star cannot be used as polarization reference and other demanding applications. This should allow even a better correction for the instrumental polarization effects in the data reduction.

2.1.3 Detectors

Schmid et al. (2012) describe the observing method of ZIMPOL, in which a large number of charge states are accumulated and shifted across different detector pixels. The handling of the detector properties and calibration is of particular importance. A *2-phase demodulation scheme is used:* Electrons accumulated on the detector are shifted many times up and down and from one pixel to the next, before the exposure is finally read. Therefore, asymmetries in the charge transfer efficiency in a fraction (<1%) of detector pixels (charge traps) affect the resulting data. A phase switch between two subsequent DITs calibrates this out for the differential polarization signal I_0-I_{90}. Therefore, all science exposures and calibration frames for ZIMPOL polarimetric observations are taken with an even number of DITs.

It is important to note that the charge traps remain in the intensity frame I_0+I_{90} of polarimetric observations. Their strength is proportional to the number of polarization cycles and affects a substantial fraction (> 0.1%) of pixels for longer integrations (> 10 s) in fast polarimetry or (>300 s) in slow polarimetry. The impact of this special feature of the ZIMPOL polarimetric mode can be strongly reduced by an appropriate observing strategy, e.g. with dithering, selecting slow polarimetry instead of fast polarimetry mode, or by taking separate frames in ZIMPOL imaging mode where this effect is not present.

Detector bias: The detector readout process includes additional readouts of pre- and over-scan pixels. This ensures a better bias subtraction for all frames. These additional readouts are visible in the raw data and appear at the border and in the middle of the array. In the standard data reduction cascade, average bias values for the overscan pixels are evaluated and subtracted for the two different readout areas of the ZIMPOL detectors. This provides a very good bias correction for imaging and slow polarimetry mode. For fast polarimetry mode two columns originating from the readout process are present which are not corrected by the overscan pixel bias subtraction method. This fixed pattern noise can be removed in a classical way by the subtraction bias frames.

Frame transfer smearing: The ZIMPOL data are taken with frame transfer CCDs. They can simultaneously take images with one half of the detector and readout the other half of the detector where the frame from the previous exposure is stored. At the end of an exposure which must last longer than the readout process (about 1.2s for fast polarimetry and imaging and 10s for slow polarimetry) the newly created frame in the image area is transferred rapidly to the readout area and a new illumination begins.

The detector illumination during the frame transfer introduces a smearing of the image in the direction of the detector columns. The smearing is proportional to the ratio of the frame transfer time, which is constant, and the DIT. For example, a 6s exposure of a point source with 100 000 counts (integrated over 5x5 pixels) and a frame transfer of about 60 ms, will produce a trace parallel to the column directions (~1000 pixels) where the illumination is enhanced by about 1 count.

The smearing effect is thus only important for short DITs in particular for non-coronagraphic, high contrast observations of saturated sources.
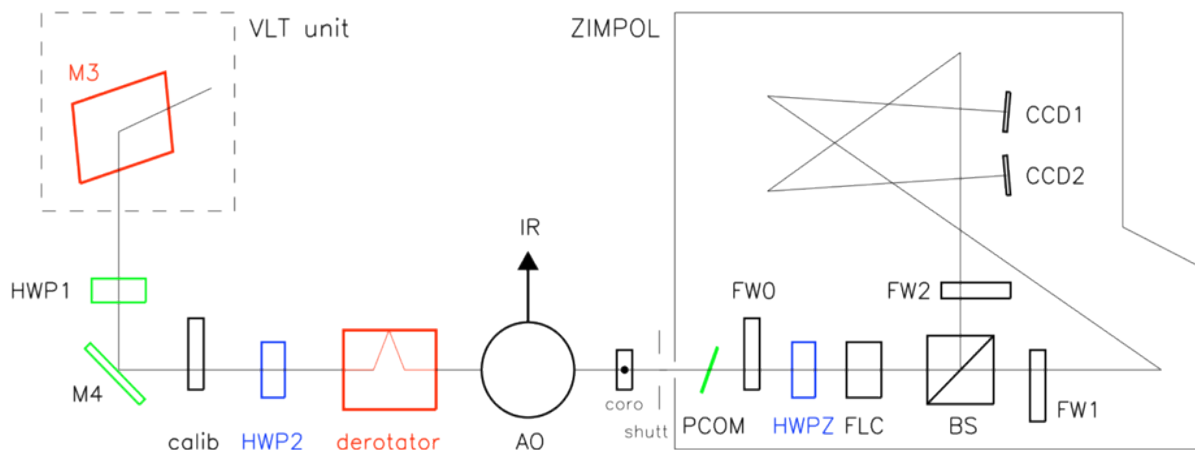
Figure 10: ZIMPOL optical path. Components, which introduce (red) or compensate (green) instrumental polarization, and those, which rotate the Stokes vector into the derotator system (blue), or instrument system (black) are indicated.

2.1.4 Imaging
The ZIMPOL imaging mode provides a higher image quality and is about 10% more efficient than polarimetric observing modes. Moreover, it does not suffer from the charge trap problem created by the charge shifting used for polarimetry.

2.1.5 Field of view
The ZIMPOL instantaneous FoV is 3.5 x 3.5 arcsec^2. This FoV is roughly centered on the coronagraph position and is identical for both CCDs. On both ZIMPOL optical arms, tip-tilt mirrors can be used to offset the field by small amplitudes. This enables dithering so that light falls onto different pixels. This scheme is commonly used to reduce the impact of bad pixels. The ability to use tip-tilt mirrors for mosaicking up to a radius of 4'' is not yet validated and not thus offered.

Instrument combinations
Dichroics allow IFS and IRDIS to take data in parallel. One dichroic setting (used in the IRDIFS_EXT mode) allows IFS observations in the Y-H range, and IRDIS observations in K at somewhat reduced performance (particularly coronagraphic).
Another setting (used in the IRDIFS mode) allows IFS observations in Y-J range, and IRDIS observations in the H band with optimum performance.
For IRDIS-alone observations, a mirror is used ensuring optimal K band performance and access to the complete 0.95 – 2.32µm spectral range.
ZIMPOL can only be used alone.

3. ADAPTIVE OPTICS PERFORMANCE

The performances given in this section are conservative, and still being consolidated (throughout the first year of operations). The following is thus a snapshot of the current performance level as measured during the acceptance tests in Europe, the integration in Paranal, and four commissioning runs on sky (between May and October 2014).

SAXO preliminary representative performance

The SPHERE Adaptive Optics module SAXO has been verified to perform nominally, and providing H-band Strehl ratio in excess of 90% for median seeing conditions (0.8"-1.2") and bright NGS (R < 9 mag). See Figure 11 and Figure 12 for details.

The AO is not limited by the NGS flux up to R~9. In between R=9 and 11, the correction remains very good but the lack of photons induces residuals that translates into a brighter residual halo in coronagraphic images. For fainter objects, AO correction can still be applied but at a slower rate, with degraded image quality.

Since P100 targets with R>11 are allowed in Service Mode. Since they require the best possible conditions, users should request them with a seeing constraint <= 1.0". For R> 11, H>9 targets, coronagraphs should be avoided as SPHERE might be operated without precise drift control on the focal-plane mask (DTTS-free mode).
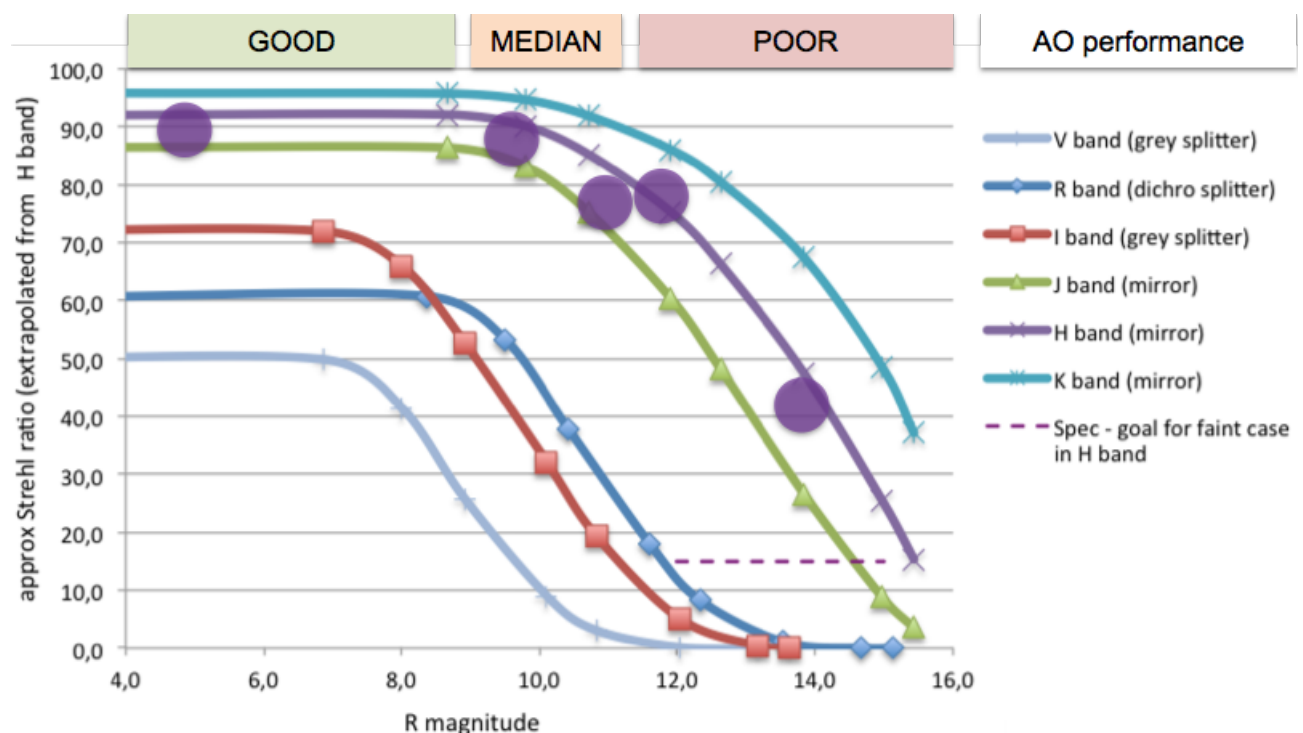
Figure 11: Theoretical and measured (purple circles) SPHERE-SAXO Strehl ratio as a function of R magnitude for good seeing conditions and different wavelength ranges from V to K (see Table 9 and Table 10 for details).

Fusco et al. 2016 (SPIE 9909) provides more on-sky performance measurements (Strehl ratio) which confirm the plot in Figure 11.
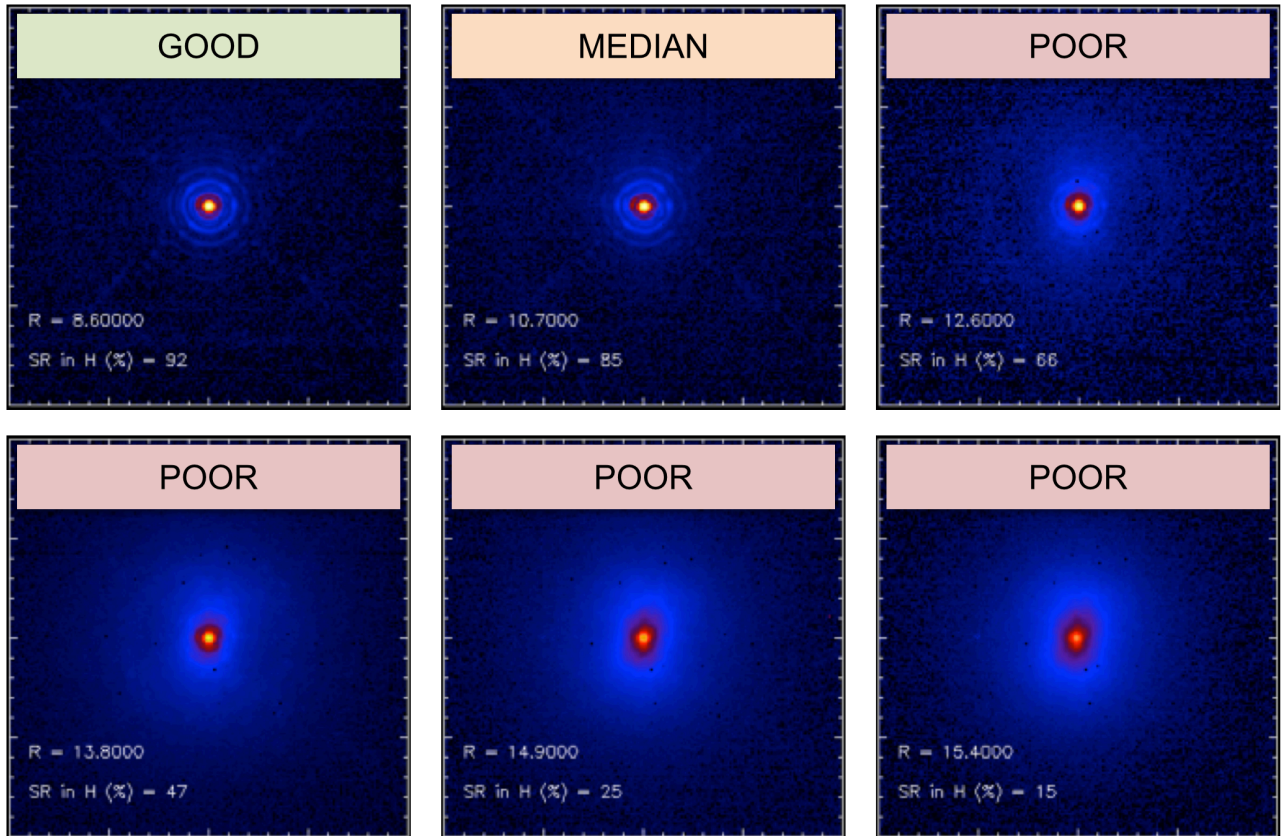
Figure 12: SPHERE PSF morphology and Strehl ratio as a function of R magnitude (see Table 9 and Table 10 for details).

IRDIS preliminary representative performance

3.1.1 IRDIS DBI

The 1σ-contrast achieved in coronagraphic imaging (IRDIFS_DBI) with filter combination DB_H23 (Figure 13) is shown as a function of angular separation (contrast curves) in Figure 14 for various differential imaging strategy combinations (SDI alone, or combined with ADI).
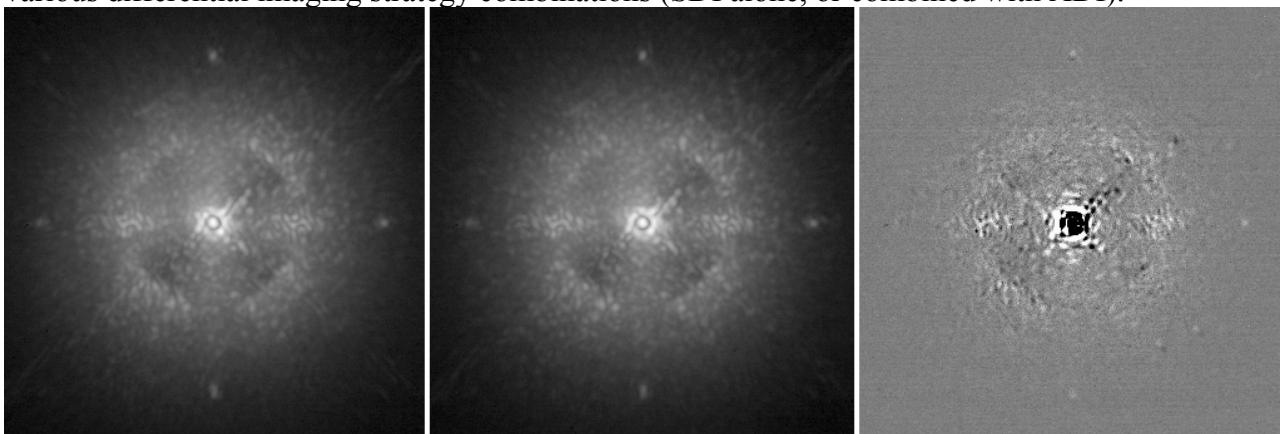
Figure 13: Coronagraphic images obtained in IRDIS H2 (left) and H3 (center) DBI filters, and the result of spectral differential imaging H2-H3 (right).
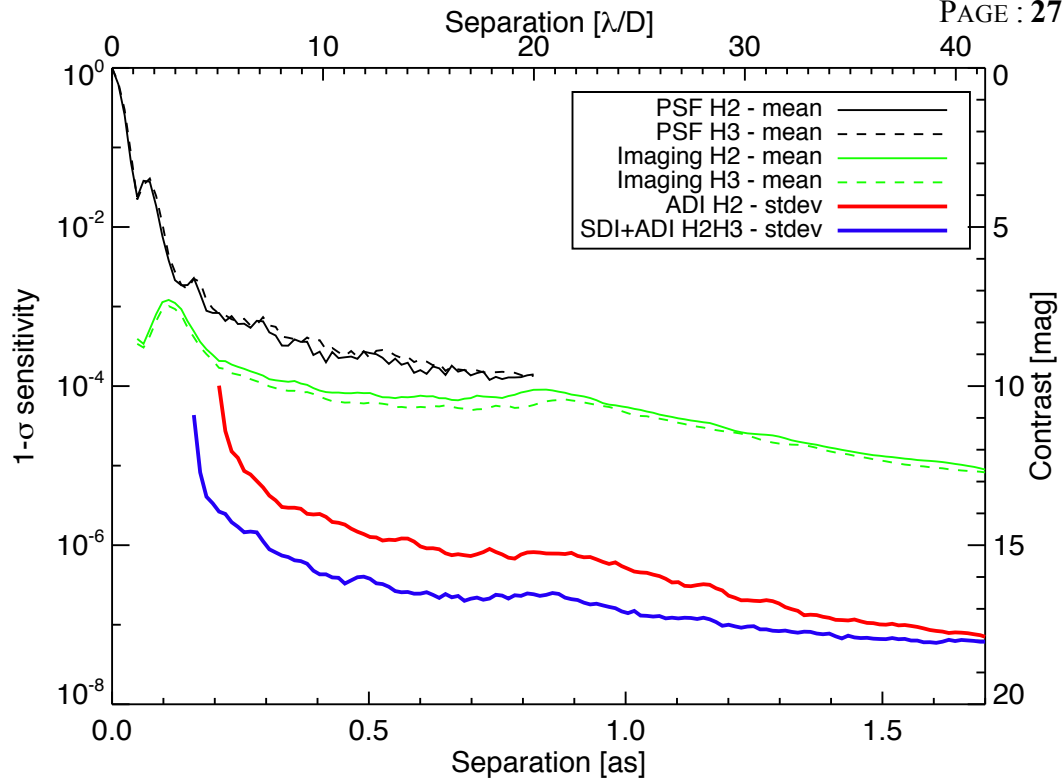
Figure 14: IRDIS DBI H2H3 contrast curves obtained on-sky for a bright target (H=0.2), in average conditions (seeing ~1.0"), with an ADI field rotation of 30 degrees. The plot shows the PSF profiles (black) and coronagraphic profiles (green) in the H2 and H3 filters, the 1σ contrast curve for ADI on the H2 data (red), and the 1σ contrast curve for SDI+ADI on the H2 and H3 data. For the ADI and SDI+ADI analysis, the algorithm throughput is taken into account and compensated, assuming a T8 spectral-type for the planet in SDI.

3.1.2 IRDIS LSS

Representative raw, and processed spectra, and contrast performance for the LSS mode of IRDIS are shown in Figure 15 and Figure 16.
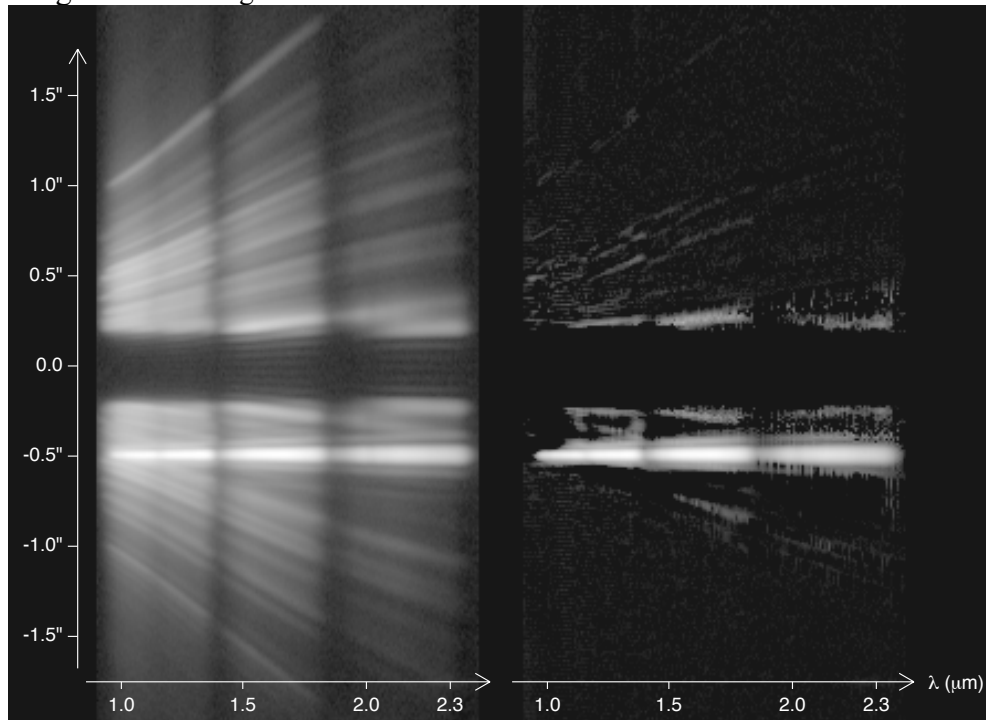
Figure 15: IRDIS LRS data obtained on PZ Tel (H=6.5). The left image is the spectrum after preprocessing and cleaning using the data reduction and handling pipeline (DRH). It corresponds to a 20 minutes exposure (DITxNDITxNEXP=20x10x6) in good conditions (seeing of 0.5"-0.6"). The spectrum of the companion PZ Tel B is visible as a straight line amidst the speckles at an angular separation of ~0.5". The obscured part between ±0.2" corresponds to the position of the opaque coronagraphic mask. The contrast of the companion is ~5.4 mag in H-band (Biller et al. 2010, ApJ, 720, 82). The right image is the data after stellar halo and speckles subtraction using the spectral difference approach described in Vigan et al. 2008 (A&A, 489, 1345). The spectra are displayed with the same logarithmic color scale.
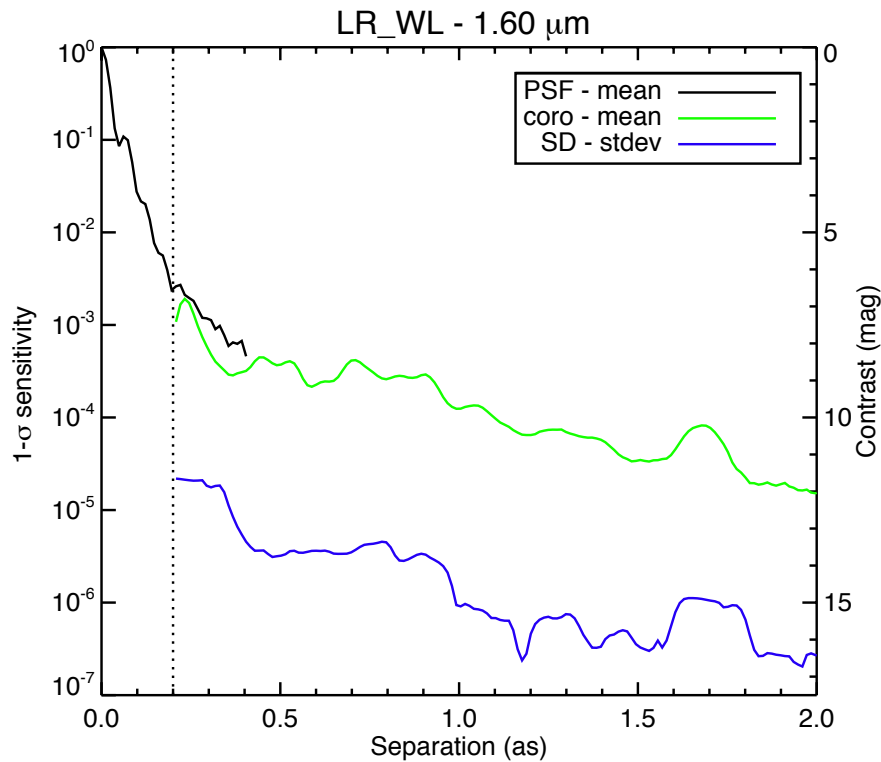
Figure 16: IRDIS LRS 1σ sensitivity curve at 1.6 µm obtained on PZ Tel (H=6.5). The plot shows the PSF profile (black), the coronagraphic profile (green) and the noise level after subtraction of the stellar halo and speckles using spectral difference (SD). The dotted vertical line represents the edge of the coronagraphic mask. At a separation of 0.5", the raw contrast in LRS data is $2-5 \times 10^{-4}$, and the speckles can be estimated and subtracted down to a level of a few 10^{-6}. However, this noise level curve does not completely represent the capabilities of IRDIS LRS mode, because one has to consider that the final characterization performance is defined by the overall quality of the spectral subtraction, and not only by the noise level in a single spectral channel, which is always optimistic. A safety margin of a factor 3 to 5 with respect to these limits has to be taken into account when foreseeing LRS observations.

IFS preliminary representative performance

The IFS contrast floor after speckle subtraction using principal component analysis on Iota Sgr is shown in Figure 17.
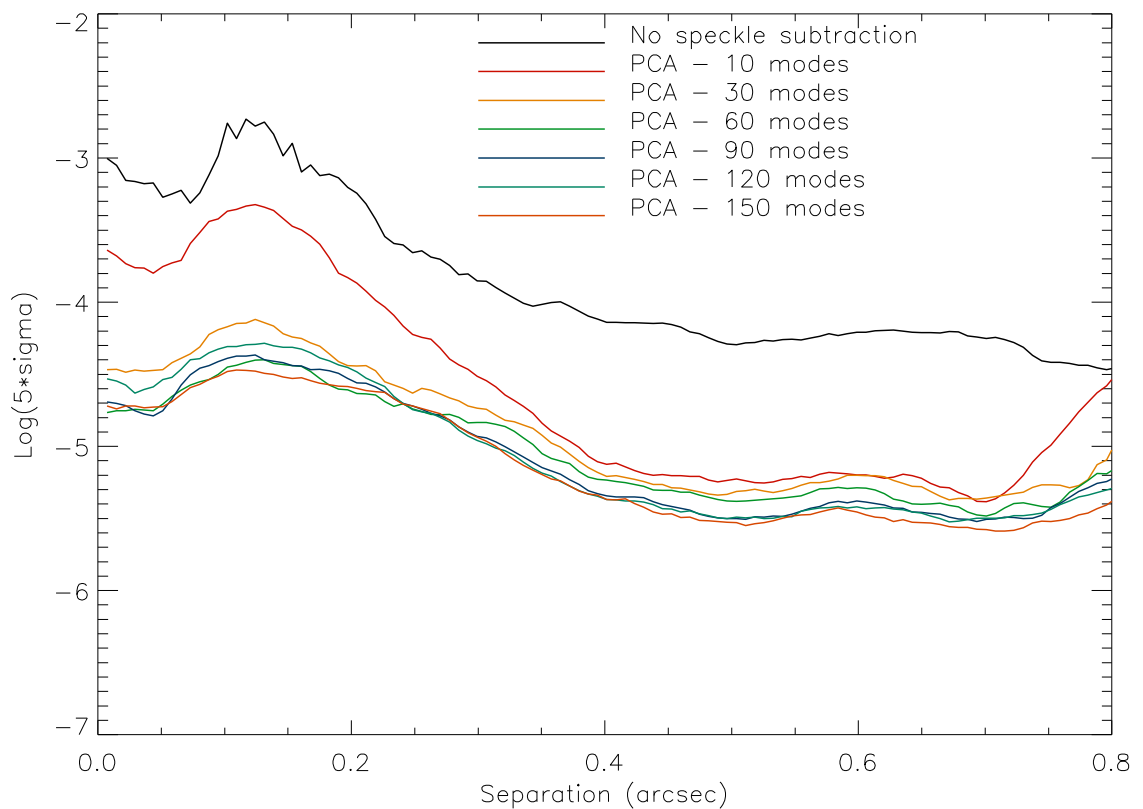
Figure 17: IFS 5σ sensitivity on Iota Sgr as function of angular separation, for different principal components retained in the speckle subtraction using both spectral and temporal diversity (ADI).
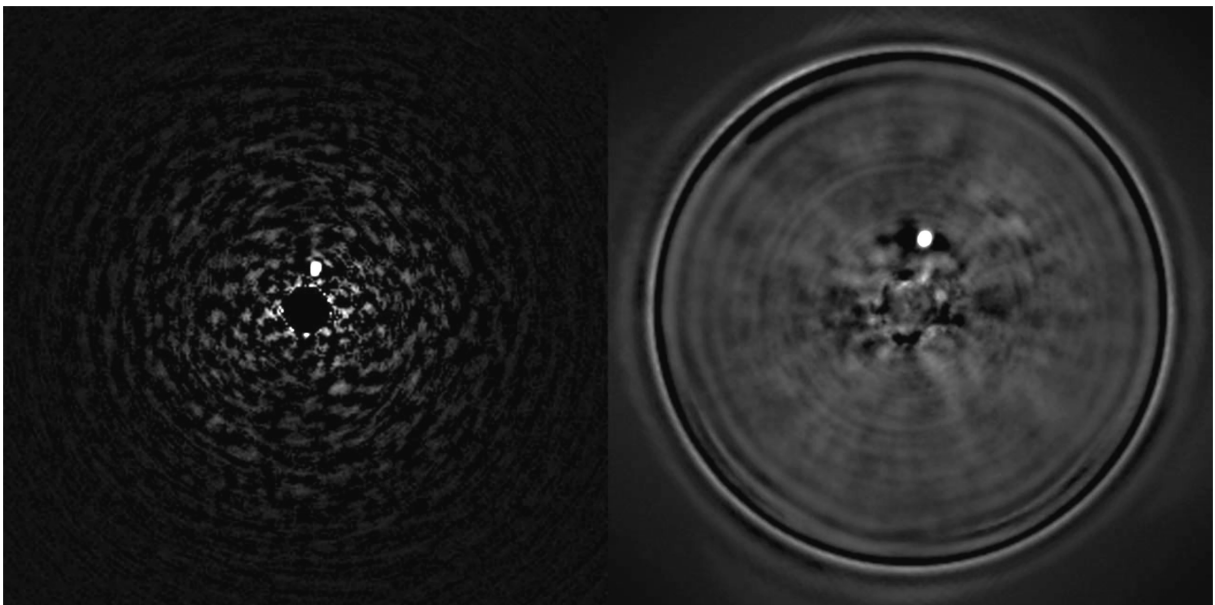
Figure 18: Detection in parallel by IRDIS (left) and IFS (right) of a faint companion at 0.24" around the bright star HR7581 (see ESO Press Release 1417, http://www.eso.org/public/news/eso1417/).

ZIMPOL preliminary representative performance
ZIMPOL performance as during commissioning is shown in Figure 19 and Figure 20.
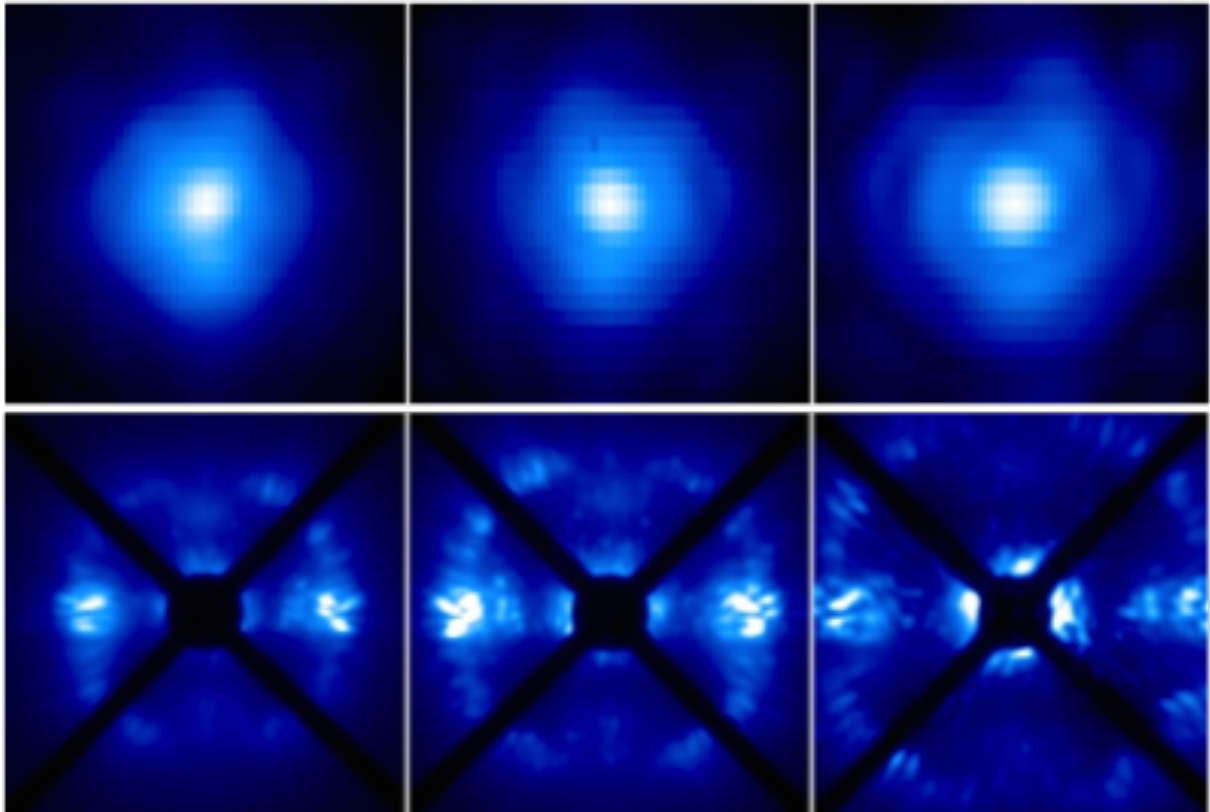
Figure 19: PSF (top) and coronagraphic (bottom) images of ZIMPOL in V, N_R, N_I filters.
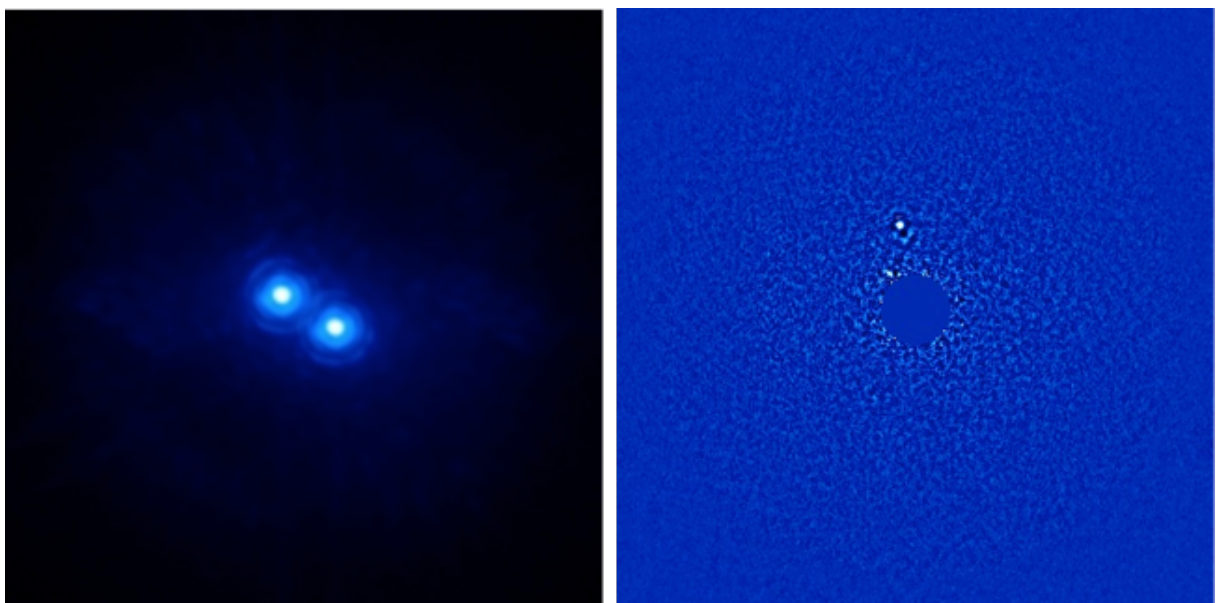
Figure 20: Left: High angular resolution imaging of a binary (150 mas separation) as seen by ZIMPOL in I band. Right: Pupil-stabilized ZIMPOL imaging providing ADI contrast close to 12 mag at 0.2" (previously unknown companion).
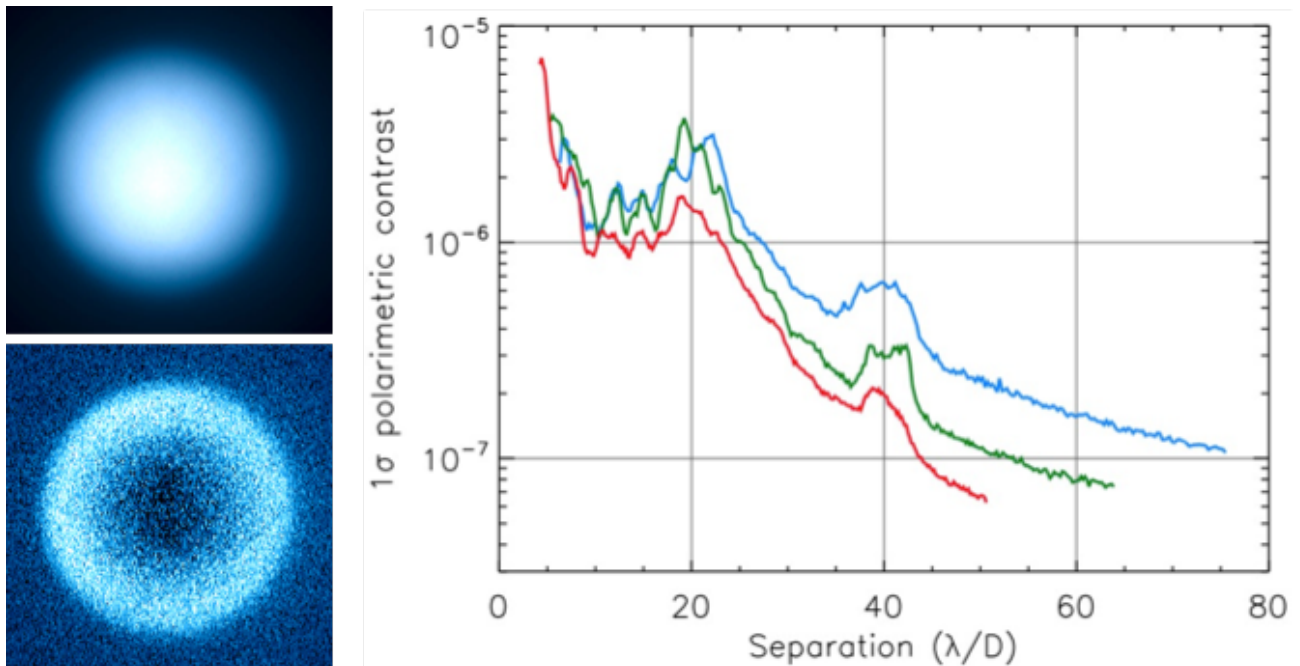
Figure 21: Top left: intensity image of Titan. Bottom Light: polarized intensity. Right: polarimetric contrast (right) on a bright target for the V (blue), N_R (green), N_I (red) filters.

SAM preliminary performance

The performance with SAM relies on the adaptive optics correction and parameters (tau0 and residual piston between the apertures, partially taken care of by the closure phase signal). It also depends on a good knowledge of the optical transfer function of the whole system (atmosphere, telescope, AO instrument). This can be provided by the use of calibrator star in the vicinity of the science target, ideally within a degree or so. Since the science target and the calibrator(s) have to be observed sequentially, the calibration of the OTF is imperfect (as the atmosphere and the telescope active optics correction evolve). The smaller the duty cycle between science and calibrator, the better. Users can build their observing sequence using concatenation of OBs. The "GoTo" acquisition template will help to switch between stars in a timely manner. It is recommended to use calibrators of the same brightness (well within 2 magnitude at R for the WFS and at the wavelengths of interest) and spectral type than the science target in order to have comparable OTF, yielding better performances.

Test observations were taken on July 2nd 2015 using all 3 masks and a variety of modes. Most data was taken on the Herbig AeBe star HD142527 which harbors a bright transitional disk and features a low-mass stellar companion at a separation of ~0.07". The early analysis of this data was discussed in a SPIE poster/proceeding: Cheetham, Girard et al. 2016 (SPIE 9907). The astrometric and spectroscopic analysis will be part of a later refeered publication (Cheetham et al., in preparation).

Figure 22 displays 4 SAM_7H PSF from the visible to the Ks band obtained from the same run. The level of wavefront correction and stability of the SPHERE Extreme AO system is enough to allow long exposures at visible wavelengths (at least with decent seeing conditions and using a bright reference star).

Preliminary contrast curves for ZIMPOL (R+I), IFS (Y to J), IRDIS (H and Ks) are displayed on Figure 24 while Figure 25 shows the equivalent in the Fourier space thanks to a Fourier transform. In the image space, the large rings correspond to the diffraction pattern of a 1-meter aperture (each hole).
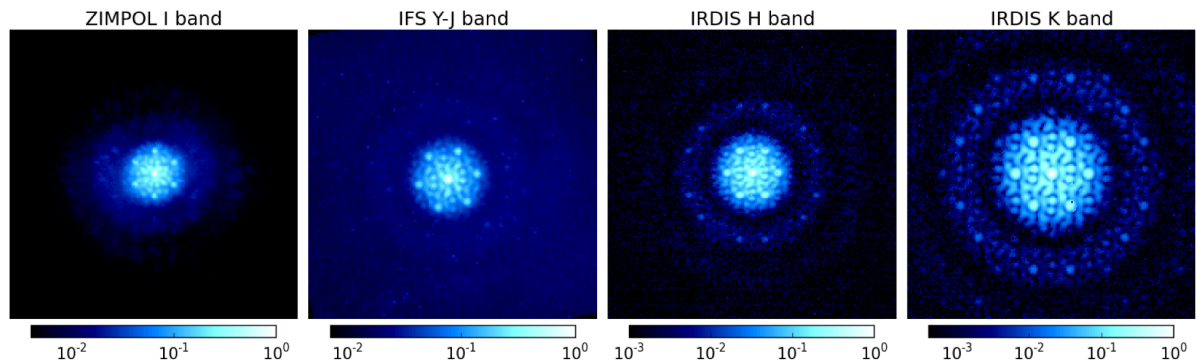
. Figure 22: SAM_7H on-sky point spread functions for 4 observing wavelengths with 3 cameras: a ZIMPOL I band exposure, a IFS wavelength slice between Y and J bands, an IRDIS H band image and an IRDIS Ks band image.
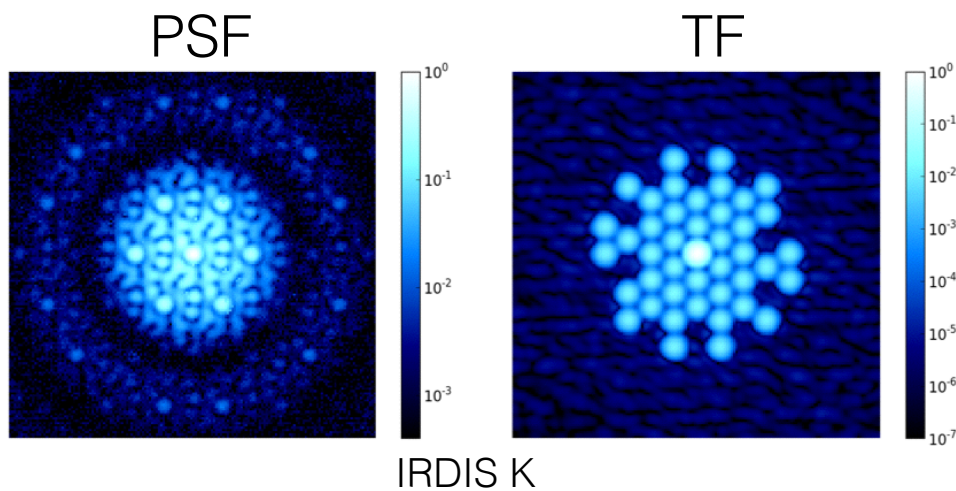
Figure 23: An image (left) produced by the aperture mask. For the 7 hole mask, the PSF is a combination of 21 sets of interference fringes. The phase and amplitude of each baseline contains information about the structure of the object being observed. The Fourier Transform of the previous image (right) allows to work in the Fourier space. Each set of interference fringes has a different frequency and direction, and so they are well separated in Fourier space and the phase and amplitude of each can be measured directly.
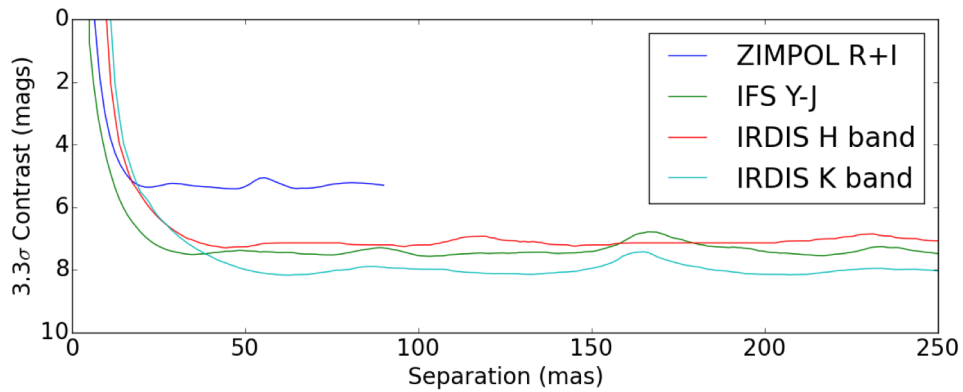
Figure 24: SAM_7H contrast limits for the detection of companions in various bands from the test data (July 2015). Each dataset consisted of approximately 1hr in execution time, including time for observations of calibrator stars. This was obtained on the F6 star HD142527 with R=8.3, J=6.5, H=5.7, K=4.98 with a seeing ~0.6-0.8". HIP113246 and HD169319 were used as calibrator stars (Cheetham et al., in prep.).
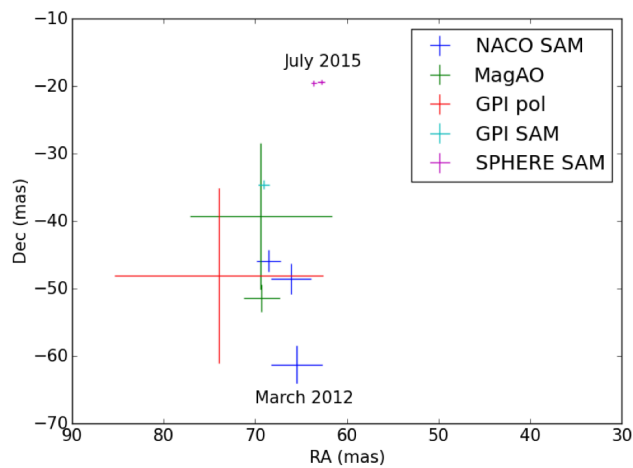
Figure 25: SAM_7H astrometry of the low-mass star companion HD142527B with respect to its host: the position uncertainty (~0.6 mas at 70 mas separation) is superior to the one obtained by other instruments and at different epochs (Cheetham et al., in prep.).

4. EXPOSURE TIME CALCULATORS

The SPHERE ETCs can be found at: http://www.eso.org/observing/etc
It returns a realistic estimation of the detection limit. This limit is expressed as the achievable image contrast as a function of separation from the central star. It covers the various observing modes, filters and coronagraph set-ups.
When applying for telescope time, please remember to add the observational overheads as detailed in Section 8.
Currently the SPHERE ETCs comply with the Phase 1 goals mostly, especially in terms of exploring the noise & SNR regimes as well as the contrast (versus angular distance) performances to identify the right mode(s) for the right project and the approximate time needed.
However, the current SPHERE ETCs are not yet suited for accurate DIT prediction, across the suite of instrument modes and filters.
For SAM, the central peak flux is roughly 45 times less than the corresponding peak flux in full aperture.
Until the online ETCs are corrected, please refer to the following page for more information:
https://www.eso.org/sci/facilities/paranal/instruments/sphere/betaETC.html
On this page you'll find the most up to date Excel DIT calculator for both IRDIS/IFS and ZIMPOL.
You can address any question to sphere@eso.org

5. QUALITY ASSESSMENT

5.1 Seeing constraints

Stable adaptive optics performance is only expected for optical seeing < 1.2''. However the wind velocity may also affect observations as described below.

5.2 Low-wind effect (LWE)

The service mode quality assessment is not trivial for SPHERE as many parameters affect the achieved contrast at a given angular separation:

> **intrinsic calibration of the common-path, AO and the given instrument,**
> **external conditions (seeing, coherence time, wind speed, etc.)**
> **many OB-depend parameters: star brightness, wavelength range and filter bandwidth,**
> **length/field rotation, differential technique(s), post-processing, etc.**

For the time being, we decided to adopt a simple scheme based on the instantaneous image quality as seen by the telescope. For that we use the telescope guide probe FWHM (~600 nm) which proves to be rather well correlated to the performance in contrast and to the seeing estimated by the SPARTA real time computer.

When a user request a "seeing" constraint on SPHERE for his/her service mode program, he/she should think in term of guide probe image quality, not DIMM seeing. Hence, a challenging program should request < 0.8 arcsec. It does not make sense to request > 1.4 arcsec. Beyond 1.2 arcsec, SPHERE AO is extremely unstable. Programs requesting 1.2 to 1.4 arsec seeing will be treated as fillers with possibly a high rate of frame selection to apply and a shallower contrast.

The following table explains the OB classification scheme for SM operations :
Table 5: QC scheme in Service Mode operations:

OB Grade	Requested seeing constraints met	6.	Seeing constraints exceeded by
A	*90% of the time*		5%
B	*50% of the time*	OR	10%
C (to be repeated)	*Less than 50% of the time*		20%

The low-wind effect appears when the outdoor wind speed (at 10 or 30m) drops below ~ 3 m/s. This is about 15 to 20% of the time and usually under good seeing conditions. The closer the wind is to 0 m/s, the stronger the effect. It is also referred as the "mickey-mouse" because it affects the PSF which can become double, triple (like "mickey-mouse" ears) or even quadruple. The effect is totally unnoticed by the AO system (Shack-Hartmann wavefront sensors are insensitive to differential piston). However, in the image plane, the PSF can be heavily affected by low-order aberrations which change on seconds to minutes time scales.

We are working on a scheme to quantify this effect (how bad is it and what are the percentage of affected frames). Meanwhile, we are recording it when it occurs and applying the scheme reported

in Table 6. If it is strong and affects > 50% of the frames, we will classify the OB as "C" (must repeat). Otherwise, if shallow and < 50% of the time, we classify the OB as "B" (if all other constraints are met) and eventually add some frames. Behind the coronagraph, the effect is such that the telescope spiders aren't well suppressed and some time-varying bright speckles appear around the mask. On the F(flux) frames without the mask, **the PSF can appear double or with "mickey-type ears" or even quadruple (when very strong)** as shown on Figure 26.

Table 6: Low-Wind-Effect

6.1.1 LWE Strength	Action for support astronomers/operators, influence on the quality assessment
Very strong	Quit operations on SPHERE or wait (i.e VM mode). Eventually try to point in the very direction of the wind. Classify C and comment "Strong low-wind effect degrading the PSF"
Strong to mild	Wait and see if the wind increases. Evaluate if it is worth finishing the OB. Classify C and comment "Significant low-wind effect degrading the PSF" OR B if it was < 50% of the time. When possible, try to add some frames to make up for it.
Mild/Nominal	Keep observing with SPHERE. Classify B and comment "Mild low-wind effect degrading the PSF on <50% of the frames" if it was present less than 50% of the time

Figure 26: Low-wind-effect qualitative assessment

Various realisations of the "low-wind effect"
on the SPHERE PSF (DTTS images)

No Effect

Typical Effect
"Mickey ears"

Strong cases
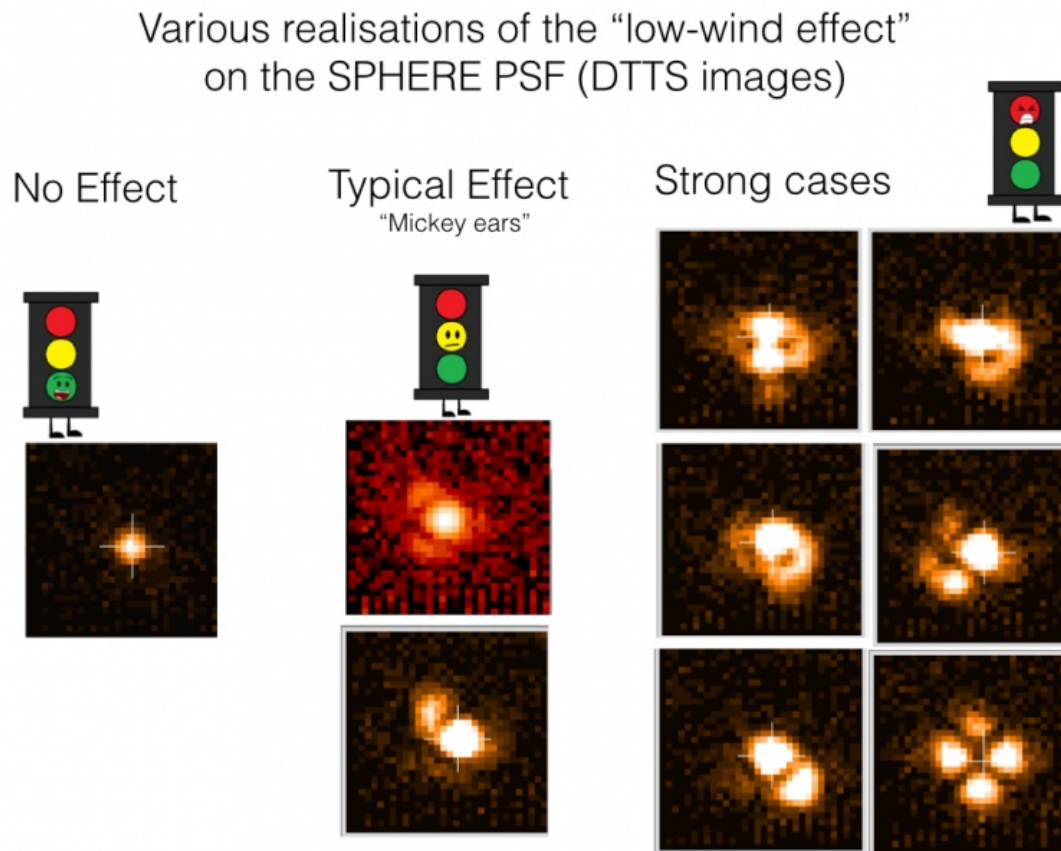
5.3 Using SPARTA files to review image quality.

SPARTA files with information on the observing conditions sampled in minute time-scales are saved in the ESO archive (http://archive.eso.org/eso/eso_archive_main.html) along with the science data. To access these files, select "SPHERE/VLT" under *Imaging*, and enter "OBJECT, AO" for *user defined type*, under *Type* in the **Data Product Info** section. From these files one can obtain the SPARTA estimates of the wind and seeing during specific observations. One can also obtain images of the PSF without the coronagraph in the H-band, recorded on the DTTS, a 0.32"x0.32" FoV detector. If the primary target was brighter than ~9-10 mag in the H-band, it should be detected on the DTTS. Hence one can check the PSF-quality, and in particular, whether the low-wind effect was present during a specific observation.

6. SPHERE OBSERVING PROPOSALS

Every semester, a call for proposal is issued by ESO. All relevant information on how to complete the so-called phase 1 proposal submission is available at:

www.eso.org/sci/observing/phase1/proposals.html

Below, we describe SPHERE observing modes and summarize them for IRDIS and IFS observations in Table 7 and for ZIMPOL in Table 8. A recommended choice of observing parameters is shown for some science cases. The feasibility of the project, the expected performance, and required telescope time should to be worked out by the proposer with the help of the ETC, adding the observational overheads listed in Section 8.

Observing modes

NIR observations of young planetary mass companions around bright stars can be performed using IRDIS and IFS simultaneously. This mode is called IRDIFS. This is the nominal infrared mode of SPHERE, recommended for surveys, with the IFS covering the Y-J wavelength range, and IRDIS offering dual-band filters in and out of the methane spectral features in the H band (around 1.65 μm). The broad-band H filter is also offered in this mode from period 97. IRDIFS offers a limited range of coronagraphs, and allows the user to choose between pupil and field tracking (pupil tracking is recommended for highest contrast performance).

IRDIFS_EXT is similar to IRDIFS but extends IFS coverage to the Y-H range, while enabling (sub-optimal) dual narrow-band observations in the K band with IRDIS. The broad-band K filter is also offered in this mode from period 97. Thanks to a wider spectral range, IRDIFS_EXT improves the IFS detection capability at small inner working angles (inside ~0.2"). This mode is recommended if additional spectral range is needed (e.g. characterization of known candidate companions).

IRDIS may also be used alone, where it offers a larger range of narrowband and broadband filter choices between 0.95 to 2.32 μm, coronagraphic, polarimetric and long-slit spectroscopic capabilities:

a. **IRDIS_DBI (dual-band imaging) offers filter pairs in the complete spectral range. This will in particular provide essential spectral information for companions out of the IFS FoV.**

b. **IRDIS_CI (classical imaging) provides a larger choice of observing parameters such as broadband filters (wider and more sensitive than DBI for faint stars) and narrowband filters.**

c. **IRDIS_DPI (dual-polarization imaging, offered from P96).**

d. **IRDIS_LSS (long slit spectroscopy) is a promising experimental mode merging long slit spectroscopy with coronagraphy (the slit is equipped with a blocking mask at its center, see Appendix for details). The IRDIS_LSS mode spectral range starts from Y, either up to H band at resolving power R~350 (with 0.09" wide slit), or up to the K band at R~50 (with 0.12" wide slit). The latter is useful for confirmation of a companion that is solely detected by IFS, or to take advantage of IRDIS's larger field of view. However, since speckles scale with wavelength, they move out of the field of view at long wavelengths, such that speckle subtraction is compromised for field of view larger than 5"x5" .**

For other science cases, such as extended sources, DPI or classical imaging is possible in all filters, with or without coronagraph, in pupil or field tracking. Please note that most differential techniques can cause significant self-subtraction for extended sources (ADI), for sources without spectral features (SDI), or unpolarized sources (PDI).

Table 7: IRDIS and IFS observing modes.

Mode	Sub-mode	Description			Main Science case
		Module/ Spectral range	Derotator	Setup/ options	
IRDIFS	IRDIFS	Simultaneous: IFS (Y-J) + IRDIS/DBI (narrow -band) or broad-band H.	Pupil or field stab.	None/ selected coronagraphs, SAM_7H	Exoplanet detection and characterization
	IRDIFS_EXT	Simultaneous: IFS (Y-H) + IRDIS/DBI (narrow -band) or broad-band K.	Pupil or field stab.	None/ selected coronagraphs, SAM_7H	Specific charact. using IFS up to H band
IRDIS alone	DBI	Dual Band Imaging, any dual-band filter pair: Y to Ks	Pupil or field stab.	None/ selected coronagraphs, SAM_7H	Charact. of companions in outer field, or confirmation of IFS detection
	DPI	Dual Polarization Imaging, any BB/NB filter: Y to Ks (BB recommended, especially J)	Field stab. Pupil Stab (VM)	None/ selected coronagraphs (CPI HWP in) SAM_7H	Polarized circumstellar disks
	LSS	Long slit spectroscopy	Field stab.	Low or medium resolution	Characterization of companions
	CI	Classical imaging, any BB/NB filter: Y to Ks	Pupil or field stab.	None/ selected coronagraphs SAM_7H	High contrast and high sensitivity (broadband) imaging

Imaging and polarimetry are available in the optical with ZIMPOL. In imaging mode "I", polarimetric devices are not used. Both detectors can either observe in the same or in different filters (e.g. Hα on/off for differential imaging). For polarimetric imaging, each arm provides a full polarimetric measurement.

Table 8: ZIMPOL observing modes.

Mode	Description		Science case
	Derotator	**Set-up/options**	
P1	Fixed	CPI HWPs in, FLC in *Options*: focal plane coronagraphic mask or clear field mask, FW1 and FW2 filters, WFS/ZIMPOL beamsplitter	Highest (absolute) precision polarimetry mode
P2	Field stab.	CPI HWPs in, ZIMPOL HWPZ and FLC in *Options*: focal plane coronagraphic mask or clear field mask, FW1 and FW2 filters, WFS/ZIMPOL beamsplitter	High precision polarimetry suited for fainter targets
I	Pupil or field stab.	All polarimetric components out *Options*: focal plane coronagraphic mask or clear field mask, FW0, FW1 and FW2 filters, FW0 ND-filters, WFS/ZIMPOL beamsplitter SAM_7H	High angular resolution imaging and Aperture Masking

The detector has 3 different readout modes (see Appendix for details). The fast polarimetry mode is used for high precision polarimetry of bright targets (with R ~ 3–7 mag). The slow polarimetry mode (with lower RON, better efficiency, but also reduced dynamic and longer minimum DIT) is more sensitive to probe the fainter environments (in the outer PSF and/or in narrowband filters). The standard imaging mode is used for non-polarimetric imaging.

Coronagraphs and filters

The choice of the coronagraph depends on the observing wavelength and inner working angle (see Tables in Sections 10.1 and 10.7). Filter sets are detailed for IRDIS in Section 10.3 and for ZIMPOL in Section 10.8. For ZIMPOL please note the AO limiting magnitudes with the grey beam splitter is ~1.74 mag brighter than with the dichroic. Also note that the use of some filters and neutral densities (located in FW0) will result in additional instrumental polarization which cannot be calibrated using the polarization compensator. Therefore the use of filters and neutral densities in the FW0 filter wheel is not recommended for ZIMPOL polarimetric imaging modes. Coronagraphs set-ups and centering, which are performed in the acquisition template, take ~5 minutes. Hence the observer is advised to limit the number of set-up changes of the coronagraph.

Sparse Aperture Masks

3 aperture masks are installed in SPHERE. All are of the same basic 7-hole design, but are located within the different sub-instruments such that SAM can be used with IRDIS (ST_SAM in the Lyot wheel), IFS (ST_SAM) and ZIMPOL (V_SAM). The general layout of the mask is shown in Figure 1. The rotation and size of each mask varies between the sub-instruments. The approximate coordinates of each mask hole for each instrument is listed in Table 1, expressed with reference to the VLT primary mirror size and projected onto the detector coordinates. However, we caution that these were measured from a single epoch in July 2015 and are provided as a guide only; the hole positions should be updated for each new set of observations.

The design of these masks requires balancing several competing factors. The 7-hole design employed in SPHERE is optimized for detecting point sources around faint targets. However, this does not preclude its use for other purposes.

AO limiting magnitudes

The most important feasibility check for SPHERE observations concerns the AO performance, measured by the Strehl ratio (SR). The SR directly impacts raw contrast level C through the rule of thumb $C \propto (1-SR)/N^2$ (Serabyn et al. 2007, ApJ 658, 1386) with N^2, the number of AO correcting elements (~1300 in SAXO).

In Table 9, we define three regimes with good, median, and poor AO corrections as a function of R magnitude and seeing as listed in Table 10. Note that these values are very conservative, and the system will likely deliver better performance, although this is not yet guaranteed (see Section 3, Figure 11).

Table 9: AO performance summary.

AO performance	H-band Strehl Ratio	R-band Strehl Ratio
Good	> 75%	> 20%
Median	50-75%	5-20%
Poor	< 50%	< 5 %

Table 10: Three regimes with good, median and poor AO corrections as a function of the R-band magnitude of the target and Seeing.

NGS mag / Seeing	Seeing < 0.8”	Seeing = 0.8”-1.2”	Seeing > 1.2”
R = 0-9 mag	Good	Median	Poor
R = 9-11 mag	Median	Median	Poor
R > 11 mag	Poor	Poor	Poor

The contrast depends weakly on the seeing in good atmospheric conditions and degrades rapidly for seeing > 1.2”, and NGS R mag > 11. For this reason, SPHERE is only offered in service mode for NGS R mag < 11.

Telescope time

For proposal submission, the astronomer should estimate the total telescope time required for the observing program. The ETC should be used to compute the integration times. When applying for telescope time, please remember to add the overheads described in Section 0. In service mode, observations are executed with observing blocks of at most 1-hour duration. An observing program must therefore take this constraint into account at Phase 1.

For the vast majority of projects, the night-time OBs will contain only one science template and the mandatory target acquisition template. The usual calibration measurements such as darks, flat-field and wavelength calibrations, are taken during the day-time as part of the calibration plan (Section 8). If for some observations, particular calibrations are needed immediately after the science exposure, these can be obtained by attaching specific calibration templates at the end of the OB or by concatenating a standard-star OB to the science OB.

For phase 2, the ESO Phase 2 Preparation Tool (P2PP) will be able to provide accurate estimates of the execution time, including overheads. It is available at:
http://www.eso.org/sci/observing/phase2/P2PP3.html

7. PREPARING OBSERVATIONS

Phase 2

After proposal submission (phase 1, Section 4), when telescope time has been granted, the observations need to be prepared during phase 2. Please consult the general guidelines on phase 2, service and visitor mode, which are available at:

- **Phase 2 preparation: http://www.eso.org/sci/observing/phase2.html**
- **Service mode: http://www.eso.org/sci/observing/phase2/SMGuidelines.html**
- **Visitor mode: http://www.eso.org/paranal/sciops/VA_GeneralInfo.html**

The observing blocks (OBs) are created with the aid of the P2PP tool during phase 2. OBs include: one acquisition template, followed by one or more templates for science observations and/or night-time calibrations. Finding charts and readme files need to be created according to the instructions available at:

http://www.eso.org/sci/observing/phase2/SMGuidelines/FindingCharts.SPHERE

And,

http://www.eso.org/sci/observing/phase2/SMGuidelines/ReadmeFile.SPHERE

Currently, NDITs above 20 are not allowed for any template, since this may cause file readout problems.

Observing constraints

The SPHERE observing constraints which can be included in Observing Blocks when preparing the observations are:

1. **Seeing: <1".2-1".4 (depending on τ_0). The optical (V-band) seeing at the position of the sky at which the telescope is pointing,**
   Transparency: SPHERE's adaptive optics system SAXO has been shown to be tolerant to THIN conditions, so user should only request photometric (PHO) or clear (CLR) conditions only for programmes requiring absolute flux measurements.
2. **Moon illumination and angular distance: SPHERE's small field of view and pixel scale is such that observations are not sensitive to the moon illumination. The angular distance, however, is recommended to be > 30º because of the VLT active optics.**
3. **Airmass: considering the maximum compensable atmospheric dispersion by ADCs, pointing is restricted to z < 60º (airmass < 2). More generally, observing close to meridian is strongly recommended for ADI performance and PSF stability. Worst pointing directions (with most variable aberrations) are at |HA| > 3hr for DEC > -40º and |HA| > 2hr for DEC > +10º.**

ESO will consider an OB as successfully executed if all the conditions in the constraint set are fulfilled. OBs executed under conditions marginally outside constraints by no more than 10% of the specified value will not be scheduled for re-execution. Unlike other Adaptive Optics-assisted instruments on Paranal, the image quality of observation conducted in service-mode will be classified according to the seeing constraint only. Once more experience is gained with the instrument performance under a wide range of observing conditions, this situation will change, and Strehl or contrast will be introduced as a formal observing constraint for SPHERE..

SPHERE has been verified to provide optimal performance under stable temperature conditions. Moreover, critical components are sensitive to temperature and humidity. For these reasons, the observatory reserves the right to interrupt observations if conditions put the instrument or the quality of the data in jeopardy. For instance:

1. **Temperature should be between 5°–18°C. Temperatures outside of this range change the DM shape at rest and reduce the tolerance to high seeing values.**
2. **Temperature variations < 1°C/h, and excursions over the night < 4°C. Strong temperature gradients will degrade the PSF stability.**
3. **Humidity should stay below 50%, as it might potentially damage the deformable mirror.**

Target acquisition templates

Each OB starts with an acquisition template. The selection of the appropriate acquisition template is detailed in
Table 11. It depends on the subsequent observing mode. Target acquisition is nominally performed in a narrow 2"x2" field of the WFS sub-apertures, and so requires precise target coordinates and proper motion. Requiring a larger FoV by imaging using IRDIS introduces unnecessary overheads times. It is important to note that all observations in a given OB should share the same sub-mode. For SPHERE, it is typically not necessary to define a specific telescope guide star. Therefore, the telescope guide star selection can be set to "catalogue", in which case a suitable telescope guide star will automatically be selected from one of the catalogues present at the telescope.
Parameters defined by the observer will be discussed in Section 9.

Table 11: List of SPHERE acquisition templates.

Acquisition template	Observing mode
SPHERE_irdifs_acq	IRDIFS, IRDIFS_EXT
SPHERE_irdis_acq	IRDIS alone in DBI or CI.
SPHERE_irdis_dpi_acq	IRDIS alone in DPI mode.
SPHERE_irdis_lss_acq	IRDIS alone in LSS.
SPHERE_zimpol_i_acq	ZIMPOL: Imaging (I).
SPHERE_zimpol_p_acq	ZIMPOL: Polarimetric Imaging P1 (derotator fixed) or P2 (field stabilized).
SPHERE_gen_acq_GoTo_acq.tsf	All modes Note: not stand alone, only for sub-sequent OBs in a concatenation.

The acquisition templates include:

a. **Telescope preset to the target coordinates and acquisition of telescope guide star.**
b. **Automatic setting of AO parameters, servo loops and checks.**
c. **Start of tracking components: derotator, ADCs, and polarization components if relevant.**
d. **Centering on the coronagraphic focal mask, if any. When the user-defined focal mask is different from the previous OB, the new mask is set in and a corresponding calibration can be performed to ensure the best centering and focus accuracy. Note that this coronagraphic device selection cannot be modified in subsequent observation templates: it remains the same in all the templates of the OB.**

General user defined parameters for IRDIFS and IRDIS templates

IRDIFS and IRDIS observation templates share many common parameters defined by the observer. They include settings of:

a. **DIT, NDIT, NEXP for IFS and IRDIS. A DIT value of 0 indicates that the smallest possible DIT value (currently 0.83 seconds) is to be used.**
b. **Number of dithering positions for IRDIS (4x4 recommended). No dithering is offered for IFS.**
c. **Observation type list. Defines the sequence of Object (O), Sky (S), Flux (F) and Star Center (C) measurements (see below) to be obtained.**
d. **Detector X and Y offset for flux measurements. Indicates the offset (in mas) which is performed to offset the source from the coronagraphic mask for the flux measurement. The recommended value (and also maximum value) is +500mas or -500mas.**
e. **Sky RA and Dec offset list. A list of sky offsets (in arcseconds) for the sky background measurement. The number of sky measurements for each "Sky" in the observation type list is equal to the number of offsets defined in the Sky RA and Dec offset list, i.e. for an RA and Dec Sky offset list of "10 -10", "-20 20" will result in two sky background measurements per "S" in the observation type list. An amplitude for the offset greater or equal to 10" is recommended, it should be less than 60". The offset are cumulative, namely "10 10" followed by "-10 -10" returns to the star position.**
f. **Deformable mirror waffle parameters. These parameters control the amplitude and the pattern of the four symmetric echoes of the PSF core in the Star Center measurement. Details are given in Appendix A 12 concerning the use of the waffle spots for accurate centring. In case of observing an object with a known companion, changing these parameters may be useful to ensure that the position of the echoes do not coincide with the location of the companion. The recommended amplitude is 0.05, corresponding to 5% of the available DM stroke. This makes a ratio between the PSF echoes and the star peak of 1.3% at H band, and scales quadratically with the wavelength.**
g. **Choice of neutral density filters.**
h. **Field orientation, for field-stabilized observations.**

Besides the on-axis (coronagraphic or not) observation of the object (observation type O), the observing template sequence should also include these observation types whenever using a coronagraph, or when observing extended objects for the third one:

Star Center - C: in the pupil-stabilized mode, the field rotates. It is thus critical to obtain the exact position of the rotation center. This is also important for accurate measurement of the separation of any potential companion. This allows measuring this position by applying a waffle pattern to the deformable mirror, which creates four replicas of the PSF away from the coronagraphic mask (see Appendix A12). Localizing the four peaks allows computing the rotation center, at the middle of the square pattern. This measurement is performed with the science template and can be repeated several times during a long science sequence. For SAM, "C" frames are not relevant.
Flux - F: a PSF core off-axis measurement can be inserted before and/or after deep coronagraphic observations in order to register the PSF core flux. Contrast curves are derived from this measurement. Off-axis measurements can be performed by moving the star and inserting a neutral density but without moving the coronagraphic focal

mask and thus without perturbing the centering accuracy. For SAM, "F" frames are not relevant.
Sky – S, optional: observes the sky background. Accurate knowledge of the background is not important for point-like objects. However, it might be important for faint extended emission.

The DIT values for the C and S observations, are not user-defined parameters, but are identical to the DIT used for the O observation. The DIT value for the F observations has to be defined separately within the observing template.

For convenience, especially if the observer is unsure about the saturation level, it is recommended to isolate a Flux F and Star Center C in two independant templates to allow the night astronomer to check the saturation level of these frames before continuing with the rest of the observations (typically observations of type O). This way, the detector integration time can be more easily adjusted, in case of detrimental over- or under-illumination of these critical frames, without aborting the whole sequence of observations.

"Go To" acquisition template

In P100, a new acquisition template called "GoTo" is introduced (pending successful commissioning):

SPHERE_gen_acq_GoTo_acq.tsf

It allows user to switch from one target to another in a timely manner. It will perform a preset to the new target (i.e. a PSF calibrator) without performing any AO nor instrument setup. This template will be instrument independent and it will not be "stand alone", it will only be used after one of the normal acquisition template has been executed at the beginning of a concatenation of OBs. The gain in overheads will be considerable, at least 5 minutes per sub-sequent OB in the concatenation (C container). More details about this template will be described in the Phase 2 version of this manual.

The R magnitude of all targets within the concatenation must not differ from the magnitude in the 1st acquisition template by more than 2 mag and with all R > 13.

IRDIFS templates

7.1.1 Observation templates and user-defined parameters

IRDIFS observation templates are detailed in Table 12. Parameters defined by the observer will be presented in Section 9.

Table 12: IRDIFS observing templates.

IRDIFS observation templates	Observing modes
SPHERE_irdifs_obs	IRDIFS observations, with IFS observing in Y-J and IRDIS in H-band, DB_H23, or DB_H34
SPHERE_irdifs_ext_obs	IRDIFS_EXT observations, with IFS observing in Y-H and IRDIS in K-band or DB_K12

For efficiency reasons it is recommended that the total duration of IFS and IRDIS exposures are similar. The neutral densities inserted in CPI are common to IRDIS and IFS. For minor differential adjustment another ND0.5 (factor $10^{-0.5}$) is available inside IRDIS for the H band dual-band filters.

7.1.2 Calibrations

Calibrating IRDIFS data involves usual day-time internal calibrations (darks/background, flat, spectral calibration of the IFS, see Section 8 for details).

IRDIS: DBI

7.1.3 Observation templates and user-defined parameters

IRDIS observation templates	Observing modes
SPHERE_irdis_dbi_obs	IRDIFS DBI

For IRDIS-only observations in dual band imaging mode, there is a single template called SPHERE_IRDIS_dbi. Parameters defined by the observer are discussed in Section 9.
The Appendix lists all the available filters. The filter pair DB_ND23 includes a ND0.5 neutral density but is otherwise identical to DB_H23.

7.1.4 Calibrations

Calibrating IRDIS-DBI data involves on-sky and internal (day-time) calibrations similar to the IRDIFS and IRDIFS_EXT modes (see Section 7.1.2). Other night-time and day-time calibrations provided as part of the SPHERE calibration plan are detailed in Section 8.

IRDIS alone Classical Imaging (CI)

7.1.5 Observation templates and user-defined parameters

IRDIS observation template	Observing mode
SPHERE_irdis_ci_obs	IRDIS CI

A complete list of user-defined parameters is presented in Section 9.

7.1.6 Purpose and properties

This mode is a general-purpose mode, which can be used in pupil, or field stabilized regime. In this mode any filters from the common filter wheel can be used. The recommended derotator rotation law to be used for observation of extended objects should be the field stabilized to avoid image smearing. Coronagraphs can also be used with any filter in classical imaging mode (see Appendix for details).

7.1.7 Calibrations

The calibrations for IRDIS CI observations are the same as for DBI observations.

IRDIS DPI   (Dual Polarization Imaging)

Dual polarimetry (via DPI) is a proxy to achieve greater contrasts at small inner-working-angles. This is provided that the object of interest features polarized scaterred light in the near IR (i.e debris and proto-planetary disks, etc.). If the latter condition is satisfied, DPI offers an enormous advantage over other high contrast differential techniques : images at orthogonal linear polarizations are taken simultaneously. If both beams have the same optical aberrations, DPI allows very efficient speckle suppression in the control radius of the AO/coronagraph.
This mode has been used in Science Verification time and by the GTO in "shared risks" because its characterization was incomplete. It is now offered starting in P96.

7.1.8 Instrumental polarization

Thanks to the SVT and P95/P94 experience, we were able to better characterize the IRDIS DPI mode. We found out that the control law of the HWP was not ideal and changed it in late April 2015.

In addition, we measured the effect of polarization cross-talks inside the instrument for four BB filters during P94 & P95.
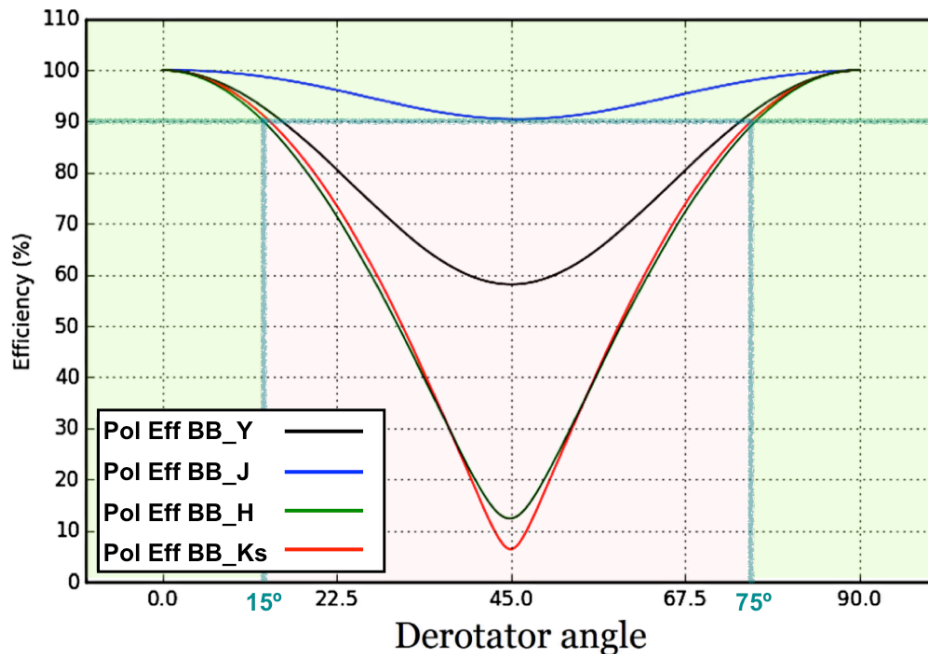
Figure 27: Measurements of the instrumental polarization efficiency (not accounting the telescope) for four broad band filters. For best use of the DPI mode, one should avoid the pink zone where the efficiency drops below 90º (> 10º loss due to cross-talks). For that, one should make sure the derotator angle stays < 15º or > 75º. J-band is the least affected and therefore the most recommended filter, especially for long observations featuring a large parallactic angle variation. At J-band the efficiency is always > 90%.
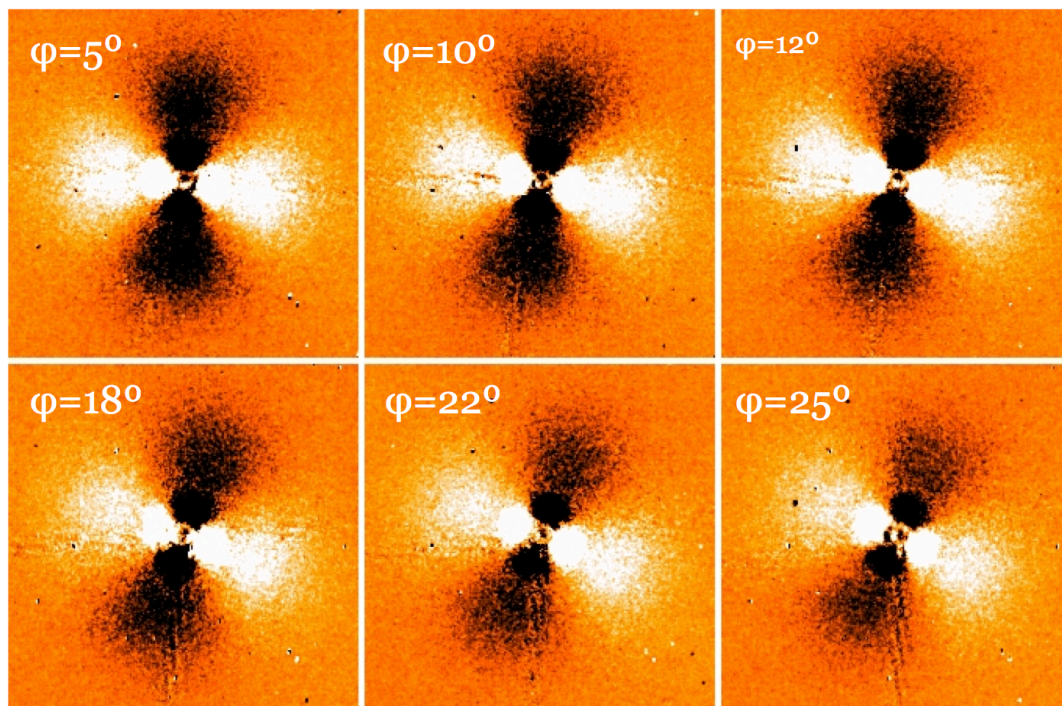
Figure 28: Effect of the instrumental polarization (efficiency loss due to increased cross-talks at a varying derotator angle). The « butterfly pattern » rotates with time and its signal to noise ratio decreases significantly. This is the polarimetric signature of a bright face-on disk (H-band observations).

Figure 28 shows the « butterfly » pattern of a bright face-on polarized disk. Its SNR and orientation varies in time. This is because of the departure, during the observation from the ideal (< 15º or > 75º) derotator position as it tracks the field, in H-band (as shown in Figure 27). This effect was even stronger before the end of April 2015 when we changed the half-wave-plate control law.

We recommend the following when using the DPI mode:

- **Use the BB filters as much as possible**
- **J-band is the least affected filter (efficiency always > 90%)**
- **For Y, H and K-band DPI, try to keep the derotator angle < 15º or > 75º. This can be done by entering a derotator position angle in the science template (bottom parameter). You can use this formula:**

Derotator position angle = <parang – alt> or = 180 + <parang – alt>

Where <parang – alt> is the mean value of the difference between the parallactic angle and altitude of the target during the template. If the amplitude of that difference is greater than 15º during the template, split the template in 2 shorter ones, and repeat the calculation.

To help you check whether your observation, at a given time will be affected by efficiency problem, an Excel table is now available here:

It calculates for a given declination and position angle (as entered in p2pp), in which regime of Figure 27 the derotator is and hence, which is the implication on the polarimetric efficiency. Time is given in Local HA (how far away one is before and

after the meridian) and the efficiency regimes are "green" when < 20º from the ideal derotator angle, yellow when > 20º and < 30º, red otherwise:

http://www.eso.org/sci/facilities/paranal/instruments/sphere/doc/IRDIS_DPI.html

Since P100, DPI is also offered in Pupil tracking (coronagraphy or SAM) in VM only.

7.1.9 Observation templates and user-defined parameters

IRDIS observation templates	Observing modes
SPHERE_irdis_dpi_obs	IRDIS DPI

For IRDIS only observations in dual polarized imaging mode, there is a single template called SPHERE_IRDIS_dpi. Parameters defined by the observer are discussed in Section 9. They include setting:

a. **DIT, NDIT, NEXP. A DIT value of 0 indicates that the smallest possible DIT value (currently 0.83 seconds) is to be used.**
b. **IRDIS Filter Combination and Neutral density filters.**
c. **Stokes parameters to be measured (Q or Q and U).**
d. **Number of polarimetric cycles**
e. **The polarization gamma parameter. This parameter reflects the on-sky orientation (measured clockwise from North) of the measured polarization in the first image of a Q cycle.**

7.1.10 Calibrations

Differential polarimetry is a proxy to achieve greater contrasts at small inner-working-angles. This is provided that the object of interest features polarized scaterred light in the near IR (i.e debris and proto-planetary disks, etc.).
Calibrating IRDIS-DPI data involves on-sky and internal calibrations similar to the IRDIS CI and IRDIFS_DBI modes (see Section 7.1.2). Other night-time and day-time calibrations provided as part of the SPHERE calibration plan are detailed in Section 8.

IRDIS alone Long Slit Spectroscopy (LSS)

7.1.11 Observation templates and user-defined parameters

IRDIS observation template	Observing mode
SPHERE_irdis_lss_obs	IRDIS LSS

User-defined parameters are:

a. **DIT, NDIT, NEXP. A DIT value of 0 indicates that the smallest possible DIT value (currently 0.83 seconds) is to be used.**
b. **Spectral resolution and range: LRS (R~350) / MRS (R~50).**

The slit selection (for width and size of the central blocking mask) is made in the acquisition template that also ensures the appropriate on-slit target centering.
The complete list of user-defined parameters is presented in Section 9.

7.1.12 Purpose and properties
Scope of LSS:
IRDIS long slit spectroscopy mode (LSS) is designed for the spectral characterization of already detected objects either at low resolution (LRS, R ~ 50) over Y to Ks, or medium resolution (MRS, R ~ 350) over Y to H. It offers the unique combination of a classical Lyot coronagraph with long slit spectroscopy.

Configurations:
In practice, the slits and opaque coronagraphic masks have been merged into a single device that is placed in the coronagraph wheel of the CPI. The specifications of the three slits that are available for LSS are listed in Table 13. In addition to the slit+coronagraphic masks, two dispersive elements are placed in the IRDIS cryostat in the Lyot stop wheel: a prism for the LRS mode and a grism for the MRS mode (the dispersion curves for these two components are available in the Appendix). The combination of the three slits and the two dispersive elements provides 4 different configurations listed in Table 14.
As a consequence of using a slit, the observations in this mode are necessarily done in field–stabilized mode to maintain the object of interest inside the slit during the observations.
Target size and spectral resolution:
Positioning of the object with respect to the slit is of significant importance in IRDIS LSS because the diffraction limit is reached inside the slit. The actual spectral resolution for point-like sources is thus set by the diffraction limit rather than the slit width. The central star halo (the star PSF core is hidden behind the coronagraphic mask) can be considered as an extended object in the sense that the speckle field of the star will fully cover the slit, decreasing the effective resolution of its spectrum.
Because the object is unresolved inside the slit, the wavelength calibration can be impacted by the position of the object. Indeed, the wavelength calibration is performed by observing an extended source through the slit, which means that it is only fully valid for the star, or if the object is perfectly centered in the slit. If the object is not well centered, this will induce a systematic shift of the wavelength for the object with respect to that of the star. Also, note that the inaccurate positioning of the object inside the slit can induce differential flux losses (see e.g. Goto et al. 2003, SPIE, 4839) that might affect the spectral slope of the continuum of the object.

Table 13: Specifications of the LSS slits+coronagraphic focal masks available in the coronagraphic wheel to use in IRDIS LSS mode.

Slit name	*Width*	*Coronagraphic mask radius*
SLIT_WL	0.12"	0.2"
SLIT_WS	0.12"	0.1"
SLIT_NL	0.09"	0.2"

Table 14: Configurations available in IRDIS LSS mode.

Configuration	*Slit*	*Dispersive element*
S_LR_WL	SLIT_WL	PRISM
S_LR_WS	SLIT_WS	PRISM
S_MR_WL	SLIT_WL	GRISM
S_MR_NL	SLIT_NL	GRISM

7.1.13 Calibrations
The calibration frames acquired automatically by the observatory include:

- **Internal background**, **Internal flat-field sequences:** a series of flat-field images is produced in all setups used during the night. In the LSS mode, a flat-field in the spectroscopic wide-band filters YJHKs (in LRS) or YJH (in MRS) are provided. It is also possible to calibrate the detector flat field using a flat acquired in the H broad-band filter if no wide-band flat field is available.
- **Wavelength calibration:** the SPHERE calibration unit provides the user with six laser emission lines covering the spectral range 988 to 2015 nm in LRS. In MRS, five emission lines are available for calibration, from 988 to 1730. This calibration is automatically obtained during day-time, after a spectroscopic observation has been done. It is however recommended that observers attach the wavelength calibration to their OB for improved accuracy. For this, the SPHERE_irdis_lss_cal_wave template should be used. The time needed to execute this template will be charged to the user.

The following additional calibrations can also be requested, but will be charged to the observer:

- **Sky background:** the acquisition of sky background frames during the night may be necessary, especially in the LRS mode covering the K band where the sky background may be bright and variable. Such background file provides an efficient correction of the thermal background of the sky + instrument, the dark features and the static bad pixels. The SPHERE_irdis_lss_obs_sky template should be used.
- **Telluric standard observation:** allows calibrating the telluric absorption on a featureless stellar spectrum. This calibration is done on request and prepared by the user with the template SPHERE_irdis_lss_obs_telluric. If the chosen star is a spectro-photometric standard, use of the widest slit is recommended to avoid the slit losses.

ZIMPOL polarimetric imaging

7.1.14 Observation templates and user-defined parameters

observation template	Observing mode
SPHERE_zimpol_p1_obs	ZIMPOL polarimetric imaging P1
SPHERE_zimpol_p2_obs	ZIMPOL polarimetric imaging P2

User-defined parameters are:

a. **Detector readout mode and exposures: DIT, NDIT, NEXP. As the polarized signal is modulated between two CCDs (cf. Fig. 8), NDIT must be an even number.**
b. **Polarization orientation and switching scheme. See section 7.1.17**
c. **Derotator: fixed (P1) or field-stabilized (P2). In case of field-stabilized observations, the field orientation. See details in Section 7.1.15.**
d. **Beam Splitter: This is selected in the acquisition template. Note that the grey beam splitter gives worse AO performance, since the light reaching the WFS decreases by 1.4 mag.**
e. **Filter: ZIMPOL filters, excluding the filters located in the common FW0, which are not currently supported for polarimetry. The selected filters may or may not be the same for both arms (in FW1 and FW2). Note that if the dichroic beam splitter (between AO WFS and ZIMPOL) is set in the acquisition template, then the choice of ZIMPOL filters is restricted to the R band, narrowband R, H-alpha broad, H-alpha continuum or (for arm 2 only) H-alpha narrow. See Section 4.1.**
f. **Stokes parameters to be measured (Q or Q and U).**
g. **Number of polarimetric cycles.**

h. **Polarization gamma parameter: Selects the on-sky orientation (measured in degrees clockwise from North) of the measured polarization in the first image of a Q cycle.**

i. **ZIMPOL polarization compensator selector: Determines whether the derotator polarization compensator is in the beam (COMP) or not (OPEN).**

j. **ZIMPOL polarization compensator tilt angle. Tilt of the compensator plate in degrees. It is recommended to leave this at the default value of 25 degrees.**

k. **Observation type list. Defines the sequence of Object (O), Flux (F) and Star Center (C) measurements to be obtained.**

l. **Detector X and Y offset for flux measurements. Indicates the offset (in mas) which is performed to offset the source from the coronagraphic mask for the flux measurement.**

m. **Deformable mirror waffle parameters. These parameters control the amplitude and the pattern of the four symmetric echoes of the PSF core in the Star Center measurement. In case of observing an object with a known companion, changing these parameters may be useful to ensure that the position of the echoes do not coincide with the location of the companion.**

n. **Field position: see Section 7.1.16.**

A complete list of user-defined parameters is presented in Section 9.

Table 15: ZIMPOL P1/P2 modes in a nutshell.

P1 mode	Highest precision polarimetry mode without derotation: • best suited for absolute polarimetric calibration • arbitrary Q/U orientation selection with HWP2 • derotator and compensator always in the same fixed position
P2 mode	Polarimetry mode with derotation: • arbitrary Q/U orientation selection with HWP2 • stable field on detector with user-defined orientation • derotator, compensator and HWP-Z move during observations

7.1.15 P1 or P2 rotation modes for ZIMPOL polarimetry

Two field rotation modes are offered for ZIMPOL polarimetry. They provide two different observing strategies:

- **P1: No field derotation. This mode is only intended for experts as special algorithms will be required to reduce the data.** For bright targets the integration times can be short enough for observations without image derotation because the rotational smearing of the signal on the detector can be neglected. The rotator is fixed in vertical position. This has the advantage that all components are fixed except for HWP1, which needs to correct for the altitude dependence of the M3 polarization, and HWP2, which rotates the polarization position angle correctly into the orientation of the derotator and the ZIMPOL system. This mode will provide the highest polarimetric sensitivity and polarimetric calibration accuracy and is best suited for the search of planets around bright stars because nothing moves after HWP2.

- **P2: Active field derotation.** This mode is suited for long integration of fainter targets. Field derotation is activated and the polarization vector is rotated by HWP2 into the rotating derotator system and rotated back by HWPZ into the ZIMPOL system. Therefore, the field is fixed but the remaining instrument polarization of about p=0.5% can have some complex, hard to calibrate drifts due to the rotating components.

7.1.16 Dithering, mosaicking

7.1.16.1 Dithering

Dithering with the tip-tilt folding mirrors in front of the detector is possible. Dithering moves the image by several pixels on the detector so that effects of individual pixels can be averaged-out or corrected. The user can select a dithering pattern which is applied to both arms. A recommended pattern is a 9 point dithering pattern with shifts of 50 mas or 14 pixels (3.5 mas each) on the detector:

The dithering positions (in pixels) are setup in the observing template as follows, for instance:

[x,y] = [-14,-14], [-14,0], [-14,+14], [0,-14], [0,0], [0,+14], [+14,-14], [+14,0], [+14,+14]

This pattern can be restricted to a 3 point or 5 point dithering pattern or additional dithering positions can be added.

7.1.16.2 Off-axis positions

Using the tip-tilt mirrors to explore the full 8 arcsec diameter is currently not offered.

7.1.17 Observing sequences for ZIMPOL polarimetry

An individual exposure with ZIMPOL polarimetry includes at least two frames taken with opposite charge shifting phasing (double phase mode). This corrects for the charge shifting effects. This minimum unit can be called within several levels of sequences. The recommended sequences for ZIMPOL polarimetry are from low level to high level:

NDIT: number of frames taken (MUST BE an even number) per exposure or data cube.

NEXPO: Number of data cubes taken per higher order sequence.

STOKES sequence: Q or QU for a HWP2 cycle (Q switch), at 0 and 45 degrees, or double cycle (QU switch) with 0, 45, 22.5 and 67.5 degrees. The QU switch sequence should be used by default. Other settings are for experts.

NPOL: Number of STOKES cycles taken within a higher order sequence.

DITH.PATTERN.LIST: List of dithering positions.

FIELD.ETA: List of image rotation angles (only for P2 mode).

Example: one can have a sequence with:

   a. **3 field orientation (list given with eta = 0, 30, 60)**
   b. **For each field orientation 3 dithering positions (e.g. list [-14, 0], [0, 0], [+14, 0])**
   c. **For each dithering position 2 (=NPOL) STOKES QU cycles**
   d. **For each HWP position 1 exposure (NEXPO=1)**
   e. **Each exposure with 50 frames of 1.2s integration time**

This yields: 50 x 1 x 4 x 2 x 3 x 3 frames or 3600 frames with a net integration time of 3960s.

7.1.17.1 Recommendations for sequences

Large NDIT (>10) reduces the observing overhead. NDIT=20 should be preferred to, e.g., NEXPO=4, NDIT=5. NDIT is limited to 20 because too large fits files can also generate errors when written to disk.

STOKES Q or STOKES QU cycles should not be too long (less than a few minutes), because the HWP2 switch corrects well for many instrumental polarization effects if the 0 – 45 degree or 22.5 – 67.5 degree switch cycle is shorter than drifts in the instrument polarization. We recommend a HWP2 switch should be made every few minutes.

DITHERINGS can correct for detector effects. A reasonable number of dithering is 3 or 5. One should also consider that ZIMPOL has a second arm where the same data can be taken simultaneously with another detector.

7.1.17.2 *Recommended sequences for different types of targets*

ZIMPOL polarimetry in P2 mode for faint sources:
One STOKES QU cycle with NDIT=2, DIT=100s (total = 800s in 4 exposures including 8 frames). This mode is appropriate for faint sources observed in slow polarimetry and yields photon noise limited or readout ZIMPOL polarization accuracy including the correction for instrumental polarization. Second arm (with the same or another filter) can be used for the identification of bad pixels and other instrumental effects.

ZIMPOL polarimetry in P1 mode of very bright star with high sensitivity:
Short exposure DIT=1.2 sec with many frames (NDIT=50) per exposure, NEXPO=2 for a total of 100 frames between each HWP2 switch. A STOKES QU cycle, where one full polarization cycle has 400 frames, has an integration time of 8 minutes. 10 such cycles (NPOL=10) form then one observing block, which may be repeated several times during the night with slight offsets of the dithering position.

7.1.18 ZIMPOL polarimetric calibrations

For ZIMPOL polarimetry the same principles for CCD detector calibrations apply. Therefore the ZIMPOL polarimetry calibration plan includes bias, dark and flat-field calibrations. One also needs a calibration of the polarimetric modulation-demodulation efficiency of ZIMPOL. The polarimetric calibration of the telescope and instrument is not required for most application because the ZIMPOL/SPHERE design has well-defined polarimetric properties. The telescope polarization is compensated to less than 1%, and the instrument polarization is self-calibrated with the half-wave plate (HWP2) switch. The zero-point of the polarization position angle will be available after commissioning to an accuracy of better than 5 degrees. Polarization cross-talks affect the measured fractional polarization p (or Q/I and U/I) by less than $\Delta p/p = 0.1$. These polarimetric properties are monitored by the observatory with the measurement and analysis of high polarization standard stars and zero polarization standard stars on a regular basis. The user should consider additional standard star measurements for science cases requiring a better accuracy in the polarimetric calibration. One can expect that the instrument will be characterized with higher precision, once more measurements become available.

Modulation-demodulation efficiency calibration: the standard polarimetric calibration to be carried out for each polarimetric observation is the modulation-demodulation efficiency calibration. These frames can be obtained during day-time with a flat-field illumination of the detectors using a linear polarizer in the beam producing a fully (100%) polarized illumination of ZIMPOL. The polarization signal measured by ZIMPOL provides then polarization efficiency (e.g. about $\varepsilon \sim 0.8$ for fast polarimetry or $\varepsilon \sim 0.9$ for slow polarimetry) and the polarization signal in the science data must be corrected by the obtained frame (Q_cal = Q_measured / ε). The modulation-demodulation efficiency calibration depends on various parameters, most importantly on the modulation frequency, the used filter, and the location on the detector. Therefore one must obtain for each polarimetric science frame a calibration taken in the same modulation mode (fast or slow) and with a similar broadband color filter. It is recommended to use for narrowband or line filter polarimetry a corresponding broadband filter calibration because they can be obtained with short exposures reducing the charge trap problem while the color dependence is sufficiently taken into account (see Section 8). The calibration frames for the modulation-demodulation efficiency are also affected by the charge trap problem. Therefore it is recommended to take these frames only with short integrations (limited number of charge shifts). For narrowband and line filter data one can use broadband filter calibrations.

Bias calibrations for polarimetry: bias subtraction for ZIMPOL is mainly based on the overscan pixel bias level. Fast polarimetry produces a fixed pattern along two columns originating from the read-out process. To remove them it is important to have a set of bias calibration (e.g. 50 frames) available. It is useful to take similar calibrations for slow polarimetry as a detector quality check.

Dark calibrations: can be useful for subtracting the dark current from long integrations. For most cases this calibration is not needed.

Intensity flat-fields for polarimetry (polarization flats): well illuminated intensity flats are required to calibrate pixel to pixel sensitivity variations. Intensity flats should be taken with the same filters as the science observations. If a coronagraph on a substrate is selected then sensitivity features due to dust and inhomogeneities of the plate can be corrected with a flat-field with the same focal plane plate inserted. The charge traps are an issue for the flat-fielding in polarimetric mode and therefore one should use short integration times. Detector fringing is an issue for the flat-fielding of frames taken with the line filters.

ZIMPOL imaging

7.1.19 Observation templates and user-defined parameters

observation template	Observing mode
SPHERE_zimpol_i_obs	ZIMPOL non-polarimetric imaging

User-defined parameters are:

a. **Detector readout mode and exposures: DIT, NDIT, NEXP**
b. **Derotator: field-stabilized or pupil-stabilized. In case of field-stabilized observations, the field orientation.**
c. **Filter: ZIMPOL filters. The selected filters may or may not be the same for both arms (in FW1 and FW2). Note that if the dichroic beam splitter (between AO WFS and ZIMPOL) is selected in the acquisition template, then the choice of ZIMPOL filters is restricted within the R band: narrowband R, H-alpha broad, H-alpha continuum or (for arm 2 only) H-alpha narrow.**
d. **Observation type list. Defines the sequence of Object (O), Flux (F) and Star Center (C) measurements to be obtained.**
e. **Detector X and Y offset for flux measurements. Indicates the offset (in mas) which is performed to offset the source from the coronagraphic mask for the flux measurement.**
f. **Deformable mirror waffle parameters. These parameters control the amplitude and the pattern of the four symmetric echoes of the PSF core in the Star Center measurement. In case of observing an object with a known companion, changing these parameters may be useful to ensure that the position of the echoes do not coincide with the location of the companion.**
g. **Field position: see before.**

The exhaustive list of user-defined parameters, as extracted from the Template Reference Manual, is presented in Section 9.

7.1.20 Purpose and properties

ZIMPOL provides an instrument mode for imaging without polarimetry. In principle, the polarimetric mode of ZIMPOL provides differential polarization signal and intensity images. But having a dedicated imaging mode ensures optimal imaging performance. The resulting data are less affected by instrumental effects (e.g. the HWP are out of the beam). Thus, if one seeks high quality imaging for targets where the polarimetric signal is not relevant then one should consider the imaging mode. Imaging provides in particular a pupil-stabilized observing mode and also features which are not available in polarimetric imaging.

The following list highlights the main advantages of the imaging mode:

- All polarimetric components are out of the beam. This enhances the throughput and reduces ghost effects and the scattered light level. Components which are not in the beam when compared to polarimetric imaging are: HWP1, HWP2, FLC modulator and eventually the polarization compensator and HWPZ.
- A pupil stabilized observing mode is offered for imaging which enables angular differential imaging (ADI).
- No charge shifting is required on the CCD. Therefore, one has no problems with the charge traps which appear in polarimetric imaging.
- The Filters in the common filter wheel are also available for imaging.
- The format of the resulting data is simpler.

Only minor drawbacks are related to the imaging mode when compared with the polarimetric imaging mode:

- Currently only the fast readout mode with a high readout noise of 20 e-/pix is offered.
- The two channels of ZIMPOL are strongly polarization sensitive. The total efficiency of one arm depends more strongly on the telescope pointing direction and the instrument configuration than in polarimetric mode.

7.1.21 Calibrations

Typical day-time (bias, flats, distortion maps) and night-time (photometric standard stars and astrometric fields/stars) calibrations are provided by the observatory (see Section 8).

8. CALIBRATION PLAN SUMMARY

Night-time calibrations

Some observing modes require attached calibration to be taken during the night. Here we detail which ones are mandatory and will be charged to the user observing time, and which ones are part of the calibrations provided by the observatory.

Whenever a coronagraph is used, the SPHERE calibration plan recommends including Flux (F) and Star Center (C) observation types in observing templates both before and after the science observing template. The purpose of the first calibration (Flux - F) is to measure the unsaturated peak flux of the star by offsetting it from the coronagraph spot, in order to ensure accurate relative photometry, and thus contrast calibration. The second calibration (Star Center - C) applies a waffle pattern on the deformable mirror to produce echoes of the PSF hidden behind the coronagraphic mask at very specific locations. The goal of (Star Center - C) is to accurately measure the position of the star behind the coronagraph, which is critical for astrometric measurements of off-axis sources.

8.1.1 Night-time calibrations provided by the observatory

The SPHERE calibration plan foresees taking photometric standard stars for all imaging modes using broadband filters, and polarimetric standard stars for all polarimetric modes (polarized and zero-polarization standard stars). The calibration plan also foresees observing reference astrometric fields (binary systems or star clusters with high precision astrometry available) without coronagraph (including ND filters if needed to avoid detector saturation) on a regular basis (frequency ~1 week).

8.1.2 Optional night-time calibrations

Photometric standard stars in narrow band filters, or wavelength calibration for IRDIS_LSS, must be requested by the user and is charged to the observer. No spectro-photometric standards or telluric standard will be taken unless explicitly requested as special night-time calibrations. The time required to do so will be charged to the observer.

Day-time calibrations

In addition, all necessary day-time calibrations will be acquired by the observatory staff during the day following the night of the observations (or within the validity period indicated in the tables below). In the following tables, "Modes" refers to the instrument mode among IRDIFS, IRDIFS_EXT, IRDIS_DBI, IRDIS_CI, IRDIS_LSS, and ZIMPOL_I, ZIMPOL_P1, ZIMPOL_P2, when applicable. "Matching parameters" describes the most critical parameter for generating the automatic calibration. For instance, darks/backgrounds will have the same DIT as the science, flats will be taken in the same filter as the science, etc. On the other hand, ZIMPOL polarimetric calibrations will be done in corresponding broadband filters (see filter correspondence table below).

Table 16: Day-time calibrations for IRDIS.

Calibration	Modes	Matching parameter(s)	Validity
Background	all	DIT	1 day
Lamp Flat	all	Filter	1 day
Distortion map	All, except IRDIS_LSS	Filter, Coronagraph combination	1 week
Wavelength calibration	IRDIS_LSS	Slit/Grism combination	1 day

Table 17: Day-time calibrations for IFS.

Calibration	Modes	Matching parameter(s)	Validity
Dark	all	DIT	1 day
Lamp Flat	all	Prism	1 week
Wavelength calibration	all	Prism	1 week
Spectra registration	all	Prism	1 day
Distortion map	all	Filter (+dichroic), Coronagraph combination	1 week

Table 18: Day-time calibrations for ZIMPOL.

Calibration	Modes	Matching parameter(s)	Validity
Bias	all	mode	1 day
Dark	all	DIT, readout mode	on request
Imaging flat	all	Filter (+dichroic), readout mode, focal plane mask on substrate (if used)	1 day
Polarimetric flat	ZIMPOL_P1, ZIMPOL_P2	Filter (+dichroic), readout mode, focal plane mask on substrate (if used)	1 day
Modulation efficiency	ZIMPOL_P1, ZIMPOL_P2	Filter (+dichroic), readout mode	1 day

NOTE: ZIMPOL distortion maps are taken weekly in V, N_R, N_I for monitoring purposes.

Table 19: Filter correspondence table for ZIMPOL calibrations.

Filter of Science	Filter for imaging and polarimetric flat	Filter for modulation efficiency
Ha_NB	Ha_NB	N_R
OI_630	OI_630	N_R
HeI	HeI	V
V_S	V_S	V
V_L	V_L	V
730_NB	730_NB	N_R
I_L	I_L	N_R
RI	RI	RI
I_PRIM	I_PRIM	I_PRIM
R_PRIM	R_PRIM	R_PRIM
N_I	N_I	N_I
N_R	N_R	N_R
B_Ha	B_Ha	N_R
CntHa	CntHa	N_R
V	V	V
Cnt820	Cnt820	N_I
TiO_717	TiO_717	N_I
CH4_727	CH4_727	N_I
KI	KI	N_I
N_Ha	N_Ha	N_R
Cnt748	Cnt748	N_I

Astrometry

8.1.3 Instrumental distortion and detector orientation in IRDIFS and IRDIFS_EXT

Observations of the gobular cluster 47 Tuc have been used to calibrate the distortion, plate scale and true north orientation at the level of the IRDIS and IFS detectors. The cylindrical mirrors in the SPHERE common path are the main source for the optical distortion, hence these distortion effects are common to IRDIS and IFS, and they dominate the telescope distorsion effects (Maire et al. 2016). The SPHERE distortion at first order is an anamorphism of 0.60±0.02% between the horizontal and vertical pixel scales. This effect if uncorrected translates into an astrometric error of 6 mas at 1″, which is larger than the astrometric specifications for SPHERE (5 mas).

The following steps are required for accurately calibrating IRDIFS data :

> **IRDIS: there a very small anamorphic distortion between the x and y axes. It can be corrected by multiplying the Y coordinate by 1.0062+/-0.0002. This value has been calibrated during commissioning and was measured to be stable within the provided error bar;**
> **IFS: similarly to IRDIS, the IFS is affected by the same anamorphic distortion, but because the IFS field is rotated by +100.56 (counter-clockwise), the corrections to be applied are 1.0059 in x and 1.0011 in y.**
> **Field orientation: once the anamorphism is corrected, the position angle on sky of any object can be determined using the following formulas:**

Stabilization	Sub-system	Formula
Field	IRDIS	$PA_{sky} = PA_{detector} + POSANGLE + TN$
	IFS	$PA_{sky} = PA_{detector} + POSANGLE + TN + IFS_{offset}$
Pupil	IRDIS	$PA_{sky} = PA_{detector} + PARANGLE + TN + PUPIL_{offset}$
	IFS	$PA_{sky} = PA_{detector} + PARANGLE + TN + PUPIL_{offset} + IFS_{offset}$

With:

$PUPIL_{offset}$: 135.99 ± 0.11 deg
IFS_{offset}: -100.48 ± 0.13 deg
TN: true North correction (see below)
POSANG: position angle offset (input in the observing template)
PARANGLE: parallactic angle

8.1.4 Plate scale and true north orientation

Basic astrometry, i.e. plate scale and true north orientation is provided by the observatory on a regular basis using a few reference calibrators. We selected as main reference fields 47 Tucanae, the Orion Trapezium B1–B4, NGC 3603, and NGC 6380 (Tab. 1 and Fig. 1), as well as a handful of long-period binaries (HIP 67745, HIP 68725, HIP 102979) with Hipparcos data and separations larger than the IFS field of view (separations ~2–5″). The catalogs of the stellar positions for these fields come from various sources: Washington Double Star (WDS) catalog for the binaries, literature for the Orion Trapezium B1–B429 , and private requests for 47 Tucanae (A. Bellini/STScI), NGC 6380 (E. Noyola/Univ. Texas Austin), and NGC 360330 (Z. Khorrami/OCA). Additional details are given in Maire et al. (2016).

The true north TN is -1.75º ± 0.08º and was shown to be stable within error bars (Maire et al. 2016).

A missynchronization problem affected all data obtained before July 13 2016. For data taken in field tracking mode before July 13 2016, a correction factor epsilon has to be added to the true north using the formula

epsilon = ATAN(TAN((TEL.ALT - 2*TEL.PARANG.START - 2*INS4.DROT2.BEGIN)*pi/180))*180/pi

This missynchronization also affects the science data taken before July 13 2016 in pupil-tracking mode, but to a smaller extent (it can however be as large as 0.1º to 0.2º) because the rotation speed of the derotator is slower in this mode. The formula for correcting this drift for pupil-tracking data is

epsilon = ATAN(TAN((TEL.ALT -2*INS4.DROT2.BEGIN)*pi/180))*180/pi

This correction factor needs to be added to the parallactic angle of each pupil-tracking frame in order to derotate accurately the image.

Beware that if you need to recalculate the parallactic angle (for instance to stamp each individual frame of a cube), the target coordinate at the epoch of observation (e.g. epoch J201X.XX) can be retrieved directly from the keyword INS4.DROT2.RA/DEC. The RA/DEC keywords are indeed given in J2000 (therefore not corrected for the precession/nutation at the epoch of observation) and rely on the coordinate on the guide star used by the telescope which is assumed to have no proper motion.

The IRDIS plate scale was evaluated in the H2 filter with the N_ALC_YJH_S coronagraph. The value is 12.255 ± 0.021 mas/pix. The plate scale can be adjusted for different filters using the following relations :

> **plate_scale(H3)=plate_scale(H2)–0.005**
> **the plate_scale for J2/J3 is 0.004 mas/pix larger than for H2/H3**
> **the plate_scale for Y2/Y3 is 0.024 mas/pix larger than for H2/H3**
> **the plate scale for non-coronagraphic observations is 0.019+/-0.001 mas/pixel smaller than that for coronagraphic observations**

The plate scale of the IFS is 7.46±0.02 mas/pix.

A web page with updated information about astrometric calibrations with SPHERE will be posted here (please visit often when performing your True North calculations):
www.eso.org/sci/facilities/paranal/instruments/sphere/doc/Astrometry.html

9. SPHERE TEMPLATE PARAMETERS

The instrument, detector and telescope are controlled by OBs, which are made up of templates. Templates are divided into three categories: acquisition, observation and calibration.
Usually, OBs consist of an acquisition template and one or more observation templates for nighttime observations and, in some limited cases, an additional nighttime calibration template. Only one acquisition template is allowed in an OB, and therefore only one preset on sky. It is not possible e.g. to group in the same OB observation templates on the science object and calibration template on a standard star. The next sections provide a short summary of the templates offered from P95. These templates should cover most needs. If this is not the case, users must contact the User Support Department (usd-help@eso.org) well before the start of observations.

SPHERE Acquisition Templates

Telescope presets can only be done via acquisition templates and all observing blocks must start with one. There are six acquisition templates and they are to be used with nine different observation templates with the following associations:

SPHERE_irdifs_acq :
SPHERE_irdifs_obs
SPHERE_irdifs_ext_obs
SPHERE_irdis_acq:
SPHERE_irdis_ci_obs
SPHERE_irdis_dbi_obs
SPHERE_irdis_dpi_acq:
SPHERE_irdis_dpi_obs
SPHERE_irdis_lss_acq:
SPHERE_irdis_lss_obs
SPHERE_zimpol_i_acq:
SPHERE_zimpol_i_obs
SPHERE_zimpol_p_acq:
SPHERE_zimpol_p1_obs
SPHERE_zimpol_p2_obs

SPHERE_gen_acq_GoTo_acq.tsf (mode independent, concatenation only)

The setups allowed by each template are shown in Tables 21–26 in terms of the parameters which may be set. For example, the SPHERE_irdifs_acq (see Table 20) allows the setting of IRDIS and IFS coronagraphs, derotator mode (field or pupil tracking), adaptive optics (AO or no AO) and position angle offset.
The parameter SEQ.AO.ST specifies weth the AO loop should be closed (T) or opened (F). Unless specific calibration purposes, the state will therefore be T (loop closed).

SPHERE Observation Templates

The templates SPHERE_irdifs_obs and SPHERE_irdifs_ext_obs both use IRDIS and IFS together. They should be used for modes IRDIFS (Y-J range with IFS and H-band range with IRDIS) and IRDIFS_EXT (Y-H range with IFS, K-band range with IRDIS) as described in section 1.7. Please note that SPHERE_iridfs_obs and SPHERE_irdifs_ext_obs templates cannot be mixed within a

single OB; a new acquisition is necessary to go from the irdifs to the irdifs_ext sub-mode and vice-versa. The parameters which can be set to define your observations are shown in Table 27 and 28. The minimum DIT allowed is actually 0.83 seconds, and setting DIT to anything less (e.g. zero) sets it to 0.83 s. The SEQ.OBSTYPE.LIST parameter allows you include obs_flux (F), star_center (C), and sky (S) along with your science observations (O) in the order you prescribe (see section 6.4). The DITs and NDITs for each of these component observations are set separately using different parameters (e.g. SEQ.IFS.DIT.STARCENTER, SEQ.IRDIS.DIT.STARCENTER). However, the dithering parameters (e.g. SEQ.IRDIS.DITH.PATTERN) control all components (FCOS).

Table 20: SPHERE_irdifs_acq

SPHERE_irdifs_acq.tsf		
Parameter	Range *(Default)*	Label
INS.COMB.ICOR	N_4Q_YJH N_4Q_Ks N_ALC_Y N_ALC_YJ_S N_ALC_YJ_L N_ALC_YJH_S N_ALC_YJH_L N_ALC_Ks N_CLC_SW_S N_CLC_LW_S N_CLC_SW_L N_CLC_LW_L N_BAR N_NC_4QPM N_NC_ALC_1 N_NC_ALC_2 N_NC_CLC_1 N_NC_CLC_2 N_NS_VLT N_NS_CLEAR N_NS_APO_1 N_NS_APO_2 *(NODEFAULT)*	Infrared IRDIS coronagraph combination
INS.COMB.ROT	PUPIL FIELD *(NODEFAULT)*	Derotator and ADC modes combination
INS.CPRT.POSANG	0.0..360.0 *(0.0)*	Derotator position angle (deg)
INS.MODE	IRDIFS IRDIFS_EXT *(NODEFAULT)*	Instrument Mode
SEQ.AO.ST	T F *(T)*	SAXO state
SEQ.TARGET.HMAG	0..18 *(0)*	Target H magnitude
SEQ.TARGET.RMAG	0..18 *(0)*	Target R magnitude
TEL.AG.GUIDESTAR	NONE SETUPFILE CATALOGUE *(CATALOGUE)*	Telescope guide star selection
TEL.GS1.ALPHA	ra *(0.)*	RA of guide star
TEL.GS1.DELTA	dec *(0.)*	DEC of guide star
TEL.TARG.ALPHA	ra *()*	RA
TEL.TARG.DELTA	dec *()*	DEC
TEL.TARG.EPOCH	-2000..3000 *(2000)*	Epoch
TEL.TARG.EQUINOX	QUERY-TARG getEquinoxList *(2000)*	Equinox
TEL.TARG.PMA	-500..500 *(0)*	Proper motion in RA
TEL.TARG.PMD	-500..500 *(0)*	Proper motion in DEC

Table 21: SPHERE_irdis_acq

SPHERE_irdis_acq.tsf		
Parameter	Range *(Default)*	Label
INS.COMB.ICOR	N_4Q_YJH N_4Q_Ks N_ALC_Y N_ALC_YJ_S N_ALC_YJ_L N_ALC_YJH_S N_ALC_YJH_L N_ALC_Ks N_CLC_SW_S N_CLC_LW_S N_CLC_SW_L N_CLC_LW_L N_BAR N_S_LR_WL N_S_LR_WS N_S_MR_WL N_S_MR_NL N_S_LR_OPEN N_S_MR_OPEN N_NC_4QPM N_NC_ALC_1 N_NC_ALC_2 N_NC_CLC_1 N_NC_CLC_2 N_NS_VLT N_NS_CLEAR N_NS_APO_1 N_NS_APO_2 N_NS_OPAQUE *(NODEFAULT)*	Infrared IRDIS coronagraph combination
INS.COMB.ROT	FIELD PUPIL *(NODEFAULT)*	Derotator and ADC modes combination
INS.CPRT.POSANG	0.0..360.0 *(0.0)*	Derotator position angle (deg)
SEQ.AO.ST	T F *(T)*	SAXO state
SEQ.TARGET.HMAG	0..18 *(0)*	Target H magnitude
SEQ.TARGET.RMAG	0..18 *(0)*	Target R magnitude
TEL.AG.GUIDESTAR	NONE SETUPFILE CATALOGUE *(CATALOGUE)*	Telescope guide star selection
TEL.GS1.ALPHA	ra *(0.)*	RA of guide star
TEL.GS1.DELTA	dec *(0.)*	DEC of guide star
TEL.TARG.ALPHA	ra *()*	RA
TEL.TARG.DELTA	dec *()*	DEC
TEL.TARG.EPOCH	-2000..3000 *(2000)*	Epoch
TEL.TARG.EQUINOX	QUERY-TARG getEquinoxList *(2000)*	Equinox
TEL.TARG.PMA	-500..500 *(0)*	Proper motion in RA
TEL.TARG.PMD	-500..500 *(0)*	Proper motion in DEC

Table 22: SPHERE_irdis_dpi_acq

Parameter	Range (Default)	Label
INS.COMB.ICOR	N_4Q_YJH N_4Q_Ks N_ALC_Y N_ALC_YJ_S N_ALC_YJ_L N_ALC_YJH_S N_ALC_YJH_L N_ALC_Ks N_CLC_SW_S N_CLC_LW_S N_CLC_SW_L N_CLC_LW_L N_BAR N_S_LR_WL N_S_LR_WS N_S_MR_WL N_S_MR_NL N_S_LR_OPEN N_S_MR_OPEN N_NC_4QPM N_NC_ALC_1 N_NC_ALC_2 N_NC_CLC_1 N_NC_CLC_2 N_NS_VLT N_NS_CLEAR N_NS_APO_1 N_NS_APO_2 N_NS_OPAQUE (*N_ALC_YJH_S*)	Infrared IRDIS coronagraph combination
INS.CPRT.POSANG	0.0..360.0 *(0.0)*	Derotator position angle (deg)
SEQ.AO.ST	T F *(T)*	SAXO state
SEQ.TARGET.HMAG	0..18 *(0)*	Target H magnitude
SEQ.TARGET.RMAG	0..18 *(0)*	Target R magnitude
TEL.AG.GUIDESTAR	NONE SETUPFILE CATA-LOGUE *(CATALOGUE)*	Telescope guide star selection
TEL.GS1.ALPHA	ra *(0.)*	RA of guide star
TEL.GS1.DELTA	dec *(0.)*	DEC of guide star
TEL.TARG.ALPHA	ra *()*	RA
TEL.TARG.DELTA	dec *()*	DEC
TEL.TARG.EPOCH	-2000..3000 *(2000)*	Epoch
TEL.TARG.EQUINOX	QUERY-TARG getEquinoxList *(2000)*	Equinox
TEL.TARG.PMA	-500..500 *(0)*	Proper motion in RA
TEL.TARG.PMD	-500..500 *(0)*	Proper motion in DEC

Table 23: SPHERE_irdis_lss_acq

Parameter	Range (Default)	Label
INS.COMB.ICOR	N_S_LR_WL N_S_LR_WS N_S_MR_WL N_S_MR_NL (*NODEFAULT*)	Infrared IRDIS coronagraph combination
INS.CPRT.POSANG	0.0..360.0 *(0.0)*	Derotator position angle (deg)
SEQ.AO.ST	T F *(T)*	SAXO state
SEQ.TARGET.HMAG	0..18 *(0)*	Target H magnitude
SEQ.TARGET.RMAG	0..18 *(0)*	Target R magnitude
TEL.AG.GUIDESTAR	NONE SETUPFILE CATA-LOGUE *(CATALOGUE)*	Telescope guide star selection
TEL.GS1.ALPHA	ra *(0.)*	RA of guide star
TEL.GS1.DELTA	dec *(0.)*	DEC of guide star
TEL.TARG.ALPHA	ra *()*	RA
TEL.TARG.DELTA	dec *()*	DEC
TEL.TARG.EPOCH	-2000..3000 *(2000)*	Epoch
TEL.TARG.EQUINOX	QUERY-TARG getEquinoxList *(2000)*	Equinox
TEL.TARG.PMA	-500..500 *(0)*	Proper motion in RA
TEL.TARG.PMD	-500..500 *(0)*	Proper motion in DEC

Table 24: SPHERE_zimpol_i_acq

SPHERE_zimpol_i_acq.tsf		
Parameter	Range *(Default)*	Label
INS.COMB.VCOR	V_CLC_S_WF V_CLC_S_NF V_CLC_MT_WF V_CLC_M_WF V_CLC_M_NF V_CLC_L_WF V_CLC_XL_WF V_BAR V_4Q_SW V_4Q_LW V_NC_WF V_NC_NF V_CLC_M_WF_B V_CLC_L_WF_B *(NODEFAULT)*	Visible coronagraph combination
INS.CPRT.MODE	FIELD PUPIL *(FIELD)*	Pupil derotator mode
INS.CPRT.POSANG	0.0..360.0 *(0.0)*	Derotator position angle (deg)
INS.ZISL.NAME	BS_GREY DIC_HA *(BS_GREY)*	Position of the ZIMPOL/WFS selector
SEQ.AO.ST	T F *(T)*	SAXO state
SEQ.TARGET.RMAG	0..18 *(0)*	Target R magnitude
TEL.AG.GUIDESTAR	NONE SETUPFILE CATALOGUE *(CATALOGUE)*	Telescope guide star selection
TEL.GS1.ALPHA	ra *(0.)*	RA of guide star
TEL.GS1.DELTA	dec *(0.)*	DEC of guide star
TEL.TARG.ALPHA	ra *()*	RA
TEL.TARG.DELTA	dec *()*	DEC
TEL.TARG.EPOCH	-2000..3000 *(2000)*	Epoch
TEL.TARG.EQUINOX	QUERY-TARG getEquinoxList *(2000)*	Equinox
TEL.TARG.PMA	-500..500 *(0)*	Proper motion in RA
TEL.TARG.PMD	-500..500 *(0)*	Proper motion in DEC

Table 25: SPHERE_zimpol_p_acq

SPHERE_zimpol_p_acq.tsf		
Parameter	Range *(Default)*	Label
INS.COMB.VCOR	V_CLC_S_WF V_CLC_S_NF V_CLC_MT_WF V_CLC_M_WF V_CLC_M_NF V_CLC_L_WF V_CLC_XL_WF V_BAR V_4Q_SW V_4Q_LW V_NC_WF V_NC_NF V_CLC_M_WF_B V_CLC_L_WF_B *(NODEFAULT)*	Visible coronagraph combination
INS.CPRT.MODE	FIELD FIXED *(FIELD)*	Pupil derotator mode
INS.CPRT.POSANG	0.0..360.0 *(0.0)*	Derotator position angle (deg)
INS.ZISL.NAME	BS_GREY DIC_HA *(BS_GREY)*	Position of the ZIMPOL/WFS selector
SEQ.AO.ST	T F *(T)*	SAXO state
SEQ.TARGET.RMAG	0..18 *(0)*	Target R magnitude
TEL.AG.GUIDESTAR	NONE SETUPFILE CATALOGUE *(CATALOGUE)*	Telescope guide star selection
TEL.GS1.ALPHA	ra *(0.)*	RA of guide star
TEL.GS1.DELTA	dec *(0.)*	DEC of guide star
TEL.TARG.ALPHA	ra *()*	RA
TEL.TARG.DELTA	dec *()*	DEC
TEL.TARG.EPOCH	-2000..3000 *(2000)*	Epoch
TEL.TARG.EQUINOX	QUERY-TARG getEquinoxList *(2000)*	Equinox
TEL.TARG.PMA	-500..500 *(0)*	Proper motion in RA
TEL.TARG.PMD	-500..500 *(0)*	Proper motion in DEC

Table 26: SPHERE_obs

SPHERE_irdifs_obs.tsf		
Parameter	Range *(Default)*	Label
DET.IFS.DIT	0 2 4 8 16 32 64 *(0)*	IFS Detector Integration Time
DET.IFS.NDIT	1..1000 *(1)*	IFS Number of DIT
DET.IRDIS.DIT	0 2 4 8 16 32 64 *(0)*	IRDIS Detector Integration Time
DET.IRDIS.NDIT	1..1000 *(1)*	IRDIS Number of DIT
INS.COMB.IFLT	DB_H23 DB_H34 DB_NDH23 BB_H *(NO DEFAULT)*	IRDIS filter combination
INS.COMB.IND.FLUX	ND_N_0.0 ND_N_1.0 ND_N_2.0 ND_N_3.5 *(NODEFAULT)*	Infrared neutral density filters combination (flux)
INS.COMB.IND	ND_N_0.0 ND_N_1.0 ND_N_2.0 ND_N_3.5 *(NODEFAULT)*	Infrared neutral density filters combination
INS.COMB.ROT	PUPIL FIELD *(NODEFAULT)*	Derotator and ADC modes combination
INS.CPRT.POSANG	0.0..360.0 *(0.0)*	Derotator position angle (deg)
SEQ.IFS.DIT.FLUX	0 2 4 8 16 32 64 *(0)*	IFS Integration Time (flux)
SEQ.IFS.NDIT.FLUX	1..1000 *(1)*	IFS Number of integrations (flux)
SEQ.IFS.NDIT.SKY	1..1000 *(1)*	IFS Number of integrations (sky)
SEQ.IFS.NDIT.STARCENTER	1..1000 *(1)*	IFS Number of integrations (star center)
SEQ.IFS.NEXPO	1..100 *(1)*	IFS exposures per dithering position
SEQ.IRDIS.DIT.FLUX	0 2 4 8 16 32 64 *(0)*	IRDIS Integration Time (flux)
SEQ.IRDIS.DITH.NPATTERN	1..100 *(1)*	IRDIS dithering pattern repetitions
SEQ.IRDIS.DITH.PATTERN	1x1 2x2 4x4 6x6 8x8 10x10 *(4x4)*	IRDIS dithering pattern sequence
SEQ.IRDIS.NDIT.FLUX	1..1000 *(1)*	IRDIS Number of integrations (flux)
SEQ.IRDIS.NDIT.SKY	1..1000 *(1)*	IRDIS Number of integrations (sky)
SEQ.IRDIS.NDIT.STARCENTER	1..1000 *(1)*	IRDIS Number of integrations (star center)
SEQ.IRDIS.NEXPO	1..100 *(1)*	IRDIS exposures per dithering position
SEQ.OBSTYPE.LIST	F C O S *(NODEFAULT)*	Observation type (F, C, O, S)
SEQ.TARG.OFFSETALPHA .LIST	0..60 *(NODEFAULT)*	Sky RA offset list (arcsec)
SEQ.TARG.OFFSETDELTA .LIST	0..60 *(NODEFAULT)*	Sky DEC offset list (arcsec)
SEQ.TARG.OFFSETX	0..400 *(400)*	Detector X offset (mas)
SEQ.TARG.OFFSETY	0..400 *(400)*	Detector Y offset (mas)
SEQ.WAFFLE.AMPLITUDE	0..0.05 *(0.02)*	DM waffle pattern amplitude
SEQ.WAFFLE.ORIENTATION	x + *(x)*	DM waffle pattern orientation
Fixed values:		
SEQ.IFS.DITH.NPATTERN	1	IFS dithering pattern repetitions
SEQ.IFS.DITH.PATTERN	1x1	IFS dithering pattern sequence

Table 27: SPHERE_irdifs_ext_obs

SPHERE_irdifs_ext_obs.tsf		
Parameter	Range *(Default)*	Label
DET.IFS.DIT	0 2 4 8 16 32 64 *(0)*	IFS Detector Integration Time
DET.IFS.NDIT	1..1000 *(1)*	IFS Number of DIT
DET.IRDIS.DIT	0 2 4 8 16 32 64 *(0)*	IRDIS Detector Integration Time
DET.IRDIS.NDIT	1..1000 *(1)*	IRDIS Number of DIT
INS.COMB.IND.FLUX	ND_N_0.0 ND_N_1.0 ND_N_2.0 ND_N_3.5 *(NODEFAULT)*	Infrared neutral density filters combination (flux)
INS.COMB.IND	ND_N_0.0 ND_N_1.0 ND_N_2.0 ND_N_3.5 *(NODEFAULT)*	Infrared neutral density filters combination
INS.COMB.ROT	PUPIL FIELD *(NODEFAULT)*	Derotator and ADC modes combination
INS.CPRT.POSANG	0.0..360.0 *(0.0)*	Derotator position angle (deg)
SEQ.IFS.DIT.FLUX	0 2 4 8 16 32 64 *(0)*	IFS Integration Time (flux)
SEQ.IFS.NDIT.FLUX	1..1000 *(1)*	IFS Number of integrations (flux)
SEQ.IFS.NDIT.SKY	1..1000 *(1)*	IFS Number of integrations (sky)
SEQ.IFS.NDIT.STARCENTER	1..1000 *(1)*	IFS Number of integrations (star center)
SEQ.IFS.NEXPO	1..100 *(1)*	IFS exposures per dithering position
SEQ.IRDIS.DIT.FLUX	0 2 4 8 16 32 64 *(0)*	IRDIS Integration Time (flux)
SEQ.IRDIS.DITH.NPATTERN	1..100 *(1)*	IRDIS dithering pattern repetitions
SEQ.IRDIS.DITH.PATTERN	1x1 2x2 4x4 6x6 8x8 10x10 *(4x4)*	IRDIS dithering pattern sequence
SEQ.IRDIS.NDIT.FLUX	1..1000 *(1)*	IRDIS Number of integrations (flux)
SEQ.IRDIS.NDIT.SKY	1..1000 *(1)*	IRDIS Number of integrations (sky)
SEQ.IRDIS.NDIT.STARCENTER	1..1000 *(1)*	IRDIS Number of integrations (star center)
SEQ.IRDIS.NEXPO	1..100 *(1)*	IRDIS exposures per dithering position
SEQ.OBSTYPE.LIST	F C O S *(NODEFAULT)*	Observation type (F, C, O, S)
SEQ.TARG.OFFSETALPHA .LIST	0..60 *(NODEFAULT)*	Sky RA offset list (arcsec)
SEQ.TARG.OFFSETDELTA .LIST	0..60 *(NODEFAULT)*	Sky DEC offset list (arcsec)
SEQ.TARG.OFFSETX	0..400 *(400)*	Detector X offset (mas)
SEQ.TARG.OFFSETY	0..400 *(400)*	Detector Y offset (mas)
SEQ.WAFFLE.AMPLITUDE	0..0.2 *(0.05)*	DM waffle pattern amplitude
SEQ.WAFFLE.ORIENTATION	x + *(x)*	DM waffle pattern orientation
Fixed values:		
Parameter	Value	Label
INS.COMB.IFLT	DB_K12 ~~BB_K~~ *(NODEFAULT)*	IRDIS filter combination
SEQ.IFS.DITH.NPATTERN	1	IFS dithering pattern repetitions
SEQ.IFS.DITH.PATTERN	1x1	IFS dithering pattern sequence

Table 28: SPHERE_irdis_dbi_obs

SPHERE_irdis_dbi_obs.tsf		
Parameter	Range *(Default)*	Label
DET.IRDIS.DIT	0 2 4 8 16 32 64 *(0)*	IRDIS Detector Integration Time
DET.IRDIS.NDIT	1..1000 *(1)*	IRDIS Number of DIT
INS.COMB.IFLT	DB_Y23 DB_J23 DB_H23 DB_H32 DB_H34 DB_K12 DB_NDH23 DB_NDH32 *(DB_H23)*	IRDIS filter combination
INS.COMB.IND.FLUX	ND_N_0.0 ND_N_1.0 ND_N_2.0 ND_N_3.5 *(NODEFAULT)*	Infrared neutral density filters combination (flux)
INS.COMB.IND	ND_N_0.0 ND_N_1.0 ND_N_2.0 ND_N_3.5 *(NODEFAULT)*	Infrared neutral density filters combination
INS.COMB.ROT	FIELD PUPIL *(NODEFAULT)*	Derotator and ADC modes combination
INS.CPRT.POSANG	0.0..360.0 *(0.0)*	Derotator position angle (deg)
SEQ.IRDIS.DIT.FLUX	0 2 4 8 16 32 64 *(0)*	IRDIS Integration Time (flux)
SEQ.IRDIS.DITH.NPATTERN	1..100 *(1)*	IRDIS dithering pattern repetitions
SEQ.IRDIS.DITH.PATTERN	1x1 2x2 4x4 6x6 8x8 10x10 *(4x4)*	IRDIS dithering pattern sequence
SEQ.IRDIS.NDIT.FLUX	1..1000 *(1)*	IRDIS Number of integrations (flux)
SEQ.IRDIS.NDIT.SKY	1..1000 *(1)*	IRDIS Number of integrations (sky)
SEQ.IRDIS.NDIT.STARCENTER	1..1000 *(1)*	IRDIS Number of integrations (star center)
SEQ.IRDIS.NEXPO	1..100 *(1)*	Number of exposures
SEQ.OBSTYPE.LIST	F C O S *(NODEFAULT)*	Observation type (F, C, O, S)
SEQ.TARG.OFFSETALPHA.LIST	0..60 *(NODEFAULT)*	Sky RA offset list (arcsec)
SEQ.TARG.OFFSETDELTA.LIST	0..60 *(NODEFAULT)*	Sky DEC offset list (arcsec)
SEQ.TARG.OFFSETX	0..400 *(400)*	Detector X offset (mas)
SEQ.TARG.OFFSETY	0..400 *(400)*	Detector Y offset (mas)
SEQ.WAFFLE.AMPLITUDE	0..0.2 *(0.05)*	DM waffle pattern amplitude
SEQ.WAFFLE.ORIENTATION	x + *(x)*	DM waffle pattern orientation

Table 29: SPHERE_irdis_ci_obs

SPHERE_irdis_ci_obs.tsf		
To be specified:		
Parameter	Range *(Default)*	Label
DET.IRDIS.DIT	0 2 4 8 16 32 64 *(0)*	IRDIS Detector Integration Time
DET.IRDIS.NDIT	1..1000 *(1)*	IRDIS Number of DIT
INS.COMB.IFLT	BB_Y BB_J BB_H BB_Ks NB_HeI NB_CntJ NB_PaB NB_CntH NB_FeII NB_CntK1 NB_H2 NB_BrG NB_CO NB_CntK2 *(NODEFAULT)*	IRDIS filter combination
INS.COMB.IND.FLUX	ND_N_0.0 ND_N_1.0 ND_N_2.0 ND_N_3.5 *(NODEFAULT)*	Infrared neutral density filters combination (flux)
INS.COMB.IND	ND_N_0.0 ND_N_1.0 ND_N_2.0 ND_N_3.5 *(NODEFAULT)*	Infrared neutral density filters combination
INS.COMB.ROT	FIELD PUPIL *(NODEFAULT)*	Derotator and ADC modes combination
INS.CPRT.POSANG	0.0..360.0 *(0.0)*	Derotator position angle (deg)
SEQ.IRDIS.DIT.FLUX	0 2 4 8 16 32 64 *(0)*	IRDIS Integration Time (flux)
SEQ.IRDIS.DITH.NPATTERN	1..100 *(1)*	IRDIS dithering pattern repetitions
SEQ.IRDIS.DITH.PATTERN	1x1 2x2 4x4 6x6 8x8 10x10 *(4x4)*	IRDIS dithering pattern sequence
SEQ.IRDIS.NDIT.FLUX	1..1000 *(1)*	IRDIS Number of integrations (flux)
SEQ.IRDIS.NDIT.SKY	1..1000 *(1)*	IRDIS Number of integrations (sky)
SEQ.IRDIS.NDIT.STARCENTER	1..1000 *(1)*	IRDIS Number of integrations (star center)
SEQ.IRDIS.NEXPO	1..100 *(1)*	Number of exposures
SEQ.OBSTYPE.LIST	F C O S *(NODEFAULT)*	Observation type (F, C, O, S)
SEQ.TARG.OFFSETALPHA .LIST	0..60 *(NODEFAULT)*	Sky RA offset list (arcsec)
SEQ.TARG.OFFSETDELTA .LIST	0..60 *(NODEFAULT)*	Sky DEC offset list (arcsec)
SEQ.TARG.OFFSETX	0..400 *(400)*	Detector X offset (mas)
SEQ.TARG.OFFSETY	0..400 *(400)*	Detector Y offset (mas)
SEQ.WAFFLE.AMPLITUDE	0..0.2 *(0.05)*	DM waffle pattern amplitude
SEQ.WAFFLE.ORIENTATION	x + *(x)*	DM waffle pattern orientation

Table 30: SPHERE_irdis_dpi_obs

SPHERE_irdis_dpi_obs.tsf		
Parameter	Range *(Default)*	Label
DET.IRDIS.DIT	0 2 4 8 16 32 64 *(0)*	IRDIS Detector Integration Time
DET.IRDIS.NDIT	1..1000 *(1)*	IRDIS Number of DIT
INS.COMB.IFLT	DP_0_BB_Y DP_0_BB_J	IRDIS filter combination
	DP_0_BB_H DP_0_BB_Ks	
	DP_0_NB_HeI DP_0_NB_CntJ	
	DP_0_NB_PaB DP_0_NB_CntH	
	DP_0_NB_FeII DP_0_NB_CntK1	
	DP_0_NB_H2 DP_0_NB_BrG	
	DP_0_NB_CO DP_0_NB_CntK2	
	DP_45_BB_Y DP_45_BB_J	
	DP_45_BB_H DP_45_BB_Ks	
	DP_45_NB_HeI DP_45_NB_CntJ	
	DP_45_NB_PaB DP_45_NB_CntH	
	DP_45_NB_FeII DP_45_NB_CntK1	
	DP_45_NB_H2 DP_45_NB_BrG	
	DP_45_NB_CO DP_45_NB_CntK2	
	(NODEFAULT)	
INS.COMB.IND	ND_N_0.0 ND_N_1.0 ND_N_2.0 ND_N_3.5 *(NODEFAULT)*	Infrared neutral density filters combination
INS.CPRT.POSANG	0.0..360.0 *(0.0)*	Derotator position angle (deg)
SEQ.IRDIS.NEXPO	1..100 *(1)*	Number of exposures
SEQ.IRDIS.POL.STOKES	Q QU *(QU)*	Stoke parameter measure
SEQ.POL.NCYCLE	1..100 *(1)*	Number of polarimetric cycles
SEQ.POL.OFFSET.GAMMA	-360..360 *(0)*	Polarization: gamma parameter (degrees)
Fixed values:		
Parameter	Value	Label
INS.COMB.ROT	FIELD	Derotator and ADC modes combination

Table 31: SPHERE_irdis_lss_obs

SPHERE_irdis_lss_obs.tsf		
Parameter	Range *(Default)*	Label
DET.IRDIS.DIT	0 2 4 8 16 32 64 *(0)*	IRDIS Detector Integration Time
DET.IRDIS.NDIT	1..1000 *(1)*	IRDIS Number of DIT
INS.COMB.IND	ND_N_0.0 ND_N_1.0 ND_N_2.0 ND_N_3.5 *(NODEFAULT)*	Infrared neutral density filters combination
INS.CPRT.POSANG	0.0..360.0 *(0.0)*	Derotator position angle (deg)
SEQ.IRDIS.NEXPO	1..100 *(1)*	Number of exposures

Table 32: SPHERE_zimpol_p1_obs

SPHERE_zimpol_p1_obs.tsf		
Parameter	Range *(Default)*	Label
DET.ZIMPOL.DIT	0..1200 *(1.3)*	Integration time
DET.ZIMPOL.NDIT	1..1000 *(2)*	Number of integrations
DET.ZIMPOL.READOUT	FastPolarimetry SlowPolarimetry *(FastPolarimetry)*	ZIMPOL read-out mode
DET.ZIMPOL.SHUTTER	Enabled Disabled *(Disabled)*	ZIMPOL detector shutter
INS.ZCSL.NAME	OPEN COMP *(COMP)*	ZIMPOL polarization compensator selector
INS.ZCTT.POS	-90.0..90.0 *(25.0)*	ZIMPOL polarization compensator, tilt angle
INS.ZIFW0.NAME	OPEN P_VIS PQ_VIS Q_VIS ND_1.0 ND_2.0 ND_4.0 Ha_NB OI_630 HeI V_S V_L 730_NB I_L *(OPEN)*	ZIMPOL common filter wheel
INS.ZIFW1.NAME	OPEN VBB I_PRIM R_PRIM N_I N_R B_Ha CntHa V Cnt820 TiO_717 CH4_727 KI *(N_R)*	Arm 1 filter
INS.ZIFW2.NAME	OPEN VBB I_PRIM R_PRIM N_I N_R B_Ha CntHa V Cnt820 N_Ha Cnt748 PUPIM *(N_R)*	Arm 2 filter
SEQ.ZIMPOL.DITH.PATTERN .LIST	-14..14 *(-14 -14 0 0 +14 +14)*	List of pixel coordinates for dithering
SEQ.ZIMPOL.FIELD.POS	0 1 2 3 4 5 6 7 8 9 *(0)*	Field position on ZIMPOL detector
SEQ.ZIMPOL.NEXPO	1..100 *(1)*	Number of exposures per dithering position
SEQ.ZIMPOL.NPOL	1..100 *(1)*	ZIMPOL - Number of polarimetric cycles
SEQ.ZIMPOL.POL.GAMMA	0..360 *(0)*	ZIMPOL - Polarization: gamma parameter.
SEQ.ZIMPOL.POL.PCOMLOOP	T F *(F)*	Initial computation of PCOM tilt angle
SEQ.ZIMPOL.POL.STOKES	Q QU QnoSwitch *(QU)*	Defines if we measure (+Q,-Q) or (+Q,-Q,+U,-U)

Table 33: SPHERE_zimpol_p2_obs

SPHERE_zimpol_p2_obs.tsf		
Parameter	Range *(Default)*	Label
DET.ZIMPOL.DIT	0..1200 *(1.3)*	Integration time
DET.ZIMPOL.NDIT	1..1000 *(2)*	Number of integrations
DET.ZIMPOL.READOUT	FastPolarimetry SlowPolarimetry *(FastPolarimetry)*	ZIMPOL read-out mode
DET.ZIMPOL.SHUTTER	Enabled Disabled *(Disabled)*	ZIMPOL detector shutter
INS.ZCSL.NAME	OPEN COMP *(COMP)*	ZIMPOL polarization compensator selector
INS.ZCTT.POS	-90.0..90.0 *(25.0)*	ZIMPOL polarization compensator, tilt angle
INS.ZIFW0.NAME	OPEN P_VIS PQ_VIS Q_VIS ND_1.0 ND_2.0 ND_4.0 Ha_NB OI_630 HeI V_S V_L 730_NB I_L *(OPEN)*	ZIMPOL common filter wheel
INS.ZIFW1.NAME	OPEN VBB I_PRIM R_PRIM N_I N_R B_Ha CntHa V Cnt820 TiO_717 CH4_727 KI *(N_R)*	Arm 1 filter
INS.ZIFW2.NAME	OPEN VBB I_PRIM R_PRIM N_I N_R B_Ha CntHa V Cnt820 N_Ha Cnt748 PUPIM *(N_R)*	Arm 2 filter
SEQ.ZIMPOL.DITH.PATTERN.LIST	-14..14 *(-14 -14 0 0 +14 +14)*	List of pixel coordinates for dithering
SEQ.ZIMPOL.FIELD.POS	0 1 2 3 4 5 6 7 8 9 *(0)*	Field position on ZIMPOL detector
SEQ.ZIMPOL.FIELD.POSANG	0..360 *(0.0)*	Field orientation on detector
SEQ.ZIMPOL.NEXPO	1..100 *(1)*	Number of exposures per dithering position
SEQ.ZIMPOL.NPOL	1..100 *(1)*	ZIMPOL - Number of polarimetric cycles
SEQ.ZIMPOL.POL.GAMMA	0..360 *(0)*	ZIMPOL - Polarization: gamma parameter.
SEQ.ZIMPOL.POL.STOKES	Q QU QnoSwitch *(QU)*	Defines if we measure (+Q,-Q) or (+Q,-Q,+U,-U)

Table 34: SPHERE_zimpol_i_obs

SPHERE_zimpol_i_obs.tsf		
Parameter	Range *(Default)*	Label
DET.ZIMPOL.DIT	0..1200 *(1.3)*	Integration time
DET.ZIMPOL.NDIT	1..1000 *(1)*	Number of integrations
DET.ZIMPOL.READOUT	StandardImaging SnapShotImaging *(StandardImaging)*	ZIMPOL read-out mode
DET.ZIMPOL.SHUTTER	Enabled Disabled *(Disabled)*	ZIMPOL detector shutter
INS.CPRT.MODE	FIELD PUPIL *(FIELD)*	Pupil derotator mode
INS.ZIFW0.NAME	OPEN P_VIS PQ_VIS Q_VIS ND_1.0 ND_2.0 ND_4.0 Ha_NB OI_630 HeI V_S V_L 730_NB I_L *(OPEN)*	ZIMPOL common filter wheel
INS.ZIFW1.NAME	OPEN VBB I_PRIM R_PRIM N_I N_R B_Ha CntHa V Cnt820 TiO_717 CH4_727 KI *(N_R)*	Arm 1 filter
INS.ZIFW2.NAME	OPEN VBB I_PRIM R_PRIM N_I N_R B_Ha CntHa V Cnt820 N_Ha Cnt748 PUPIM *(N_R)*	Arm 2 filter
SEQ.ZIMPOL.DITH.PATTERN.LIST	-14..14 *(-14 -14 0 0 +14 +14)*	List of pixel coordinates for dithering
SEQ.ZIMPOL.FIELD.POS	0 1 2 3 4 5 6 7 8 9 *(0)*	Field position on ZIMPOL detector
SEQ.ZIMPOL.FIELD.POSANG	0..360 *(0.0)*	Field orientation on detector
SEQ.ZIMPOL.NEXPO	1..100 *(1)*	Number of exposures per dithering position

SPHERE Night-time Calibration Templates

There are three calibration templates that can be useful for night time observations to support science. SPHERE_irdis_lss_obs_sky SPHERE_irdis_lss_obs_sky allow to get additional sky backgrounds and a telluric standard star respectively, in LSS mode, and SPHERE_zimpol_i_cal_star_center estimates the stellar position just as with the IRDIS star_center observations. The parameters which may be modified for these templates are shown in Tables 36-38.

Table 35: SPHERE_irdis_lss_obs_sky

SPHERE_irdis_lss_obs_sky.tsf		
To be specified:		
Parameter	Range *(Default)*	Label
DET.IRDIS.DIT	0 2 4 8 16 32 64 *(0)*	IRDIS Detector Integration Time
DET.IRDIS.NDIT	1..1000 *(1)*	IRDIS Number of DIT
INS.COMB.IFLT	S_LR S_MR *(NODEFAULT)*	IRDIS filter combination
INS.COMB.IND	ND_N_0.0 ND_N_1.0 ND_N_2.0 ND_N_3.5 *(NODEFAULT)*	Infrared neutral density filters combination
INS.CPRT.POSANG	0.0..360.0 *(0.0)*	Derotator position angle (deg)
SEQ.SKY.TARG.OFFSETALPHA.LIST	0..60 *(NODEFAULT)*	Sky RA offset list (arcsec)
SEQ.SKY.TARG.OFFSETDELTA.LIST	0..60 *(NODEFAULT)*	Sky DEC offset list (arcsec)

Table 36: SPHERE_irdis_lss_obs_telluric

SPHERE_irdis_lss_obs_telluric.tsf		
To be specified:		
Parameter	Range *(Default)*	Label
DET.IRDIS.DIT	0 2 4 8 16 32 64 *(0)*	IRDIS Detector Integration Time
DET.IRDIS.NDIT	1..1000 *(1)*	IRDIS Number of DIT
INS.COMB.IND	ND_N_0.0 ND_N_1.0 ND_N_2.0 ND_N_3.5 *(NODEFAULT)*	Infrared neutral density filters combination
INS.CPRT.POSANG	0.0..360.0 *(0.0)*	Derotator position angle (deg)
SEQ.TARG.OFFSETX	0..500 *(500)*	Detector X offset (mas)

Table 37: SPHERE_zimpol_i_obs_star_center

SPHERE_zimpol_i_obs_star_center.tsf		
To be specified:		
Parameter	Range *(Default)*	Label
DET.ZIMPOL.DIT	0..1200 *(1.1)*	Integration time
DET.ZIMPOL.NDIT	1..1000 *(1)*	Number of integrations
SEQ.WAFFLE.AMPLITUDE	0..0.2 *(0.05)*	DM waffle pattern amplitude
SEQ.WAFFLE.ORIENTATION	x + *(x)*	DM waffle pattern orientation

10. DATA REDUCTION

Obtaining calibration files from the ESO archive
Darks and flats are taken every morning after SPHERE observations, in the appropriate filters and with the appropriate exposure times for the science data. Moreover, to check the health of the instrument, calibrations are also taken on a weekly basis using standard setups (see chapter on the calibration plan). One can download necessary calibration files from the ESO Data Archive (archive.eso.org/eso/eso_archive_main.html). For example, to download IRDIS calibrations from the archive page, one can enter the *Start* and *End* UT dates for the data they want. Furthermore, one can select *SPHERE/VLT* under *Imaging, CALIB* under *Category, Dark* under *Data Product Info:Type.* If desired one can also choose the exposure time under *Instrumental Setup: Exptime.* Pressing the *Search* button displays the calibrations available for download. **To pin point calibrations more rapidly and avoid downloading unnecessary files, one can use the SPHERE specific form which allows to narrow down the searchs with help of header keywords**:

`archive.eso.org/wdb/wdb/eso/sphere/form`

The data reduction procedures are described in the SPHERE pipeline manual. For a short summary we outline the principal steps for each instrument:

IFS reduction cascade summary

1. **Correction using a dark frame taken with the IFS shutter closed and all internal lamps off. In this step hot pixels and cosmic ray hits are removed and the background subtracted. The IFS background is dominated by thermal emission, which depends on the temperature of the instrument.**
2. **Correction for the wavelength-dependent detector flat-field (pixel-to-pixel response variations). This needs at least three detector flats taken at different wavelengths, possibly another one taken in white light. These are taken with IFS shutter closed and one of its internal calibration sources switched on.**
3. **Wavelength calibration using a pixel description table that holds the wavelengths assigned to each pixel, its illumination fraction, and spectrum ID. This table is made in two steps: First, spectra are detected on an external flat-field frame with IFS shutter open and the external white light calibration source switched on. Then, a wavelength solution is found on a frame where again IFS shutter is open and 3 or 4 of the monochromatic external calibration sources are switched on. Wavelength calibration is obtained using an integrating sphere and laser lines at 0.9877, 1.1237, 1.3094, and 1.5451 (μm).**
4. **Application of an IFU flat. This corrects for throughput variations between individual lens-lets (spaxels). It is derived from the same flat-field as used in the first step 3.**
5. **Construction of a cube of evenly spaced monochromatic planes. This is actually the endpoint of the automated pipeline. Note that it does not combine several cubes. The results can be fed to (manually operated) data analysis recipes or dedicated software packages.**

IRDIS reduction cascade summary

10.1.1 DBI, classical imaging
Data reduction of DBI and classical imaging mode data is as follows:

1. **Correction using a dark frame.**
2. **Application of the internal flat-field.**
3. **Determination of the position of the optical axis in each of the two simultaneous images. To do this, a dedicated calibration is used where a waffle pattern is applied to SPHERE's high-order deformable mirror. This causes four off-axis peaks to appear (even in coronagraphic images), the positions of which are detected and measured. Their centers of illumination are then used as center of rotation and to align the two frames.**
4. **The combination of all input frames. This includes optionally de-rotation, spectral differencing, and angular differencing.**

10.1.2 Long slit spectroscopy
Data reduction of LSS mode data is as follows:

1. **Correction using dark.**
2. **Application of internal flat.**
3. **Wavelength calibration, taken the same way as for IFS.**
4. **Combination of all input frames. Output is a frame that has wavelengths assigned to each pixel. The extraction of a spectrum, e.g. a correction for telluric absorption that is measured in the same way on a calibration star, is left to the user.**

The DPI mode of IRDIS works essentially the same way as the other imaging modes. The pipeline does not currently provide any (polarimetric) analysis recipes.

ZIMPOL reduction cascade summary
Because of the stripe mask on the ZIMPOL detector, all recipes include a pre-processing step that re-orders the image rows into logical and viewable images. All recipes provide these pre-processed data as optional output.

10.1.3 Imaging
The principal calibration steps for imaging are:

1. **Subtraction of the bias level. The default method is a subtraction of the mean value for the overscan pixels. A bias frame subtraction can be used if a fixed read-out noise pattern is present.**
2. **Possibly a subtraction of a dark frame of matching exposure time or interpolated to a matching exposure time. For short integration times (e.g. <30 s) this is not needed. Noise in the dark frame may add noise to the science image.**
3. **Flat-fielding with flat field calibration frames taken with the same filter (and the same focal plane coronagraph plate if a coronagraph on a substrate is used).**
4. **Combination of all frames using optionally some filtering of outliers. The combination includes back-shifting of dithered images and optionally also the derotation of the frames.**

The ZIMPOL QuickLook RTD (real time display) shows the pre-processed, overscan bias subtracted image of the first frame in an exposure.

10.1.4 Polarimetry
The principle calibration steps for polarimetry are:

1. **Subtraction of the bias level. For slow polarimetry a subtraction of the mean value for the overscan pixels provides good results. For fast polarimetry, a bias frame subtraction should be used to remove the fixed read-out column feature.**
2. **Dark current correction as for imaging**
3. **Correction for the modulation-demodulation efficiency. This is derived from frames illuminated evenly by the 100% polarized flat field calibration source and corrects for the pixel-dependent efficiency to in shifting charges back and forth during integration, thus measuring polarization. The modulation-demodulation efficiency calibration is only applied to the polarization frame.**
4. **Flatfielding as for imaging. The flatfielding is only applied to the intensity frame.**
5. **Combination of all frames as for imaging (with dithering and rotation corrections) and derivation of the intensity image and Q, or U polarization state.**

The ZIMPOL QuickLook RTD shows the pre-processed, overscan bias subtracted intensity frame (top) and the polarimetrically combined fractional polarization frame (bottom) for the two first frames of an exposure.

AO performance monitoring

The AO system of SPHERE generates parameter files accessible through the archive.
These file are multi-extension fits files containing binary tables and images. One file is generated every time a new acquisition template is run. It stores every 20s the strehl, atmospheric parameters estimated by the real time calculator (turbulent wind speed, Fried parameter, seeing) and other AO internal parameters (flux on the visible wavefront sensor and infra-red DTTS camera) and every 30s the image of the DTTS camera (for coronagraphic near-infrared observations).
This information can be useful for atmospheric and performance monitoring and the DTTS image can be used to monitor the photometry.
These files are accessible in the dedicated SPHERE archive query form
http://archive.eso.org/wdb/wdb/eso/sphere/form by entering OBJECT,AO in the DPR TYPE field (User defined input) in addition to the night of observation.

OVERHEADS

The most important contributors to overheads are:

a. **Target acquisition: this strongly dominates the overheads when staying on the same target less than 1hr.**
b. **Detector: overheads associated to the detector operations.**

Additionally, the HW setup changes (including dithering, filter or HWP swapping) also contribute, depending on the observing sequence.

Target acquisition

Target acquisition (whenever a new target is pointed at) includes the telescope preset (= 6 min, see, e.g. http://www.eso.org/sci/facilities/paranal/cfp/cfp95/overheads.html), AO loop closing (including the measurement of flux, performance, and the check of the selected setup). Given the small fields of view of the 3 instruments accurate coordinates and proper motions of all targets are mandatory. In case the initial pointing is not accurate enough to guarantee that the AO sensors detect the star within its ~2'' FoV, larger FoV images should be obtained by the operator. This could easily cost an additional 2 minutes.

If the coronagraph set-up has been changed (or if the previous check is older than typically one hour), it is recommended to repeat the coronagraph centering.

Observing Blocks (OBs) typically last 1 hour. Hence, in Service Mode, single OBs or the first OB in a concatenation must take into account the overhead for centering given in Table 38. In Visitor Mode, the overhead mentioned in Table 38 should be taken into account every hour.

Table 38: Target acquisition execution times for all acquisition templates, including the 6 min of telescope preset, along with typical execution times for star center (C), and flux (F).

Action	Approximate duration
Acquisition	10 min **(including 6 min of telescope preset)**
Coronagraph centering	+ 5 min
Star Center – C	+ 3.5 min
Flux – F	+ 3.5 min

NIR observation overheads

The formula to compute execution time for IRDIS and IFS, including overheads, are:

time_IFS = (O_START_IFS + NDIT_IFS * (DIT_DELAY_IFS + DIT_IFS + ROT_IFS) + O_EXP_IFS) * NEXP_IFS

time_IRD = ((T_START_IRD + NDIT_IRD * (DIT_DELAY_IRD + DIT_IRD + ROT_IRD) + O_EXP_IRD) * NEXPO_IRD + O_DITH_IRD) * NDITHER * NPATTERN

The total execution for an IRDIFS sequence is :

time_obs = MAX(time_IFS, time_IRD)

In these formulas, DIT_IFS and DIT_IRD are the detector integration times for IFS and IRDIS, NDIT_IFS and NDIT_IRD the number of DITs, NEXP_IFS the number of IFS exposures, NDITHER the number of dithering positions for IRDIS, NEXPO_IRD the number of exposures per dithering position, ROT_IFS and ROT_IRD the readout times, DIT_DELAY_IFS and

DIT_DELAY_IRD an additional readout delay, and O_* various detector and mechanical overheads for IFS and IRDIS. The value of these overheads are given in the table below.
Note that the minimum DIT for IRDIS is 0.838 s for IRDIS, while it is 1.65 s for IFS. You have to take this different into account when trying to match the execution time of IRDIFS observations.

Table 39: Overheads for IFS and IRDIS observations

Operation	IFS	IRDIS
O_START	0.3	0.3
DIT_DELAY	0.2	0.1
ROT	1.65	0.838
O_EXP	1.1	1.1
O_DITH_IRD		1.77

ZIMPOL observation overheads
The formula to compute typical ZIMPOL execution times, including overheads is:
(DIT + O_DIT) * NDIT * NEXPO * CYCLE * NPOL * NDITH * NETA + O_EXPO * NEXPO * CYCLE * NPOL * NDITH * NETA + O_NPOL * CYCLE * NPOL * NDITH * NETA + O_DITH * NDITH * NETA + O_ETA * NETA
Where DIT is the detector integration time, O_DIT, the DIT overhead, NDIT, the number of DITs, NEXPO, the number of exposures per position, O_EXPO, the exposure overhead, NPOL, the number of polarimetric cycles (CYCLE = 1 for QnoSwitch, 2 for Q, 4 for QU), NDITH, the number of dithering positions, O_DITH the overhead associated with dithering, NETA, the number of field angles, O_NETA, the overhead associated with derotator setting.

Table 40: ZIMPOL approximate overheads.

Mode	FastPol	SlowPol	StdI
O_DIT	0.1	0.1	0.1
O_EXPO	3	13	3

Table 41: HW setup overheads in ZIMPOL observations.

Operation	Overhead
O_NPOL	5
O_DITH	5
O_ETA	5

Typical examples (CYCLE = 2, Q):

	DIT	NDIT	NEXPO	NPOL	NDITH	NETA	OST	Duration		Effic.
								(s)	**(min)**	
SlowPol	50	2	2	2	1	3	2400	2852	47	0.84
FastPol	1.2	50	1	2	3	3	2160	2688	45	0.8
StdI	5	6	2	N/A	40	N/A	2400	2888	48	0.83

APPENDIX

A1. Detector properties

A1.1 IRDIS and IFS detectors

IRDIS and IFS are equipped with a 2Kx2K Hawaii-2RG arrays manufactured by Teledyne Imaging Sensors. The detectors are operated with cryogenic preamplifiers located next to the focal plane and operating at temperatures of ~80 K. The data acquisition system is the ESO New Generation Controller (NGC). The controller reads all the 32 video channels of each of the two Hawaii-2RG detectors in parallel.

Table 42: IRDIS and IFS detector properties.

	IRDIS	**IFS**
Detector arrays	2k x 2k (2k x 1k read) Hawaii-2RG	2k x 2k Hawaii-2RG
Readout mode	Non destructive sampling (NonDest)	Non destructive sampling (NonDest)
Readout noise	4 (long DIT) - 10 (short DIT) e^- rms/pix/readout	4 (long DIT) - 10 (short DIT) e^- rms/pix/readout
Dark current	Negligible	Negligible
Gain	1.75 e^-/ADU	1.8 e^-/ADU
Quantum efficiency	>95% from Y to K	>95% from Y to H
MINDIT/readout time	0.83s	1.66s
Linearity and saturation	0.1% up to 10^5 e^- 15000 ADU for DIT=0.83s 25000 ADU for DIT=4s 30000 ADU for DIT>8s	0.1% up to 10^5 e^- 15000 ADU for DIT=1.66s 25000 ADU for DIT=8s 30000 ADU for DIT>16s

A1.2 ZIMPOL detectors

The ZIMPOL detectors CCD1 and CCD2 consist of 4k x 2k pixel, back-illuminated, frame transfer CCDs (e2v CCD 44-82 bi) with 15 μm x 15 μm pixels. They have two read-out registers which work in parallel, each reading out half a line. The 2k x 2k CCD is in all modes operated like a 1k x 1k pixel CCD with 2 x 2 pixel binning allowing faster read-out and providing an effective pixel size of 30 μm x 30 μm. The saturation limit is at 65000 while linearity is at 63000 ADUs.

Table 43: ZIMPOL detector and readout mode properties.

	Fast polarimetry	**Slow polarimetry**	**Standard Imaging**
Science application	high precision polarimetry of targets with intermediate brightness (R ~ 3-7 mag) in broad band filters	photon noise limited polarimetry of faint targets, or bright star observations of the outer PSF or in narrow band filters	Standard imaging, when polarization information is not needed
Modulation: frequency, time	967 Hz, 1.03 ms	27 Hz, 37ms	N/A
Row shift time (binned row)	54.7 μs	72.3 μs	N/A
Detector field of view*	3.5"×3.5", 1024 × 512 pix	3.5"× 3.5", 1024 × 512 pix	3.5"×3.5", 1024 × 512 pix
Integration times: min-max	1.2 – 100 s	10 – 1000 s	1.2 – 1000 s
Frame transfer time	56 ms	74 ms	66 ms
Max. frame rate	0.86 Hz	0.1 Hz	0.86 Hz
Shutter use	Not offered	Not offered	Not offered
Readout: noise, frequency	20 e⁻, 625 kHz	3 e⁻, 100 kHz	20 e⁻, 625 kHz
Gain, well depth	10.5 e⁻/ADU, 670 ke⁻	1.5 e⁻/ADU, 100 ke⁻	10.5 e⁻/ADU, 670 ke⁻
Dark current	0.2 e⁻/(s pix)	0.015 e⁻/(s pix)	0.2 e⁻/(s pix)

Effective field of view for one polarization mode I_0 or I_{90}.
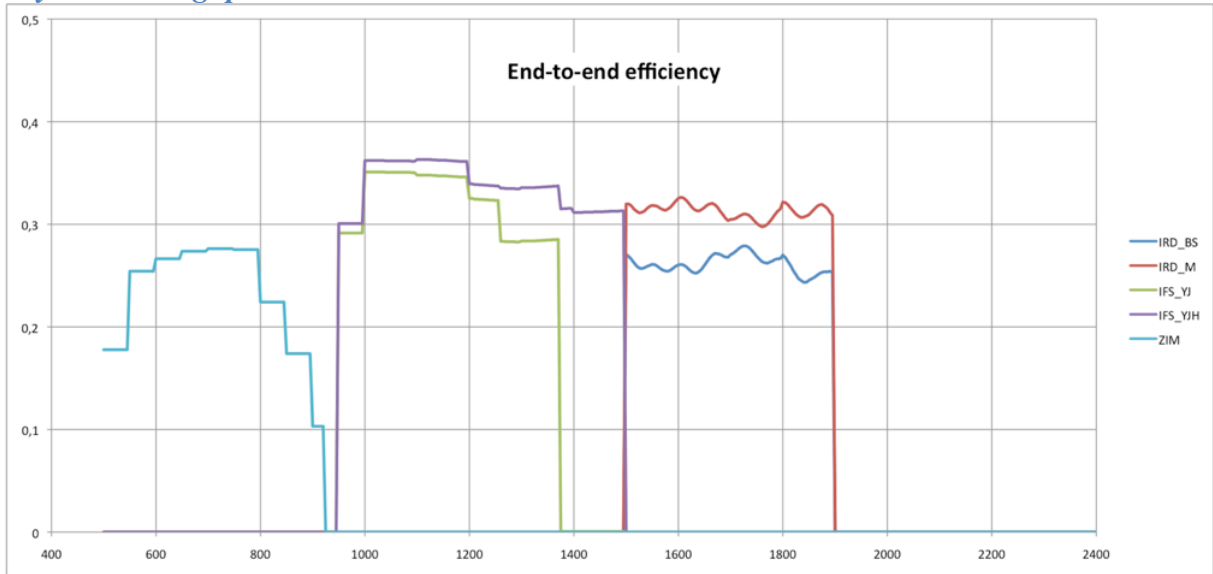
A2. System throughput

Figure 29: Transmission from SPHERE entrance to the science detectors, including the detector efficiency, assuming i) no coronagraph, ii) ZIMPOL path goes through the GREY beamsplitter (80% to ZIMPOL), and iii) the H dichroic separating the flux between IFS (up to 1450 nm) and IRDIS. Note that IRDIS cannot observe in K band in this setup.
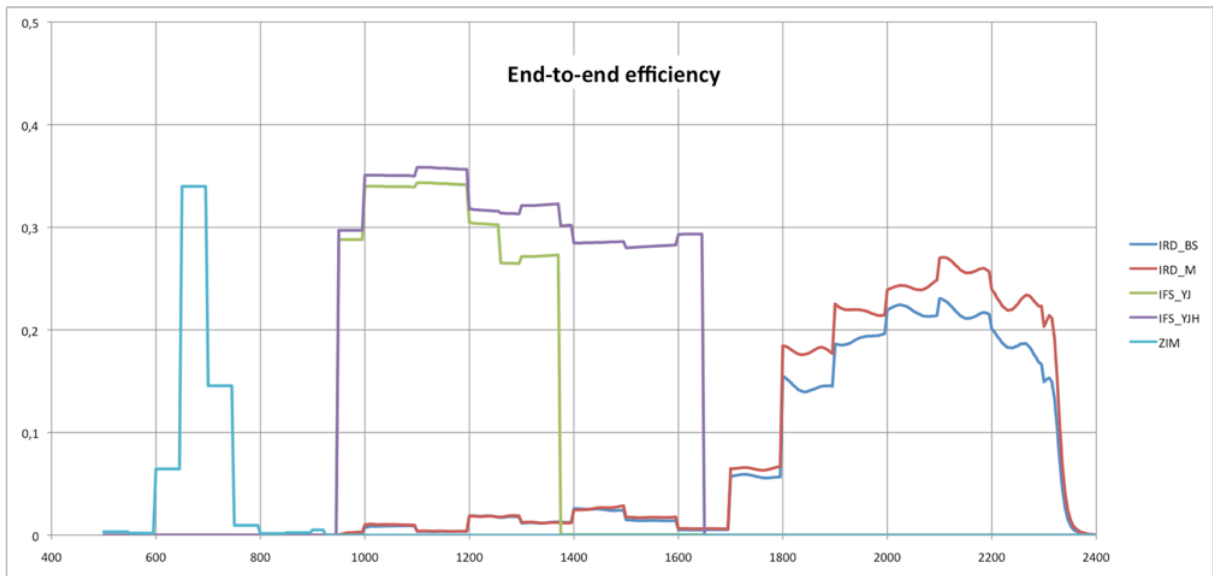

Figure 30: Transmission (as above) with different beamsplitters. In visible: separation between WFS and ZIMPOL uses a dichroic sending more light to ZIMPOL but in R band only; in NIR: the IFS/IRDIS dichroic 'K' feeds IFS with the its full Y-H range, with lower efficiency for IRDIS in K band only.
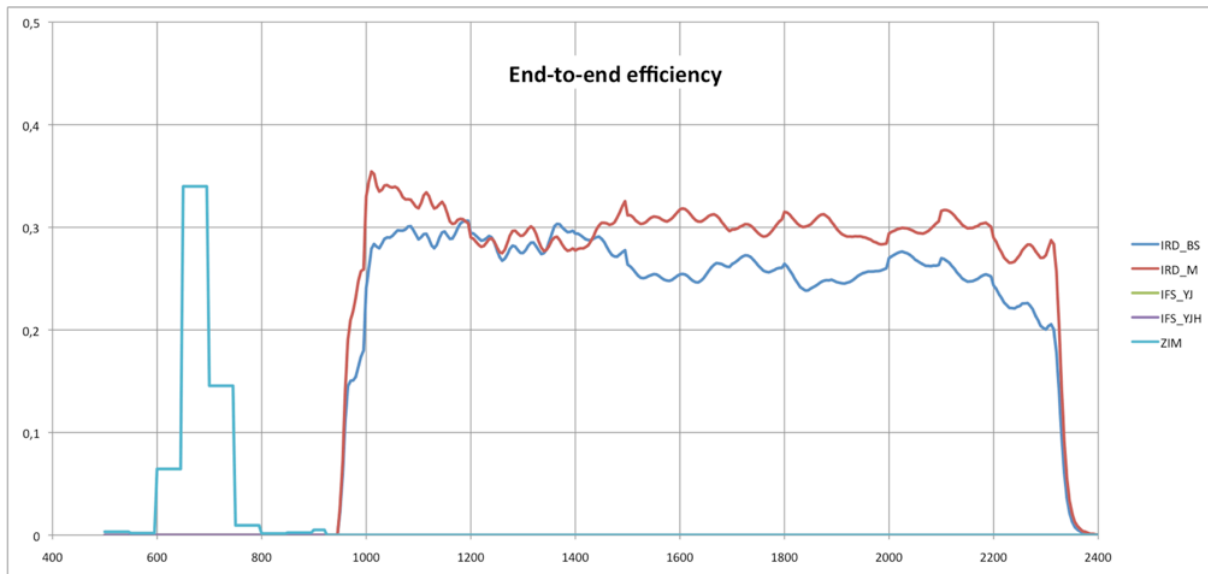
Figure 31: Transmission (as above) in IRDIS alone configuration where all the NIR light is sent to IRDIS.

A3. Neutral densities

Since neutral densities prevent most photons from reaching the detector, their use in science templates should be avoided when possible. Instead, a coronagraph should be considered when trying to prevent saturation. If accurate photometry or astrometry of the primary target is desired, Star center and Flux observations should be considered.

The transmission curves of the VIS and NIR neutral density filters are available here :
https://www.eso.org/sci/facilities/paranal/instruments/sphere/inst/filters.html

A3.1 CPI

The transmissions as a function of wavelength of the neutral density filter of CPI are displayed in Figure 32. These ND filters are common to IRDIS and IFS.
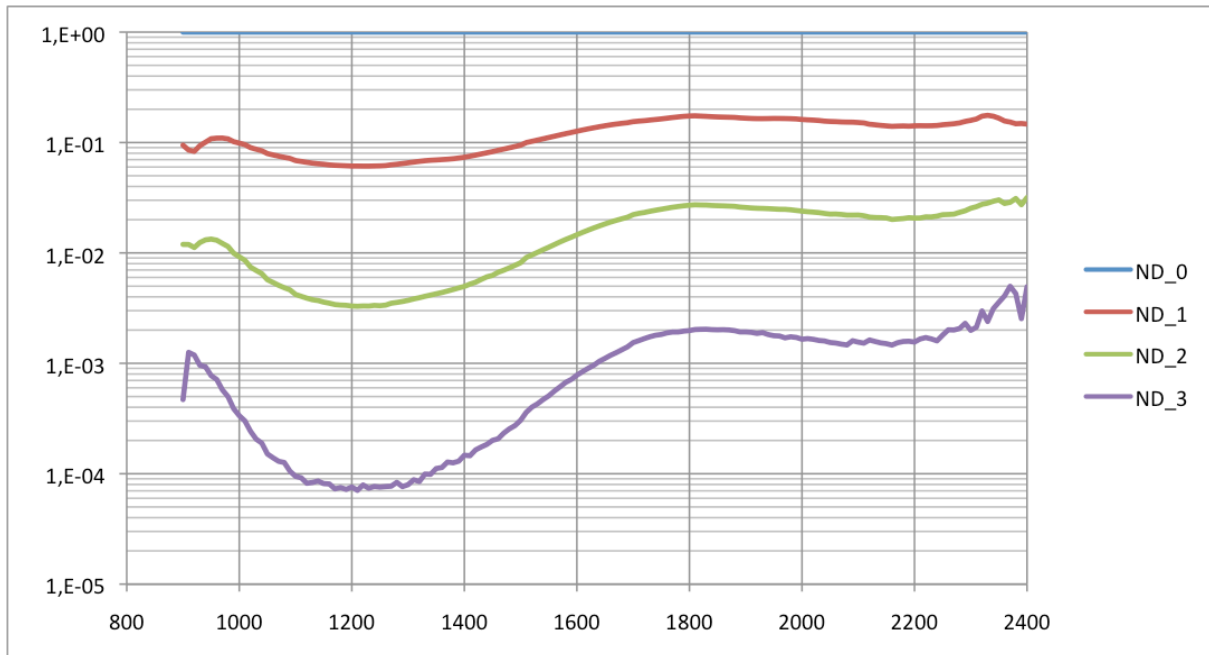
Figure 32: Transmission CPI NIR densities as a function of wavelength (nm).

A3.2 IFS

A filter wheel is mounted within IFS. These filters allow appropriate exposure levels for the IFS internal flat-field lamp. The wheel hosts three neutral density filters (ND1, ND2, ND3). The filters are identical to those in the CPI. They are inclined with respect to the optical axis, to avoid ghosts. This causes a small shift of the optical path.

A3.3 IRDIS

When observing with IRDIS-H in parallel to IFS, it might be useful to reduce the flux seen by IRDIS without affecting IFS data. This can be achieved by using the filter BBF-ND-H (consisting of H + a neutral density filter) instead of BBF-H.

A3.4 ZIMPOL

The transmission as a function of wavelength of the neutral density filters ND1, ND2 and ND4 mounted in filter wheel FW0 are shown in Figure 33.
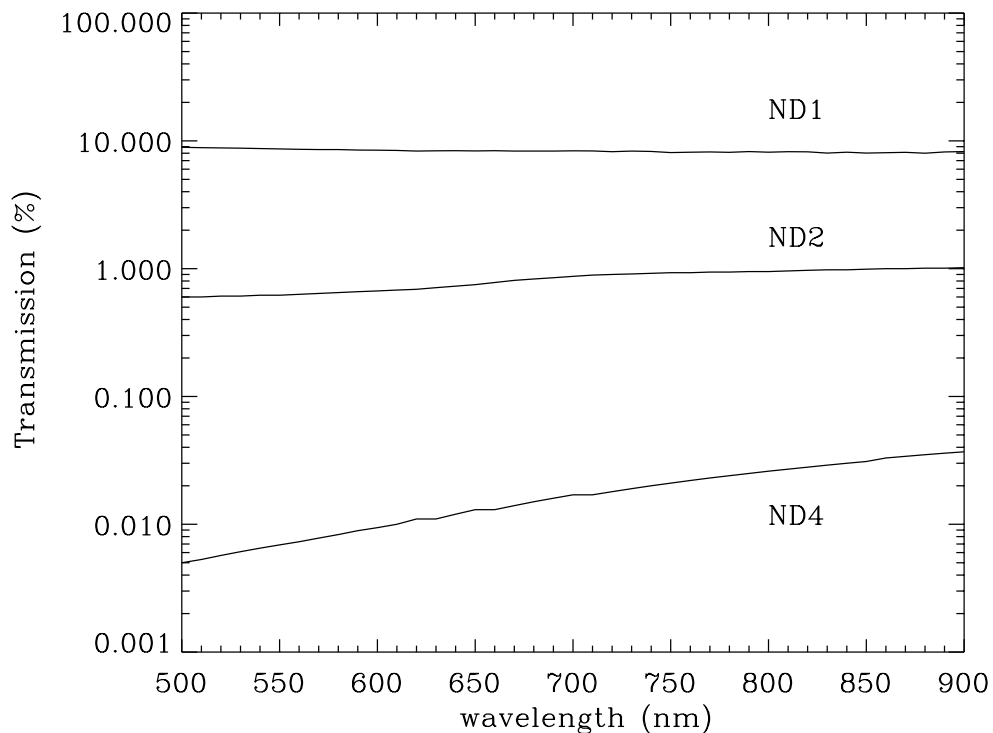
Figure 33: Spectral transmission of the ZIMPOL neutral density filters ND1, ND2 and ND3 (as provided by the manufacturer).

A4. IRDIS beam-splitter

The IRDIS internal beam-splitter separates the flux between the left and the right detector halves. The left (right) half is illuminated by light that is reflected (transmitted) by the splitter. The beam-splitter introduces flux differences between the two detector halves of less than 10% while slightly larger differences are observed for polarized light.

A5. IRDIS filters

IRDIS requires four types of filters: wideband filters (WBF), broadband filters (BBF), narrowband filters covering specific atomic or molecular lines (NBF), and dual band filters used pair wise for dual-band imaging (DBF). WBF, BBF, and NBF are referred to as common filters because they are located in a filter wheel situated in front of the beam separation optics. The DBFs are organized in pairs, located after the beam separation optics. Figure 34, Figure 35 and Figure 36 illustrate the various IRDIS filter transmissions.

Filter available as a function of observing mode:

- **CI can use any filter (except DBF).**
- **DPI can use any of the BBF and NBF.**
- **DBI can use only the DBF.**

The transmission curves of all IRDIS filters are available here :
https://www.eso.org/sci/facilities/paranal/instruments/sphere/inst/filters.html

DBF are used in conjunction with BBF (acting as blocking filters). In templates, the user is not asked for setting individual wheels but only pre-defined relevant combinations, as presented in Table 45.
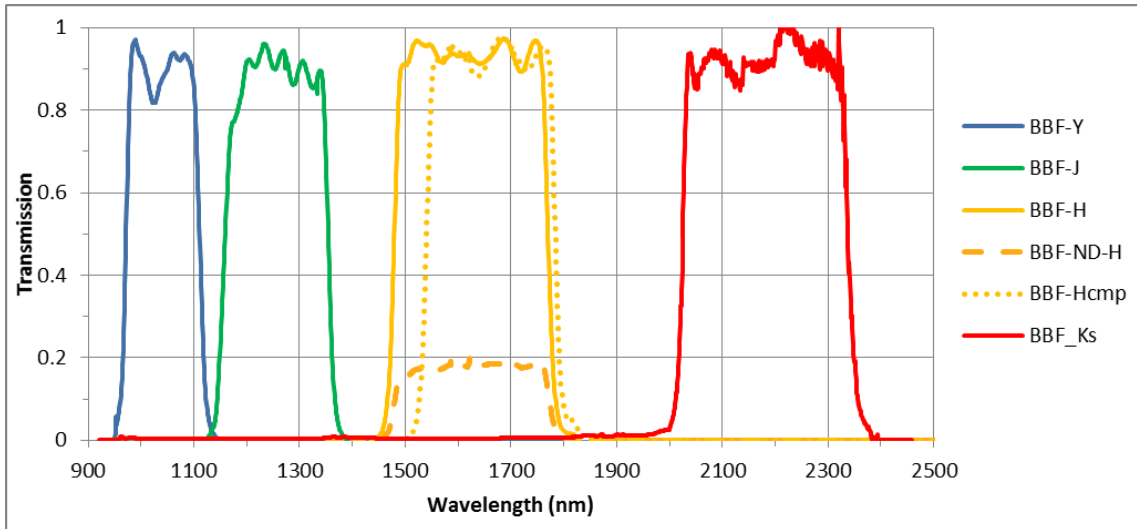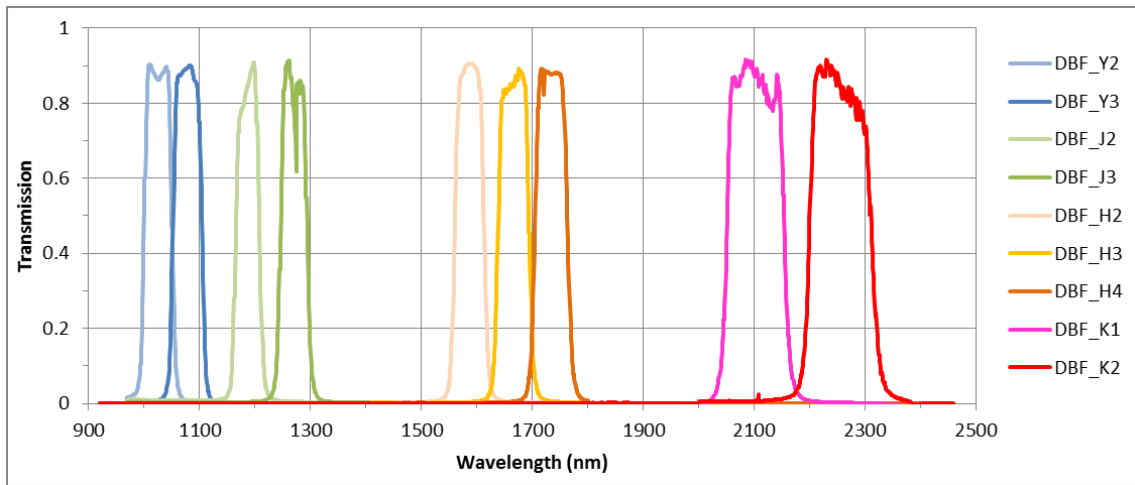
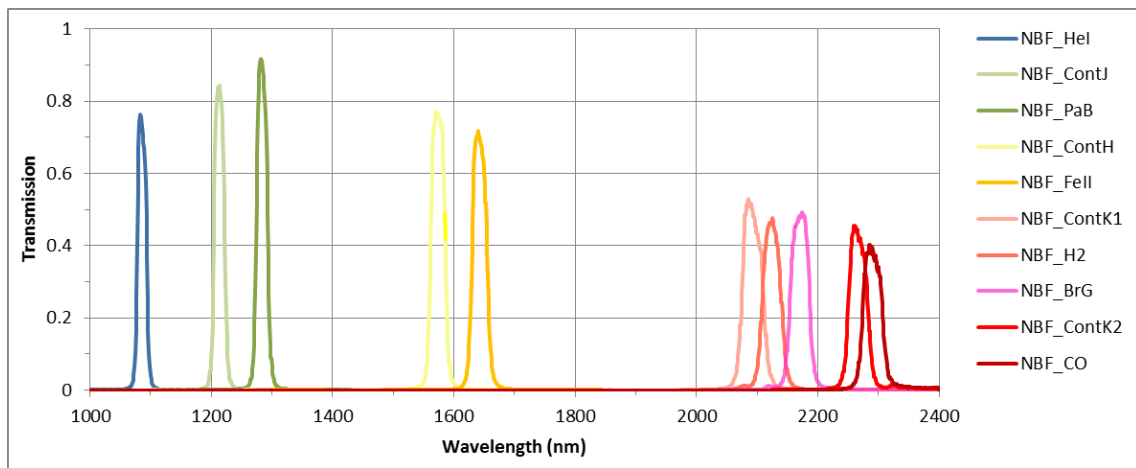Figure 34: IRDIS BB filters.

Figure 35: IRDIS DB filters.

Figure 36: IRDIS NB filters.
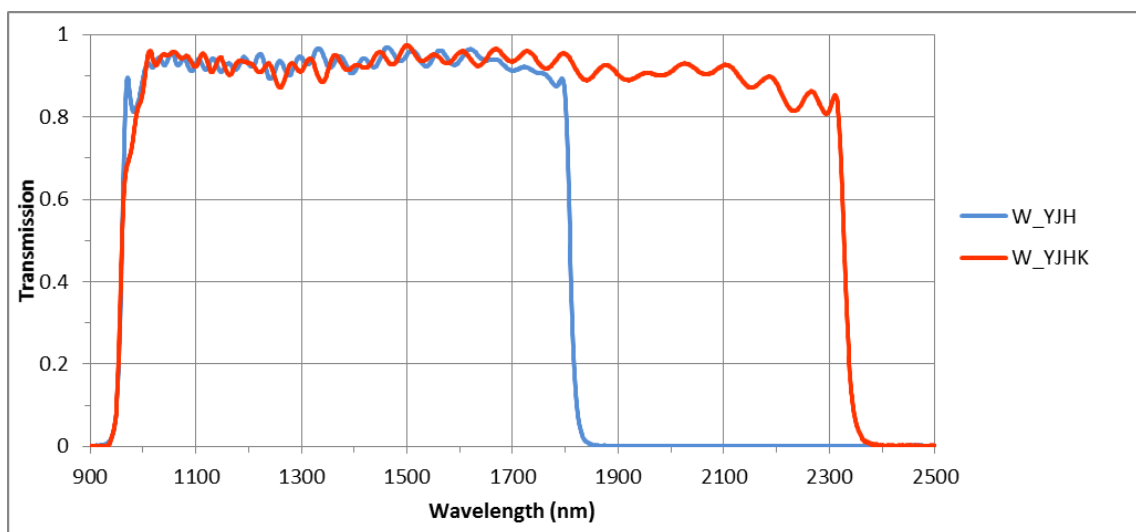
Figure 37: IRDIS wideband filter.

Table 44: IRDIS relevant filter combinations.

Name	Mode	λ_c (nm)	$\Delta\lambda$	IRFW1	IRFW2	Modes
DBI						
DB_Y23	*DBI, Y2-Y3*	1025.8 - 1080.2	44.8 - 45.5	B_Y	D_Y23	DBI, CI
DB_J23	*DBI, J2-J3*	1189.5 - 1269.8	47.6 - 50.8	B_J	D_J23	DBI, CI
DB_H23	*DBI, H2-H3*	1588.8 - 1667.1	53.1 - 55.6	B_H	D_H23	DBI, CI
DB_H32	*DBI, H3-H2*	1589.0 - 1665.3	53.1 - 55.6	B_H	D_H32	DBI, CI
DB_H34	*DBI, H3-H4*	1665.0 - 1736.4	55.6 - 57.7	B_Hcmp2	D_H34	DBI, CI
DB_K12	*DBI, K1-K2*	2102.5 - 2255	102 - 109	B_Ks	D_K12	DBI, CI
DBI + ND filter						
DB_NDH23	*Including ND 0.5*			B_ND-H	D_H23	DBI, CI
DB_NDH32	*Including ND 0.6*			B_ND-H	D_H32	DBI, CI
Broadband						
BB_Y	*Full Y band*	1042.5	139	B_Y	CLEAR	DPI, CI
BB_J	*Full J band*	1257.5	197	B_J	CLEAR	DPI, CI
BB_H	*Full H band*	1625.5	291	B_H	CLEAR	DPI, CI
BB_Ks	*Full Ks band*	2181.3	313.5	B_Ks	CLEAR	DPI, CI
Narrowband						
NB_HeI	*HeI (1083nm)*	1092.3	17.1	N_HeI	CLEAR	DBI, CI
NB_ContJ	*ContJ (1211nm)*	1215.7	18.3	N_ContJ	CLEAR	DBI, CI
NB_PaB	*PaB (1282nm)*	1281.3	20.9	N_PaB	CLEAR	DBI, CI
NB_ContH	*ContH (1574nm)*	1557.8	24.5	N_CntH	CLEAR	DBI, CI
NB_FeII	*FeII (1644nm)*	1645.5	26.1	N_FeII	CLEAR	DBI, CI
NB_ContK1	*ContK1 (2098nm)*	2102.7	33.0	N_CntK1	CLEAR	DBI, CI
NB_H2	*H2 (2122nm)*	2128.2	32.4	N_H2	CLEAR	DBI, CI
NB_BrG	*BrG (2167nm)*	2162.9	37.4	N_BrG	CLEAR	DBI, CI
NB_CO	*CO (2294nm)*	2287.5	35.1	N_CO	CLEAR	DBI, CI
NB_ContK2	*ContK2 (2267nm)*	2270.5	34.0	N_ContK2	CLEAR	DBI, CI
Spectroscopy						
S_LR	*YJHKs*	*1644*	*1370*	W_YJHKs	CLEAR	LSS
S_MR	*YJH*	*1384.5*	*851*	W_YJH	CLEAR	LSS

A6. NIR Coronagraphs

NIR coronagraphs include classical Lyot coronagraphs (CLC) and apodized Lyot coronagraphs (ALC). The available coronagraphs combinations for particular wavelengths and optical elements are summarized in Table 45. The value N_NS_CLEAR indicates that no coronagraph will be used. Since only ALC coronagraphs are offered in service mode, when "Coron" is chosen on the Exposure Time Calculators (ETCs), the choice of coronagraph and returned performances are implicitly the ones corresponding to ALCs.

Table 45: List of NIR coronagraph combinations with filters and slit. The most common combinations are highlighted in green.

Instrument	Wavelength/	Service mode	Visitor mode

mode	Filter	Recommended* Coronagraph	Small IWA** Coronagraph	Large IWA Coronagraph
IRDIFS or IRDIS alone	IFS-YJ, DB_H23, DB_H34, DB_ND23, DB_NDH23, BB_H	N_ALC_YJH_S (IWA~0''.15)	N_ALC_YJ_S (IWA~0''.08)	N_ALC_YJH_L (IWA~0''.2)
IRDIFS-EXT	IFS-YJH, DB_K12, BB_Ks	N_ALC_YJH_S (IWA~0''.15)	N_ALC_YJ_S (IWA~0''.08)	N_CLC_SW_L (IWA~0''.35)
IRDIS alone	DB_Y23, BB_Y, NB_HeI	N_ALC_YJH_S (IWA~0''.15)	N_ALC_YJ_S (IWA~0''.08)	N_ALC_YJH_L (IWA~0''.2)
IRDIS alone	DB_J23, BB_J, NB_CntJ, NB_PaB	N_ALC_YJH_S (IWA~0''.15)	N_ALC_YJ_S (IWA~0''.08)	N_ALC_YJH_L (IWA~0''.2)
IRDIS alone	BB_H, NB_CntH, NB_FeII	N_ALC_YJH_S (IWA~0''.15)	N_ALC_YJ_S (IWA~0''.08)	N_ALC_YJH_L (IWA~0''.2)
IRDIS alone	DB_K12, BB_Ks	N_ALC_Ks (IWA~0''.2)	N/A	N_CLC_LW_L (IWA~0''.35)
IRDIS alone	NB_CntK1, NB_BrG, NB_CntK2, NB_H2, NB_CO	N_ALC_Ks (IWA~0''.2)	N/A	N_CLC_LW_L (IWA~0''.35)
IRDIS LSS	N_S_LR_WL, N_S_MR_WL	Not offered in service mode	N/A	N_S_LR_WL, N_S_MR_WL (IWA~0''.2)

*Three special coronagraphs (only available in visitor mode, for expert users) are not included in the table. For shorter wavelengths, ALC configurations are optimized depending on band and focal mask: **ALC_Y, ALC_YJ_S, ALC_YJ_L**.

A6.1 ALC coronagraphs

The optimal transmission profile of the apodizer depends on the size (in λ/D) of the focal mask. Practically, a given focal mask has a given size in microns, not in units of λ/D. This means that, when observing in broadband filters, a given apodizer and focal mask combination is optimal only at a particular wavelength. The performance of the coronagraph decreases rapidly at longer wavelengths but slowly at shorter wavelengths. The ALC combinations include

- 2 apodizers, APO1 and APO2, optimized for 4 and 5.2 (λ/D) focal masks,
- 3 focal masks, ALC1, ALC2, ALC3, with diameters of 145, 185 and 240 (mas).

The ALC Lyot stop has good transmission (92%) with a large outer radius (96% of VLT pupil). The transmission and resolution are limited by the entrance apodizer. Optimal approved combinations of apodizer-mask-Lyot stop have been preselected, and cannot be changed for now. These combinations are described in Table 46.

Table 46: Definition of the coronagraph combination

Coronagraph combination name	Applicable band	Apodizer	Lyot Mask and diameter in mas
N_ALC_YJH_S	YJH	APO1	ALC2 (185mas)

N_ALC_YJH_L	YJH	APO2	ALC3 (240mas)
N_ALC_YJ_S	YJ	APO1	ALC1 (145mas)
N_ALS_YJ_L	YJ	APO2	ALC2 (185mas)
N_ALC_Ks	YJHKs	APO1	ALC3 (240mas)

A characterization of the transmission profile of N_ALC_YJH coronagraph (radius 92.5mas) was measured with IRDIS (H2/H3 filter) and the IFS (Y to J mode) by placing a star behind the coronagraph and offsetting it from the center of the mask.

Numerical end-to-end simulations confirm accurately the measurements of the transmission and are shown in the Figure 38. The vertical axis correspond to the ratio between the star flux at a given separation and the star flux measured at large separation outside the influence radius of the coronagraphic mask. For the IFS, we measured a small chromatic dependence of the transmission profile which is not reproduced by the simulation (possibly ADC residuals or normalization effects) so we provide a single transmission curve from Y to J.

The measured inner working angle (IWA defined as the separation that yields a transmission of 50%) are 95mas and 99mas for the IFS YJ and IRDIS H2 respectively. About 90% of the flux is recovered at a separation of 130mas from the mask center in all configurations.

In case of a detection close the coronagraph IWA or to provide contrast curves below 200mas, correcting for the transmission profile of the coronagraph is required. The digitized version of this curve can be found at .
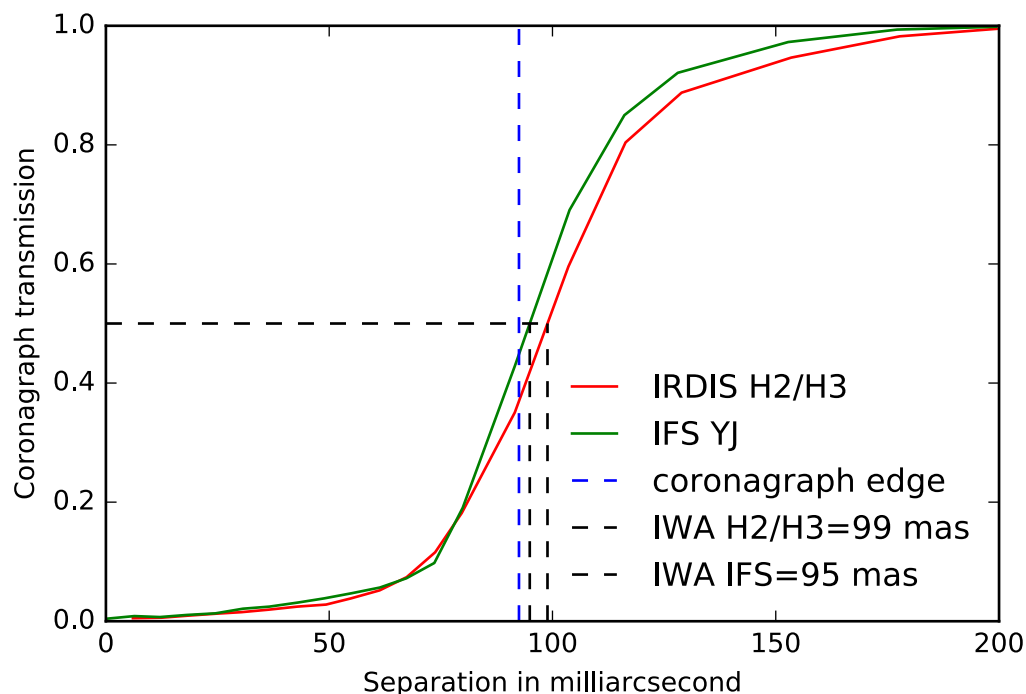

Figure 38 Transmission profile for the N_ALC_JYH_S coronagraph

A7. IFS dispersive components

There are two alternative dispersive elements in IFS. Both are Amici prisms designed either for the Y-J or the Y-H band. The prisms are associated with filters that define the pass-band of each spectrum, avoiding overlap of consecutive spectra along the dispersion direction. Prism parameters are listed in Table 47.

Table 47: IFS prisms parameters.

Parameter	Y-J	Y-H
Spectral length (pixels)	35.4	35.3
Wavelength Range (µm)	0.96-1.34 µm	0.97-1.66 µm
Average dispersion (nm/pixel)	10.52	19.15
Average Spectral resolution (per FWHM)	55.1	34.5

A8. IRDIS dispersive components

A8.1 LSS

LSS requires a long slit located in the coronagraphic focal plane and a dispersive component (prism or grism) that is located in the IRDIS pupil plane. The corresponding focal plane and pupil plane combinations for LSS are listed in. Naming conventions for named LR_N_L to MR_W_S are:

- LR for low resolution and MR for medium resolution,
- N for narrow (90 mas) and W for wide (120 mas) slit width, both larger than the PSF,
- L for large (400 mas) and S for small (200 mas) size of the central blocking mask.

A8.2 Prism

LRS mode uses a double prism designed for zero deviation close to the center of the spectral range and close to linear dispersion function. The wavelength λ to pixel y relation for the prism is fit by:

$$\lambda = \lambda_0 + c_1*(y-y_0)/100 + c_2*((y-y_0)/100)^2 + c_3*((y-y_0)/100)^3 + c_4*((y-y_0)/100)^4$$

The laser line is at λ_0=1545.07 nm and its position determines y_0. Fit parameters are: c_1 = -9.1293 for channel M or c_1= -9.12795 for channel BS; c_2, c_3 and c_4 are equal for both channels. The relative orientation of the double prisms introduces a higher variance in λ_0 and c_1 than for the grism.

A8.3 Grism

The pixel–wavelength relation is linear for the grism. Fitting parameter c_1 = -1.13878 +/- 0.00022 (nm/pixel) is related to the focal length of the camera mirror. As the two mirrors are slightly different, this term is slightly different for the two channels. In the fit, y_0 corresponds to a constant offset and varies with slit position. The two parameters, y_0 and λ_0, are determined as above.

A9. Visible Coronagraphs

The coronagraphs in the visible are all classical Lyot coronagraphs (CLC). The selection of a coronagraph includes setting of different devices: the focal mask and the pupil stop. The CLC focal masks, which have various diameters, are suspended or deposited on substrates (with no suspending wire), and include a field stop (either full ZIMPOL FoV or restricted to inner 1'' FoV for window mode). Relevant combinations are listed in. Naming conventions are:

- CLC, NC: for the type of coronagraph (Classical Lyot Coronagraph or no coronagraph).
- S, M, L, XL: for the size of the focal mask from small to very large (93, 155, 310 and 1240 mas, respectively).
- WF: for the wide field stop.

Table 48: List of visible coronagraph combinations. Recommended configurations are highlighted in green.

Mode	Filter	Recommended* Coronagraph	Medium/large/ extra large IWA Coronagraph
ZIMPOL_P1	RI, R_PRIM, I_PRIM, V, N_R, N_I, KI, TiO_717, CH4_727, Cnt748, Cnt820, CntHa, N_Ha, B_Ha	V_CLC_M_WF	V_CLC_S_WF/ V_CLC_L_WF/ V_CLC_XL_WF
ZIMPOL_P2	RI, R_PRIM, I_PRIM, V, N_R, N_I, KI, TiO_717, CH4_727, Cnt748, Cnt820, CntHa, N_Ha, B_Ha	V_CLC_M_WF	V_CLC_S_WF/ V_CLC_L_WF/ V_CLC_XL_WF
ZIMPOL_I	RI, R_PRIM, I_PRIM, V, V_S, V_L, N_R, 730_NB, N_I, I_L, KI, TiO_717, CH4_727, Cnt748, Cnt820, HeI, OI_630, CntHa, B_Ha, N_Ha, Ha_NB	V_CLC_M_WF	V_CLC_S_WF/ V_CLC_L_WF/ V_CLC_XL_WF

*Not in the table is the **V_CLC_MT_WF** mask (155 mas), which includes a grid of dots that is useful for calibration purposes and/or accurate astrometric reference.*

The selection depends on the required halo rejection, none-saturation capability and IWA:
- No coronagraph (V_NC_WF or V_NC_NF): Should be used when the science goal concerns the target itself or its immediate environment at the resolution limit. The N_NC_NF option uses a field stop of 1" (useful for – not yet offered- windowed read-out modes), whereas the full field-of-view is accessible with the V_NV_WF option. Saturation effects are limited thanks to the high CCD pixel-well and by the short DIT possible especially in window mode. Neutral density filters can be inserted unless observing with filters mounted on the FW0. If saturation occurs, the charge leakage is quite limited close to the saturated peak and over the columns. Observations performed so far indicate that artefacts introduced by saturations are very small.
- CLC with increasing mask diameter between 93 and 1240 (mas).
- Special case of V_CLC_MT_WF: this on-substrate 155 mas mask also includes a grid of dots that is useful for calibration purposes and/or accurate astrometric reference.

A10. ZIMPOL filters
ZIMPOL has three filter wheels, FW0 located in front of the polarization modulator and beam splitter, FW1 located in arm 1 of ZIMPOL and FW2 located in arm 2 of ZIMPOL. FW0 contains besides filters for imaging also polarization calibration components and neutral density filters. Recommendations are:

Filters located in FW0 can be used for imaging and they provide the same band-pass in both arms. FW0 cannot be combined with neutral density filters, as they are located in the same wheel. It is not recommended that the FW0 filter be used for polarimetric measurements because they may introduce polarimetric effects that are difficult to calibrate. The combination of FW0 filters with FW1 or FW2 filters is not supported.

Filters located in FW1 and FW2 can be used for imaging, differential imaging and polarization. Different filters can be used in FW1 and FW2, but one needs to be aware that the detector operation (e.g. exposure time) is identical in both arms. The combination of a narrowband filter with a broadband filter may therefore cause an underexposed image in one arm and an overexposed image in the other arm.

The list of relevant combinations, and their names are listed in Table 49. Note that if the dichroic beam splitter is used between ZIMPOL and WFS then only a small wavelength range in the R-band can be observed. This reduces the useful filters to those highlighted in green in Table 49.
The transmission curves of all ZIMPOL filters are available here :
www.eso.org/sci/facilities/paranal/instruments/sphere/inst/filters.html

Table 49: Measured band-pass of ZIMPOL filters. We list wavelengths (nm), where the transmission is 50% of its maximum, the 50% width and its central wavelength.

Filter	λ_{min}	λ_{max}	FWHM	λ_0
RI	590.1	880.6	290.5	735.4
R_PRIM	552	700.6	148.6	626.3
I_PRIM	713.3	866	152.7	789.7
V	513.7	594.3	80.6	554
V_S	513	550.2	37.2	531.6
V_L	560.9	602	41.1	581.5
N_R	617.5	674.2	56.7	645.9
730_NB	705.5	760.4	54.9	733
N_I	776.5	857	80.5	816.8
I_L	842.4	898.8	56.4	870.6
KI	759.6	780.8	21.2	770.2
TiO_717	706.9	726.6	19.7	716.8
CH4_727	720	740.5	20.5	730.3
Cnt748	737.1	757.7	20.6	747.4
Cnt820	807.4	827.2	19.8	817.3
HeI	585.3	590.7	5.4	588
OI_630	626.8	632.2	5.4	629.5
CntHa	642.8	646.9	4.1	644.9
B_Ha	652.9	658.4	5.5	655.6
N_Ha	655.85	656.82	0.97	656.34
Ha_NB	656.04	657.02	0.98	656.49

NOTE: The filters highlighted in green are compatible with the dichroic beamsplitter.

A11. Polarimetric calibration components

ZIMPOL is optimized for the measurement of linear polarization. Here we present a short summary of the critical polarimetric calibration components, the reader is invited to read Bazzon et al. 2012 (SPIE 8446, 93B) for further details about the polarimetric concept.

The most important components for the polarimetric calibration are the linear polarizer and HWPZ. Less important are the quarter-wave plate and the circular polarizer. Note that:

- **The achromatic (dichroic glass) polarizer is made of structured absorptive nanoparticles. It provides a contrast <10^{-3} between 600-900 nm and 10^{-2} between 500-600 nm.**
- **Circular polarization is measured with an achromatic quarter-wave plate made out of MgF$_2$ and quartz. The retardance error is less than ±6% between 500-900 nm.**
- **The circular polarizer is a combination of a linear polarizer with the fast axis at 45° (±0.5°) followed by a quarter-wave plate with the fast axis at 0°. Both components are of the same. Since the quarter-wave plate is not perfectly achromatic the circular polarizer has a small leakage of linear polarization of several %.**

The reference orientation for the polarimetric alignment is given by the polarizing beam-splitter of ZIMPOL. The transmitted beam (CCD 1) has a linear polarization parallel to the ZIMPOL bench and the reflected beam (CCD 2) an orientation perpendicular

A12. Waffle spots

When a coronagraph is used with Irdis or Zimpol, the position of the star behind the coronagraph can be known by applying a waffle pattern to the DM. This is critical because most post-processing techniques rely on the accurate registration of the star. The pattern creates four replicas of the PSF, called satellite spots, at a separation of about 14 λ/D. The orientation of this pattern can be chosen, between an x shape (position angle of the spots of 45º, 135º, 225º and 315º as shown in Figure 39) or a + shape (position angle of 0º, 90º, 180º and 270º). These spots can be used to find the star center by intersecting the line joining opposite spots, as illustrated in Figure 39. Non coronagraphic observations of a star with the waffle pattern on were obtained to calibrate the accuracy of this technique as illustrated in Figure 40. The star center as estimated from the intersection of the two lines joining opposite satellite spots and from a direct 2d fit on the PSF core agrees within better than 2.5mas
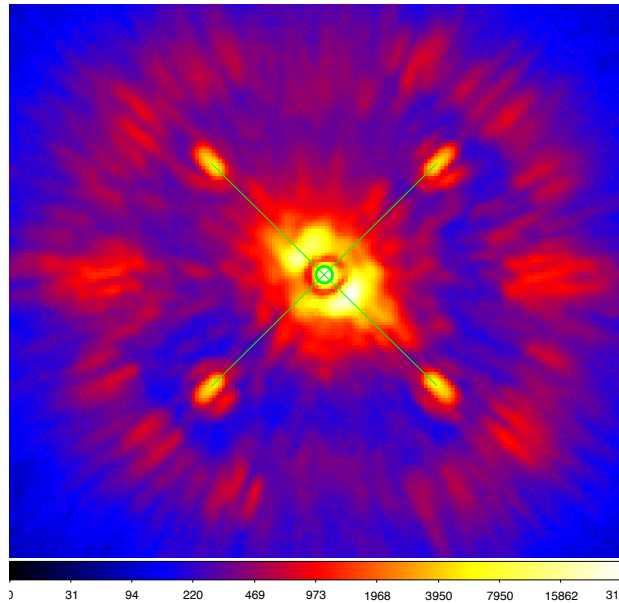
Figure 39. Irdis image in broad-band H, with the N_ALC_YJH coronagraph, with the waffle pattern applied to the DM, creating four satellite spots. These spots are elongated with broad-band filters and point source with narrow-band filters. The green lines start and end points were computed by fitting a 2D Gaussian on each spot, they intersect on the star center, indicated by a green thick circle.
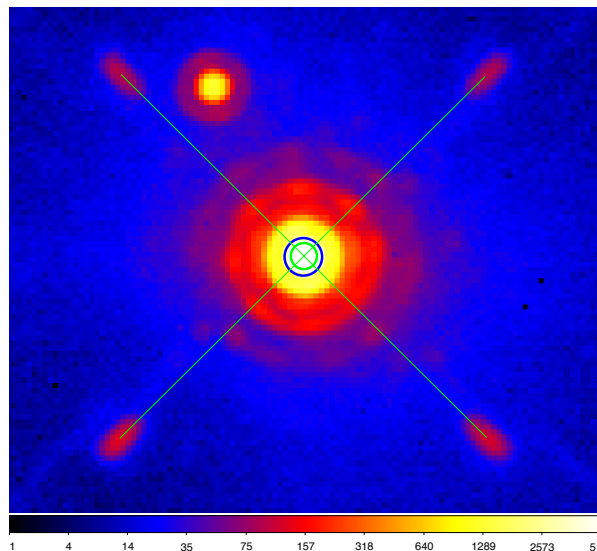

Figure 40 Non coronagraphic image of a star (happening to have a binary companion) in broad-band H with Irdis, after applying a waffle pattern to the DM for calibration purposes. The green thick circle indicates the intersection of the green lines, while the blue thick circle indicates the star position (Gaussian fit). Both agree within 2.5mas.